DIPLOMARBEIT | MASTERTHESIS

# Thermal and Visual Performance Assessment and Parametric Improvement of a Historical Educational Building in Greece through Passive Strategies

unter der Leitung von

Univ.-Prof. Dipl.-Ing. Dr.techn. Ardeshir Mahdavi

Sen. Sci. Dipl.Ing. Dr.techn. Ulrich Pont

E 259-3 Forschungsbereich für Bauphysik und Bauökologie

Institut für Architekturwissenschaften

eingereicht an der

Technischen Universität Wien

Fakultät für Architektur und Raumplanung

von

Eleni Marmaridou, BSc

[redacted]

Wien, Juni 2022

# KURZFASSUNG

Dynamische Energie- und Tageslichtsimulationen mit verschiedenen Softwareinstrumenten werden zunehmend verwendet und optimiert, um eine richtige Bewertung der Energieeffizienz von Gebäuden sowie des thermischen und visuellen Komforts zu ermöglichen. Unter diesen Softwaretools bietet Grasshopper, eine parametrische visuelle Skriptschnittstelle, die in der computergestützten Designanwendung Rhinoceros 3D ausgeführt wird, eine zunehmend stabile Umgebung, die über verschiedene Plug-Ins (z. B. Ladybug Tools) mit Energie- und Tageslichtmodellierungs-Engines verbunden ist.

Das Ziel dieser Forschungsarbeit ist zweierlei:

- Zum einen wird die Effizienz einer solchen Schnittstelle für dynamische Gebäudeenergie- und Tageslichtsimulationen bewertet,

- zum anderen steht die detaillierte Energie- und Tageslichtanalyse und -optimierung eines Schulgebäudes im Mittelpunkt dieser Arbeit.

Dabei wird die Bewertung dieses Gebäudes mit den genannten Instrumenten durchgeführt. Das Schulgebäude ist das "Knabengymnasium" der Stadt Drama in Nordgriechenland. Es ist ein Denkmal des kulturellen Erbes Griechenlands, das zwischen 1928 und 1932 erbaut wurde. Der derzeitige Zustand des Gebäudes kann kaum als zufriedenstellend bezeichnet werden, da es nur gelegentlich instandgehalten wird. Es handelt sich um ein repräsentatives Gebäude unter einer Vielzahl von Schulgebäuden, denen der Status des kulturellen Erbes in Griechenland zugewiesen worden ist. Diese Gebäude können laut Gesetzgebung von einer effizienten Nutzung der Energie ausgenommen werden (T.O.T.E.E., 2017). .

Die Studie der Schule wird durchgeführt, indem bestimmte Parameter der vorhandenen thermischen und visuellen Leistung der Schule gesammelt und anhand bestimmter Gebäudeleistungsindikatoren bewertet werden. Diese Indikatoren werden durch Simulationen berechnet und gemäß den bestehenden Vorgaben bewertet. Sie betreffen den Wärmekomfort im Gebäude während der Belegungszeit eines ganzen Jahres sowie die Energie- und Tageslichtleistung der Schule und insbesondere den Heiz-, Kühl- und elektrischen Lichtbedarf für den Energieteil sowie die durchschnittliche Beleuchtungsstärke und Gleichmäßigkeit jeder Wärmezone, räumliche Tageslichtautonomie und Punktblendungswahrscheinlichkeitswerte für den Tageslichtteil. Es muss erwähnt werden, dass der thermische Komfort durch den „adaptiven Komfortrechner“ der Legacy-Plug-ins Ladybug 0.0.69 und Honeybee 0.0.66 bewertet wurde, der den thermischen Komfort der Bewohner für ausschließlich natürlich belüftete, freilaufende

Gebäude berechnet . Da es sich bei dem untersuchten Gebäude jedoch nicht um ein freilaufendes Gebäude handelt, ist die Analyse der adaptiven Theorie nicht konsistent, sondern wurde durchgeführt, um einen Eindruck einer relevanten Erkundung zu vermitteln.

Anschließend wird ein parametrisches Modell erstellt, das mehrere mögliche Optimierungsmethoden für die oben genannten Kennzahlen vorschlägt, und zwar in Übereinstimmung mit den Vorgaben des "Amtes Moderner Monumente" Griechenlands und durch Umsetzung einer Reihe passiver Maßnahmen. Diese Maßnahmen umfassen das Hinzufügen einer Isolierung zu Außenwand-, Dach- und Bodenkonstruktionen, die Unterbringung verschiedener Innenschirme, Optionen zur Nachrüstung von Fenstern und das Hinzufügen oder nicht von Lichtfächern. Die Ergebnisse der verschiedenen Szenarien werden gleichzeitig mit einem populären Tool zur Erkundung des Designraums visualisiert, das als Design Explorer bezeichnet wird. Mit diesem Tool ist es möglich, die Auswahl der Strategien basierend auf den zu erreichenden Entwurfs- und Planungszielen einzugrenzen. Auf diese Weise können die verschiedenen Leistungsaspekte anhand quantitativer Kennzahlen verglichen werden.

Letztendlich können die Ziele und Anforderungen der verschiedenen Interessenten effizient diskutiert und unterstützt werden.

**Schlüsselwörter**

Energie- und Tageslichtsimulation, Grasshopper-Schnittstelle, parametrische Studie, Energieeffizienz- und Tageslichtmetriken, thermischer und visueller Komfort

# ABSTRACT

Dynamic energy and daylight simulations through different software instruments are increasingly used and optimized to enable the efficient assessment of buildings' energy efficiency and thermal and visual comfort levels. Among these software tools, Grasshopper, a parametric visual scripting interface running within the Rhinoceros 3D application, offers an increasingly stable environment connected to energy and daylight modeling engines via different plug-ins (e.g. Ladybug 0.0.69 and Honeybee 0.0.66 Legacy Plug-ins). The aim of this research is dual. On the one hand, the efficiency of such an interface for dynamic building energy and daylight simulations is assessed. On the other hand, the detailed energy and daylight analysis and improvement of a school building are in focus of this work. Thereby, the assessment of this building is conducted with the mentioned instruments. The school building is the "Boys' High School" of the city of Drama in northern Greece. It is a cultural heritage monument of Greece, built during the period 1928-1932. Currently, the building's status quo can be considered as poorly and sporadically maintained, as for most school buildings under cultural heritage state in Greece. An important reason that explains this phenomenon is the fact that these buildings can be excluded from the buildings' efficiency legislation of the country (T.O.T.E.E., 2017).

The school's study is conducted by collecting certain data of the school's existing thermal and visual performance and assessing them through certain building performance indicators. These indicators are computed through simulations and are evaluated according to existing Standards. They concern the thermal comfort inside the building during the occupancy hours of a whole year, as well as the school's energy and daylight performances and in specific, its heating, cooling, and electric light loads for the energy part and the illuminance, uniformity, spatial daylight autonomy and point glare probability values for the daylight part. It has to be mentioned that the thermal comfort was assessed through the "adaptive comfort calculator" of the Ladybug 0.0.69 and Honeybee 0.0.66 Legacy Plug-ins which calculates the occupants' thermal comfort levels for solely naturally ventilated, free-running buildings. Since the building studied though is not a free-running one, the analysis of the adaptive theory is not consistent, but it was conducted to give an impression of a relevant exploration.

Subsequently, a parametric model that suggests multiple possible improvement methods for the above-mentioned indicators is created, in accordance with the Standards of the "Ephorate of Contemporary Monuments" of Greece and by implementing a set of passive strategies. These strategies include the addition of insulation to the exterior wall, roof, and floor constructions, the implementation of different interior shades, various window retrofit options, and the addition of

light shelves. The results of the different scenarios are visualized through a popular design space exploration tool, known as Design Explorer. Through this tool, it is possible to narrow down the selection of strategies based on the design and planning goals that are to be achieved. In this way, the different performance aspects can be compared based on quantitative metrics. As a result, the goals and requirements of the different interested parties can be discussed and supported efficiently.

**Keywords**

Energy and Daylight Simulation, Grasshopper Interface, Parametric Study, Energy Performance and Daylight Metrics, Thermal and Visual Comfort

# ACKNOWLEDGEMENT

I would like to thank my supervisor Univ. Prof. Dr. Ardeshir Mahdavi, for his guidance and his helpful suggestions throughout my work.

I am also grateful to the staff of the Department of Building Physics and Building Ecology of the Vienna University of Technology, that provided me with the necessary tools and guidance to complete this study.

I would also like to express gratitude to the headmaster Mr. Symeonidis and the teachers of the “Boys´ High School” of Drama who helped me acquire the blueprints of the school facilities, together with other useful material, and offered me their knowledge and advice on the topic.

Furthermore, I am grateful to the Municipality of the city of Drama that granted me entrance permission to the school for all the necessary in-situ observations.

Special thanks go to my friend Shiva Khosravi for her wholehearted support on this attempt of mine.

Last but not least, I would like to thank my parents, Christos Marmaridis and Eleftheria Anthopoulou, and my sisters Margarita Marmaridou and Anastasia Marmaridou who helped me along the process, offering me their knowledge and presence in any way I needed it.

The research presented in this thesis was inspired, in part, by the master thesis “Restoration of the “Boys’ High School” of Drama - Assessment of its bearing capacity – Interventions” (2010) of the civil engineer Konstantinos Paraschou for the Department of Civil Engineering of the Aristotle University of Thessaloniki.

# CONTENTS

# 1. INTRODUCTION

## 1.1 Motivation

The thermal and visual performance of buildings in general and school buildings in particular, is of utmost importance for several reasons. On the one hand, it concerns the occupants' thermal and visual comfort in a learning environment, which is what makes its interior livable. On the other hand, it gives information about the school buildings' energy and environmental performance (reduced energy costs, reduced greenhouse gas emissions, etc.) (Daschalaki and Sermetzoglou, 2011).

Currently in Greece, there are legislations based on European and International Standards concerning the suggested energy demand and thermal and visual comfort levels, both for new and existing school buildings, These are the Laws 4122/2013-G.G. A'42/19.02.2013 and 4602/2019-G.G. A'45/09.03.2019/Article70, the regulation K.EN.A.K.: "Greek Regulation for the Energy Efficiency of Buildings", which includes the "TEE-KENAK" software that is responsible for the calculation of the energy efficiency of buildings in Greece, as well as all the T.O.T.E.E.20701/2017 guides issued by the Technical Chamber of Greece that state all the technical instructions for the application of an energy study.

Still, the cultural heritage school buildings have the right to be excluded from compliance with the existing legislation, which means that new interventions usually happen without a holistic approach and more often than not, only when there is an urgent need for them (T.O.T.E.E., 2017). As a result, these school buildings are usually far from any energy efficiency and/or comfort standards. They are often inadequately insulated and/or heated in order to avoid high costs and their occupants have to endure conditions that make the school's environment uncomfortable. Lack of thermal comfort can mean too cold, too hot, too humid, or not humid enough environments that can negatively influence the teaching and learning processes and affect a person's wellness and concentration (Keco, 2017). Similarly, lack of visual comfort can mean too dark, too bright, or high-glare environments and has effects on the vision and in extension to the concentration and general wellness of the occupants (Alexandri and Karapetsis, 2016). Sometimes the effects can be not only short-term, but also long-term, which shows the urgent need for a holistic approach on the matter (Alexandri and Karapetsis, 2016).

The continuous advancement of a state-of-the-art technology on dynamic-state energy and daylight simulations offers the possibility of systematic calculations of the energy loads and thermal and visual comfort levels of buildings. Grasshopper's Ladybug 0.0.69 and Honeybee 0.0.66 Legacy Plug-ins package is “a collection of free computer applications that support environmental design and education” as it is stated in Ladybug Tools Forum (2021) and aims to create a stable environment that is connected to multiple energy and daylight modeling engines. It is also offering a potentially highly efficient approach to parametrically improving the energy performance indicators and the thermal and visual comfort indicators and visualizing them through a user-friendly environment. As such, assessing the efficiency of this tool for conducting parametric dynamic energy and daylight simulations can provide some insight into the potential of these instruments for other comparable inquiries as well as user experiences for other users.

## 1.2 Background

### 1.2.1 Historical data

#### 1.2.1.1 The city of Drama and the educational sector

Drama is a city and municipality located in northeastern Greece. It is the capital of the regional unit of Drama which is part of the East Macedonia and Thrace administrative region. The city (population 44,823 in 2011) is the economic center of the municipality (population 58944 in 2011), which in turn comprises 60% of the regional unit's population. It is built at the foot of Mount Falakro, in a verdant area with abundant water sources at a 115 m elevation and its coordinates are: Latitude 41°9′N and Longitude 24°8 E. It has a humid, continental climate in the mountainous areas, while the lowlands have a Mediterranean one and it belongs to the 4th Climatic Zone of Greece (Zone D), as it can be seen in Figure 1. Today, the city bases its economy mostly on agriculture, small-scale mining (particularly of marble), and forestry (Regional Unit of Drama, 2022).


*Figure 1 The four climatic zones according to KENAK from the warmest to the coldest (source: T.O.T.E.E., 2017)*

From the second half of the 19th century and while still under the Turkish occupation, the flourishing of trade in Drama and the rise of the Christian orthodox population led to efforts for spiritual flourishing as well. According to written testimonies, until 1840 the schools of Drama operated in the narthex of the city's church. This narthex was later replaced by a small lodge that housed the so-called "School", which was later enlarged to accommodate both the boys' and the girls' schools. This "School" was maintained until 1881 (Marmaridou, 2013).

After 1897 and the war between Greece and Turkey, the Bulgarian committees started being more active in the area until 1904. They initially tried to attract population through spiritual development by sending priests and teachers. The Patriarchate of Constantinople followed the same method in return and important construction work was implemented in the period 1902-1909 (amongst others, the Primary School of Drama “Ekpedeftiria” was built in 1909 and it can be seen in Figure 2) (Marmaridou, 2013).

*Figure 2 The first Primary School of Drama “Ekpedeftiria”, built in 1909 (source: dramini.gr, 2020)*

The end of the Turkish occupation in Drama was declared through the start of the Balkan wars. In 1918 the city passed to the Greek state again and with the exchange of populations, 92000 non-orthodox people left its area until 1929, while according to the Statistical Yearbook of 1930, it was the first choice for orthodox refugees’ settlement. Drama acquired a Greek character from the third decade of the 20th century, at the time when the Greek state started applying a holistic educational reformation, including the construction of many new school buildings with the "Boys' High School" of the city, which can be seen in Figure 3, amongst them (Marmaridou, 2013).


*Figure 3 The "Boys' High School" of Drama, built in the years 1928-1932 (Photo by the author, 2013)*

After the Second World War, more school buildings were built in the city, but only after 1979 the need for thermal protection started being considered more systematically. Still, only for the heat losses during the winter period. Furthermore, none of the school buildings constructed before the above year were thermally improved at the time, as only the new ones were relevantly attended. (T.O.T.E.E., 2017).

From 2010, the application of the TEE-KENAK software started in Greece. It was created to issue Energy Performance Certificates (EPC) for both new and renovated buildings. It introduced an integrated energy planning in the design and construction/renovation of buildings, setting the minimum requirements and specifications that they must meet. The cultural heritage monuments, with the "Boys' High School" of the city amongst them, had the right to be excluded from a holistic energy improvement approach and only undergo changes in case of need. Moreover, these changes had to always be according to the regulations of the "Ephorate of Contemporary Monuments" of Greece, making sure that there would be no alterations of their historical character and appearance. As a result, only recently and because of the rise of relevant needs, the municipality of Drama has published announcements for energy upgrade studies of such buildings (T.O.T.E.E., 2017).

#### 1.2.1.2 School buildings in the History of Modern Greece and Relevant Building Standards

One of the main aims of Kapodistrias, the first governor of the Greek state between 1828-1832, was the construction of school buildings. The first buildings had one storey, a rectangular-shaped plan and were built far from crowded areas. Those schools had large windows at a 2-meter distance from the ground to ensure good air circulation. During the reign of Otto Friedrich Ludwig (1832-1862), schools would operate in churches or other buildings that were not suitable for teaching. The few new school buildings reminded of rectangular farmhouses, had a height of 5-7 m and the distribution of windows in the classrooms was arranged in a way to ensure better natural ventilation. In the 1860's "Guide" there were architectural specifications that suggested construction by taking into account medical and sanitary terms. So, in the second half of the 19th century the above schools were considered inappropriate for teaching. Some of them were small and dirty and the sunlight was absent (Marmaridou, 2013).

At the end of the 19th century, it started being considered that the school buildings should be built in central areas that would be far from noisy and polluted surroundings. Again, there was a number of regulations concerning the classrooms' dimensions, window distribution, shading, natural ventilation, capacity and natural light penetration, as well as the size of the courtyards and the location of the toilets, that tried to achieve more livable conditions in the classrooms and outside of them. In 1894, the engineer D. Kallias drafted the first architectural regulation for the school space and proposed a uniform and scientific way for the construction of such buildings so that, amongst others, the rules of hygiene and aesthetics would be fulfilled. He suggested that large, airy plots should be chosen, and spacious classrooms should be designed, with a height of 4 m which would allow natural light through rectangular or arched windows, sometimes on the one side and sometimes on both sides of them. He also defined the minimum space per student to 0.90-1.25 $m^2$. Finally, he suggested the application of natural ventilation and heating systems. The number of schools that were built was limited, since the financial resources were not enough and with the reformation law of 1911 their construction stopped completely (Marmaridou, 2013).

In June 1930, the Minister of Education, G. Papandreou, wanted to increase the number of schools and signed a 1000000-pound loan in Stockholm with the company Aktiebolaget Kreuger and Roll. Since then, the Greek state took over the construction of school buildings. That was the period when many Greek architects were applying the rules of the Modern architectural movement in large-scale school buildings, amongst other projects of theirs, which were occasionally decorated with elements of local architecture (Marmaridou, 2013).

After 1960, with the constitution of the "Organization of School Buildings" of Greece, the production of schools got industrialized, because of the need for fast reconstruction after the Second World War and any kind of cultural, ideological or morphological factor was no longer being taken into account. The school buildings in Greece fell into two categories at the time. The first included those erected before 1960 which were mainly built with stone and had wooden roofs. The second included those built after 1960 according to the "Organization of School Buildings" regulations. The schools were built uniformly concerning the proportions of the classrooms, the corridors as well as the rest of the spaces and regardless of the climatic zone in which they belonged to although the country presented climatic diversity (Marmaridou, 2013).

It was not until 1979, with the thermal insulation regulation that the thermal insulation of buildings started being considered and the country got divided into three climatic zones. Still, the regulation aimed solely at reducing heat loss during the winter, while it would not take into account the energy consumption during the summer. Furthermore, it only concerned the new buildings, without any care for the existing ones (T.O.T.E.E., 2017).

In Greece after the 90's, it was considered necessary to study the climatic conditions prevailing in each area so that the building would be able to respond as well as possible to the needs of users. In fact, in some cases, the microclimate had to be studied (Tsiouka, 2018).

In the framework of the Directive 91/2002/EC of the European Parliament and of the Council "On the Energy Efficiency of Buildings", Greece had the obligation to comply until January 2006 with the issuance and implementation of a relevant legislation. The first step was the issuance of the Law 3661/2008-Government Gazette A΄89 "Measures to reduce the Energy Consumption of Buildings and other provisions". According to the law, there was the obligation to issue a relevant "Regulation for the Energy Efficiency of Buildings" (K.EN.A.K.) which, among other things, should specify the minimum technical specifications and energy efficiency requirements of new and radically renovated buildings in Greece, as well as the methodology for calculating their energy efficiency (semi-fixed monthly step status of the European Standard ELOT EN ISO 13790 and other relevant standards). In specific, it requires the determination of the annual energy consumption for heating, cooling and lighting, but not only through determining the "static" coefficients. It additionally includes in the calculations items such as: active solar systems, passive solar systems, photovoltaic cells, natural ventilation, sun protection, RES etc (T.O.T.E.E., 2017).

The Directive 91/2002/EC was amended by the Directive 31/2010/EC and Greece's compliance with the new directive took place with the issuance of the new law 4122/2013-Government Gazette A'42 "Energy Efficiency of Buildings-Harmonization with the Directive 2010/31/EU of the European Parliament and of the Council and other provisions". All the technical instructions are available in the T.O.T.E.E. 20701/2017 guides, issued by the Technical Chamber of Greece (T.O.T.E.E., 2017).

With the Law 4602/2019-Government Gazette A'45 concerning the "Research, exploitation and management of the geothermal potential of the country, establishment of the Hellenic Authority for Geological and Mineral Surveys, ownership separation of natural gas distribution networks and other provisions" which came into force on 09.03.2019, there is a series of changes in the energy efficiency standards that have to be met by new buildings in the public and private sector. In specific, from 01.01.2021 all new buildings must be buildings with almost zero energy consumption. By decision of the Minister of Environment and Energy, special cases of buildings were determined, for which the cost-benefit analysis for the economic life cycle of a specific building has a negative result. Those buildings are exempted from this obligation. Furthermore, each new, almost zero energy consumption building or each new that can be exempted from the above obligation and each radically renovated one, require a prerequisite for the issuance of each new building permit from 01.01.2020. They require an Energy Efficiency Study (EES) which is submitted to the competent Building Service. This study must document that the building meets the technical specifications and minimum energy efficiency requirements (T.O.T.E.E., 2017).

#### 1.2.1.3 School Buildings of the era 1928-1932

As the Greek state was passing from the 19th to the 20th century, the society started acquiring a more urban and industrial character. The government of Venizelos took over the urban modernization of Greece according to the western standards of Capitalism and liberal bourgeois democracy and amongst others, it tried to reform the educational system through a proposal formed in 1913. It was not until the reformations of 1917 though, with the introduction of the vernacular in schools, and later, with the reformations of 1929 that the approach became more complete (Marmaridou, 2013).

The topic of the construction of school buildings in the Greek state was developed initially a bit more independently, as it was faced as a factor that did not play an important role in the attempt of a holistic educational reformation. Gradually though, it became clear that this topic also demanded a more systematic approach, as the direct correlation of a building with the effectiveness of teaching was becoming more and more obvious and issues of hygiene demanded arrangement. As a result, the establishment of an “Architectural Service for School Buildings” was proposed in 1898, but it was not until 1911 that a bill that made the creation of a separate architectural study for each new school building obligatory, was submitted. Those studies had to follow the demands of the location concerning the building's typology and morphology and at the same time certain compositional standards. After 1920, the Architectural Service for School Buildings of the Greek Ministry of Education produced a great number of architectural studies for new school buildings, as well as for the reformation and repair of existing ones. The high demands though, did not allow for architectural studies according to the local factors, in most cases (Marmaridou, 2013).

From 1928 and according to the “Construction of school buildings in the whole Greek state” program, approximately 3000 of those were built. Most of them were based on revised typologies of the period 1920-28, while a certain number of those were modern architectural compositions of architects working at the Architectural Service for School Buildings of the Greek Ministry of Education. The school building became a fully structured concept and the school an institution in the service of the state. The Boys High School of Drama (1928-32) also belongs to the logic of this period (Marmaridou, 2013).

Along with the above developments, there were certain developments in the Greek architectural expression as well, which of course affected the construction in the educational sector. The prevailing architectural idiom until the second decade of the 20th century was that of Neoclassicism and can be acknowledged in 358 school buildings constructed during that period. Some eclectic architectural expressions could also be spotted starting from the last decade of the 19th century, while architectural quests within the folk tradition of the Greek state were also taking place. This was especially true after the Asia Minor Catastrophe and the exchange of populations that initiated a more general movement of research in the recent and not so recent past of the foundations for the construction of a unified national culture. From the second decade of the 20th century the Modern movement influence was also starting to find its place in the architectural expression of Greece and especially in the school building constructions, as its standards seemed to meet the requirements of such buildings for achieving high functionality and saving time and money (use of reinforced concrete) (Marmaridou, 2013).

The constructed school buildings varied in size and usually had one or two storeys and more rarely three. The building plan provided for up to fourteen classrooms arranged in a row, with the entrance usually placed in a vestibule between two classrooms. It also provided for rooms for other activities, such as offices, toilets, gyms, locker rooms, libraries, physics-chemistry laboratories, etc. The toilets and the changing rooms were always placed either on the ground floor or the basement and usually close to the gym that could be either part of the main building or an independent one. The spaces that stored the heating systems, as well as any auxiliary spaces, were located underground, in spaces that met the necessary ventilation and lighting standards. Moreover, schools had to also adapt to the climatic conditions of each place. Thus, in cold and wind-exposed areas the classrooms were designed to face south and the corridors with their windows to the north, while in areas with a dry and mild climate the classrooms would face north and the corridors to the south, having the form of a balcony or a portico (Marmaridou, 2013). The structural frame of the building was made of reinforced concrete, while the filling walls were either made of masonry with high thermal insulation capabilities, or of double brick wall with a gap. There was a second alternative, with the stone masonry walls being the vertical bearing elements, while reinforced concrete was used for the horizontal ones, i.e. slabs and beams. Finally, wherever the conditions allowed for it, it was proposed to build insulated roofs of reinforced concrete that could be used as recreation areas by students. In contrast, in mountainous areas, the solution of the wooden roof with tiles was chosen, underneath which a slab of reinforced concrete was often added. Finally, for the provision of uniform lighting, especially in the classrooms, a longitudinal arrangement of openings was designed (Marmaridou, 2013).

### 1.2.2 Current Greek Standards for Energy Efficiency of Buildings

Currently in Greece, every new or radically renovated construction has to follow the instructions of the "Regulation for the Energy Efficiency of Buildings" (K.EN.A.K.), as already mentioned. All its technical instructions are available in the T.O.T.E.E. 20701/2017 guides, issued by the Technical Chamber of Greece. Moreover, these guides are updated and state that from 01.01.2020, all new buildings must be buildings with almost zero energy consumption, with a few exceptions. Furthermore, each one of the new or radically renovated buildings requires an Energy Efficiency Study (EES) for the issuance of each new building permit. This study documents that each building meets the technical specifications and minimum energy efficiency requirements (Government Gazette A'45, 2019).

According to the Government Gazette A’42 (2013) some categories of buildings are excluded from the application of K.EN.A.K. and the cultural heritage monuments are amongst them. Still, little by little, more announcements for energy upgrades get published for this category of buildings, as well. This happens because of a need to solve issues concerning energy efficiency and thermal and visual comfort.

In the T.O.T.E.E. (2017) guide, one can find the specifications for the national parameters that are required for the application of the methodology of calculations of the energy efficiency of buildings, as it is defined in the "Regulation for the Energy Efficiency of Buildings" (K.EN.A.K.). The parameters are shaped according to the technologies applied in the construction of buildings (construction materials and electromechanical systems), the operating profile of the buildings, the internal operating conditions and the specific climatic conditions for each area. The parameters, apart from supporting the methodology for calculating the energy efficiency of buildings, are also facilitating and defining the framework of the process of inspecting buildings and heating, cooling and air conditioning systems. On top of that, for each building, depending on its end use, specific parameters that have to do with the human factor and mainly with the internal profits in which it participates, are taken into account. The following sections present the parameters in categories.

#### 1.2.2.1 Specifications for the operating conditions per end use of a building or part of a building

According to the T.O.T.E.E. (2017) guide, these specifications have to do with the opening hours, the desired room temperatures, the desired relative humidity, the fresh air requirements per building use, the water consumption, the mains water temperature and the internal gains from users and appliances. Table 1 shows that the secondary school buildings operate for 8 hours on weekdays and from the 9th of September till the 9th of May.

Table 1 Typical opening hours of buildings per use (source: T.O.T.E.E., 2017)

| Basic building categories | Uses of buildings or thermal zones | Operating hours | Operating days per week | Operating period in months |
|---|---|---|---|---|
| Education | Kindergarden | 8 | 5 | 9 (Sept.-May) |
| | Primary education, secondary education | 8 | 5 | 9 (Sept.-May) |
| | Higher education, classroom | 13 | 5 | 10(Sept-June) |
| | Tutoring, conservatory | 7 | 5 | 9 (Sept.-May) |
| Temporary Accommodation | Annual-operation hotel | 24 | 7 | 12 |
| | Summer-operation hotel | 24 | 7 | 7 (Apr-Oct) |
| | Winter-operation hotel | 24 | 7 | 8 (Sept-Apr) |
| | Annual-operation guest house | 24 | 7 | 12 |
| | Summer-operation guest house | 24 | 7 | 7 (Apr-Oct) |
| | Winter-operation guest house | 24 | 7 | 8 (Sept-Apr) |
| | Boarding school and dormitory | 24 | 7 | 12 |
| | Hotel bedroom, boarding school room etc. | 12 | 7 | Depending on use |
| | Common area of hotel, boarding school, etc. | 24 | 7 | Depending on use |

Table 2 shows that for the calculation of the energy efficiency of buildings, the temperature value for the winter period should be set to 20 °C, while for the summer period to 26 °C. Moreover, the heat that is released per user of a secondary school building is 80 $W.m^{-2}$, as Table 3 shows.

Table 2 Determined values of temperature and relative humidity of interiors for the calculation of the energy efficiency of buildings (source: T.O.T.E.E., 2017)

| Uses of buildings or thermal zones | Temperature [°C] | | Relative Humidity [%] | |
|---|---|---|---|---|
| | Winter period | Summer period | Winter period | Summer period |
| Theater, cinema | 20 | 26 | 35 | 50 |
| Concert area | 20 | 26 | 35 | 50 |
| Exhibition space, museum | 20 | 23 | 35 | 50 |
| Conference room, amphitheater, courtroom | 20 | 26 | 35 | 45 |
| Bank | 20 | 26 | 35 | 45 |
| Multipurpose hall | 20 | 26 | 35 | 50 |
| Indoor gym, indoor swimming pool | 18 | 25 | 35 | 45 |
| Corridors and other common auxiliary spaces | 18 | 26 | 35 | 50 |
| Bathroom (shared) | 22 | 26 | 40 | 50 |
| Kindergarden | 20 | 26 | 35 | 45 |
| Primary education, Secondary education | 20 | 26 | 35 | 45 |
| Higher education, Classroom | 20 | 26 | 35 | 45 |
| Tutoring, Conservatory | 20 | 26 | 35 | 45 |

Table 3 User heat released per building use for the calculation of its energy efficiency (source: T.O.T.E.E., 2017)

| Uses of buildings or thermal zones | Thermal power per person [W / person] | Thermal power per unit of built area [W / m2] | average attendance rate |
|---|---|---|---|
| Kindergarden | 80 | 40 | 0,16 |
| Primary education,<br>Secondary education | 80 | 40 | 0,18 |
| Higher education,<br>classroom | 80 | 40 | 0,32 |
| Tutoring, conservatory` | 80 | 44 | 0,16 |

### 1.2.2.2 Parameter specifications for building elements

As stated in the T.O.T.E.E. (2017) guide, these parameters may refer to technical characteristics and thermophysical properties of building materials, typologies of masonry, typologies of openings, thermal bridges, shading, passive systems etc.

The specifications that can be applied in the simulations can be seen on the following tables. Table 4 gives the maximum allowed values of the thermal transmittance coefficient of the various structural elements per climatic zone in case of a radical renovation of an existing building. The values of the “Zone D’” column are the ones that are used in this study.

Table 4 Maximum allowed values of the thermal transmittance coefficient of the individual structural elements per climatic zone in case of radical renovation of an existing building (source: T.O.T.E.E., 2017)

| **Structural element** | **Maximum permissible coefficient of thermal transmittance U [W/(m²·K)]** | | | |
|---|---|---|---|---|
| | **Zone A'** | **Zone B'** | **Zone C'** | **Zone D'** |
| Outdoor horizontal or inclined surface in contact with exterior air (roof) | 0,50 | 0,45 | 0,40 | 0,35 |
| Exterior wall in contact with the exterior air | 0,60 | 0,50 | 0,45 | 0,40 |
| Floor in contact with the exterior air | 0,50 | 0,45 | 0,40 | 0,35 |
| Horizontal or inclined roof in contact with a closed unheated space | 1,20 | 0,90 | 0,75 | 0,70 |
| Wall in contact with a closed unheated space | 1,50 | 1,00 | 0,80 | 0,70 |
| Floor in contact with a closed unheated space | 1,20 | 0,90 | 0,75 | 0,70 |
| Horizontal or inclined roof in contact with the ground | 1,20 | 0,90 | 0,75 | 0,70 |
| Wall in contact with the ground | 1,50 | 1,00 | 0,80 | 0,70 |
| Floor in contact with the ground | 1,20 | 0,90 | 0,75 | 0,70 |
| Window frame in contact with the exterior air | 3,20 | 3,00 | 2,80 | 2,60 |
| Window frame without glazing in contact with the outside air | 3,20 | 3,00 | 2,80 | 2,60 |
| Glass facade of a building non-opening or partially-opening in contact with exterior air | 2,20 | 2,00 | 1,80 | 1,80 |
| Window frame in contact with an unheated space | 5,70 | 5,20 | 4,80 | 4,40 |
| Window frame without glazing in contact with an unheated space | 5,70 | 5,20 | 4,80 | 4,40 |
| Glass facade of a building non-opening or partially-opening in contact with an unheated space | 4,00 | 3,60 | 3,10 | 2,90 |

Table 5 gives some typical values of thermal transmittance coefficients of windows without any external protective sheets in [$W.m^{-2}.K^{-1}$] which can be referenced if the existing windows offer no relevant information.

Table 5 Typical values of thermal transmittance coefficients of windows $U_w$ and doors in [$W.m^{-2}K^{-1}$] without external protective sheets (source: T.O.T.E.E., 2017)

| Frame Type | Frame Percentage $F_f$ | Single Glazing | Double Glazing | | Double Glazing with low E membrane | |
|---|---|---|---|---|---|---|
| | | | with air gap 6 mm | with air gap 12 mm | with air gap 6 mm | with air gap 12 mm |
| | [ % ] | [W/(m².K)] | [W/(m².K)] | [W/(m².K)] | [W/(m².K)] | [W/(m².K)] |
| Metallic frame without thermal break | 20% | 6,0 | 4,1 | 3,7 | 3,6 | 3,0 |
| | 30% | 6,1 | 4,5 | 4,1 | 4,0 | 3,5 |
| | 40% | 6,2 | 4,8 | 4,5 | 4,4 | 4,0 |
| Metallic frame with thermal break of 12 mm | 20% | – | 3,6 | 3,2 | 3,1 | 2,6 |
| | 30% | – | 3,5 | 3,2 | 3,1 | 2,7 |
| | 40% | – | 3,5 | 3,2 | 3,0 | 2,8 |
| Metallic frames with thermal break of 24 mm | 20% | – | 3,4 | 3,0 | 3,0 | 2,3 |
| | 30% | – | 3,3 | 3,0 | 2,9 | 2,4 |
| | 40% | – | 3,2 | 3,0 | 2,9 | 2,4 |
| Synthetic frame | 20% | – | 3,4 | 3,0 | 2,9 | 2,2 |
| | 30% | – | 3,3 | 2,9 | 2,9 | 2,3 |
| | 40% | – | 3,2 | 2,9 | 2,9 | 2,4 |
| Wooden frame | 20% | 5,0 | 3,2 | 2,9 | 2,7 | 2,1 |
| | 30% | 4,7 | 3,1 | 2,8 | 2,6 | 2,1 |
| | 40% | 4,3 | 3,0 | 2,7 | 2,6 | 2,1 |
| Double frame (wooden)* | 20% | 2,4 | – | – | – | – |
| | 30% | 2,3 | – | – | – | – |
| | 40% | 2,1 | – | – | – | – |
| Double frame (aluminum )* | 20% | 3.9 | – | – | – | – |
| | 30% | 3.6 | – | – | – | – |
| | 40% | 3.3 | – | – | – | – |

| Exterior doors without glazing [W/(m².K)] | | |
|---|---|---|
| Material | In contact with the exterior air | In contact with an unheated space |
| Metal | 6,0 | 4,0 |
| Synthetic | 3,5 | 2,7 |
| Wood | 3,5 | 2,7 |

Going on to Table 6, there can be seen some typical reflectance and absorptance values of the solar radiation for certain materials, while Table 7 gives the emissivity values of the thermal radiation for certain materials.

Table 6 Typical values of reflectance and absorptance of solar radiation (source: T.O.T.E.E., 2017)

| Surface description | Reflectance | Absorptance |
|---|---|---|
| **Vertical building ele  ents** | | |
| White plaster, smooth surface | 0,70 | 0,30 |
| Light-colored plaster (eg light gray, beige, yellow, pink or light blue) | 0,60 | 0,40 |
| Medium shade plaster (eg gray, beige, dark ocher, salmon) | 0,40 | 0,60 |
| Dark plaster (eg dark oil, brown, gray) | 0,20 | 0,80 |
| Visible brickwork or stonework | 0,20 | 0,80 |
| Visible light brick or stonework | 0,40 | 0,60 |
| Glossy metal surfaces (eg aluminum foil) | 0,80 | 0,20 |
| Opaque glass front part (eg glass coated panels) | 0,40 | 0,60 |
| Green facade (with evergreen plants) | 0,30 | 0,70 |
| **Horizontal building elements (ceilings)** | | |
| Red tile | 0,40 | 0,60 |
| Very dark roof coatings (tarpaulins) | 0,10 | 0,90 |
| Dark roofs coatings (eg coating with slate slabs, asphalt tiles) | 0,20 | 0,80 |
| Light-colored roof coatings (eg paving slabs, tarpaulins with | 0,35 | 0,65 |
| Quartz tile | | |
| Glossy metal surfaces (eg reflective films) | 0,80 | 0,20 |
| Gravel | 0,70 | 0,30 |
| Green roof | 0,30 | 0,70 |

Table 7 Emissivity values of the thermal radiation (source: T.O.T.E.E., 2017)

| Surface description | Emissivity |
|---|---|
| Usual building material | 0,80 |
| Glass | 0,90 |
| Glossy metal surfaces | 0,20 |
| Gravel | 0,30 |
| Green roof or Green wall (with evergreen plants) | 0,80 |

#### 1.2.2.3 Parameter specifications for the technical systems of heating, cooling, air conditioning and domestic hot water

These parameters concern standard efficiencies of heating, cooling and domestic hot water production systems, losses of distribution systems, performance of air conditioning auxiliary systems (circulators, pumps, room thermostats, etc.), efficiency of heat recovery systems and air conditioning terminal units, etc. (T.O.T.E.E., 2017).

In the energy simulations of this study with Ladybug 0.0.69 and Honeybee 0.0.66 Legacy Plug-ins, an ideal air loads system is used. By definition, as stated in the Ladybug Tools Forum (2021), this system does not include a coefficient of performance (COP). It can only give information about the heat removed or added to a zone by the system and not the values of electricity or fuel that it might take to add or remove this heat.

Still, the focus of the study is on minimizing the heating, cooling and electric light demands and maximizing the visual and thermal comfort through passive methods, so that the suggested HVAC system will have as low demands as possible. So, the focus of the study is on the implementation of passive strategies and not on the calculation of an actual HVAC system. This purpose can be served well by an ideal air loads system.

#### 1.2.2.4 Parameter specifications for electrical, electronic and technical systems

These parameters may refer to the efficiency of lighting systems, desired levels of lighting per use of spaces, utilization of natural light and efficiency of cogeneration systems of electricity & heat. They might also refer to efficiency of renewable energy systems for buildings (solar panels, geothermal, solar air conditioning, photovoltaics, etc.), energy consumption from engines, pumps, circulators, etc., efficiencies of central and local automatic control devices and energy management in buildings (thermostats, inverters, etc.) (T.O.T.E.E., 2017).

Table 8 shows that the suggested general lighting levels for school buildings include a 300 lx illuminance at a 0.8 m-height reference plane. Furthermore, the suggested UGR value is 19 and the Uniformity equal to 0.6. Finally, the minimum Luminous Efficiency of lighting systems according to the guide has to be 60 $lm.W^{-1}$.

Table 8 General (non-specific) lighting level of the reference building per building use (source: T.O.T.E.E., 2017)

| Uses of buildings or thermal zones | Lighting level [ℓx] | measurement reference level | Unified Glare Rating UGR | Lighting uniformity (min / average price) Uo |
|---|---|---|---|---|
| etc | | | | |
| Kindergarden | 300 | 0,8 | 19 | 0,6 |
| Primary education, Secondary education | 300 | 0,8 | 19 | 0,6 |
| Higher education, Classroom | 500 | 0,8 | 19 | 0,6 |
| Tutoring, Conservatory | 500 | 0,8 | 19 | 0,6 |

### 1.2.3 European Daylight Standard (CEN - EN 17037)

Daylight is considered the preferred method for the illumination of the majority of indoor spaces for multiple reasons. It can offer the necessary illuminance and visual comfort levels when handled correctly. It can also offer the advantages of the exposure to the sunlight to the occupants, as well as views to the outside. Last but not least, it can reduce the energy invested in electric light. So, for all those reasons the European Daylight Standard specifies certain methods for achieving a good balance of daylight indoors, and for providing an adequate view out. Furthermore, it gives recommendations on the duration of the exposure to the sunshine within occupied rooms, as well as on how to limit glare. These methods can be applied to all spaces that may be regularly occupied by people. This study will focus on the illuminance and visual comfort target levels (CEN, 2018).

Starting with the daylight provision calculation, the Standard offers two different methods. The first gives values for target daylight factors (DT) and minimum target daylight factors (DTM) to be achieved depending on the given site. The second one, which is chosen in this study, provides us with the steps for the calculation of illuminance levels on the reference plane of our choice using climatic data for the given site and an adequate time step. As it can be seen, Table 9 gives values for target illuminances and minimum target illuminances that are to be achieved. According to it, a space is considered to provide adequate daylight if a target illuminance level is achieved across a fraction of the reference plane within a space for at least half of the daylit hours (CEN, 2018).

Table 9 Recommendations of daylight provision by daylight openings in vertical and inclined surfaces (EN, 2018)

| Level of recommendation for vertical and inclined daylight opening | Target illuminance $E_T$ lx | Fraction of space for target level $F_{plane,\%}$ | Minimum target illuminance $E_{TM}$ lx | Fraction of space for minimum target level $F_{plane,\%}$ | Fraction of daylight hours $F_{time,\%}$ |
|---|---|---|---|---|---|
| Minimum | 300 | 50 % | 100 | 95 % | 50 % |
| Medium | 500 | 50 % | 300 | 95 % | 50 % |
| High | 750 | 50 % | 500 | 95 % | 50 % |

The second criterion refers to the maximum acceptable glare values and in specific, it uses the Daylight Glare Probability (DGP) method to assess protection from glare for spaces where the activities are relevant to reading, writing, or using display devices and the occupants are not able to choose their position and viewing direction. This method can be applied to a space with vertical or inclined daylight openings, but it is not applicable to a space with horizontal ones. The DGP-threshold values, as it can be seen on Table 10, must not exceed a certain fraction of the reference usage time (CEN, 2018).

Table 10 Different proposed levels of threshold DGP for glare protection (EN, 2018)

| Level of recommendation for glare protection | $DGP_{e < 5\%}$ |
|---|---|
| Minimum | 0,45 |
| Medium | 0,40 |
| High | 0,35 |

### 1.2.4 Current European Standard of lighting requirements of indoor workplaces which meet the needs for visual comfort and performance

The CEN - EN 12464-1 European Standard specifies the lighting requirements for indoor workplaces, so that a high visual comfort is ensured. According to the CEN/CENELEC Internal Regulations, amongst other countries, the national standards organization of Greece is bound to implement it, as well (EN, 2011).

Table 11 shows in detail what the lighting requirements for interior spaces, tasks and activities in educational buildings are. In specific, it gives, amongst others, the values of the minimum demanded average illuminance of a grid of sensors of the space studies, as well as of the Unified Glare Rating for each type of interior space, task, or activity.

Table 11 Lighting requirements for interiors (areas), tasks and activities (EN, 2011)

| 6.2 | Educational buildings | | | | |
|---|---|---|---|---|---|
| Ref. no. | Type of interior, task or activity | $\bar{E}_m$ lx | $UGR_L$ - | $R_a$ - | Remarks |
| 6.2.1 | Classrooms, tutorial rooms | 300 | 19 | 80 | Lighting should be controllable. |
| 6.2.2 | Classroom for evening classes and adults education | 500 | 19 | 80 | Lighting should be controllable. |
| 6.2.3 | Lecture hall | 500 | 19 | 80 | Lighting should be controllable. |
| 6.2.4 | Black board | 500 | 19 | 80 | Prevent specular reflections. |
| 6.2.5 | Demonstration table | 500 | 19 | 80 | In lecture halls 750 lx. |
| 6.2.6 | Art rooms | 500 | 19 | 80 | |
| 6.2.7 | Art rooms in art schools | 750 | 19 | 90 | $T_{CP} \geq 5000$ K. |
| 6.2.8 | Technical drawing rooms | 750 | 16 | 80 | |
| 6.2.9 | Practical rooms and laboratories | 500 | 19 | 80 | |
| 6.2.10 | Handicraft rooms | 500 | 19 | 80 | |
| 6.2.11 | Teaching workshop | 500 | 19 | 80 | |
| 6.2.12 | Music practice rooms | 300 | 19 | 80 | |
| 6.2.13 | Computer practice rooms (menu driven) | 300 | 19 | 80 | DSE-work: see 4.11. |
| 6.2.14 | Language laboratory | 300 | 19 | 80 | |
| 6.2.15 | Preparation rooms and workshops | 500 | 22 | 80 | |
| 6.2.16 | Entrance halls | 200 | 22 | 80 | |
| 6.2.17 | Circulation areas, corridors | 100 | 25 | 80 | |
| 6.2.18 | Stairs | 150 | 25 | 80 | |
| 6.2.19 | Student common rooms and assembly halls | 200 | 22 | 80 | |
| 6.2.20 | Teachers rooms | 300 | 19 | 80 | |
| 6.2.21 | Library: bookshelves | 200 | 19 | 80 | |
| 6.2.22 | Library: reading areas | 500 | 19 | 80 | |
| 6.2.23 | Stock rooms for teaching materials | 100 | 25 | 80 | |
| 6.2.24 | Sports halls, gymnasiums, swimming pools (general use) | 300 | 22 | 80 | For more specific activities, the requirements of EN 12193 shall be used |
| 6.2.25 | School canteens | 200 | 22 | 80 | |
| 6.2.26 | Kitchen | 500 | 22 | 80 | |

Last but not least, the EN 12464-1 European Standard gives information about the demanded Uniformity levels of the different types of interior spaces, tasks or activities, as it can be seen on Table 12.

Table 12 Standard values for lighting of indoor and outdoor workplaces and sports facility lighting (EN, 2011)

| **Educational premises** | | $\bar{E}_m$ | $UGR_L$ | $U_O$ | $R_a$ |
|---|---|---|---|---|---|
| Nursery school, play school | Play rooms | 300 | 22 | 0.40 | 80 |
| | Nurseries | 300 | 22 | 0.40 | 80 |
| | Handicraft rooms | 300 | 19 | 0.60 | 80 |
| Educational buildings | Classrooms, tutorial rooms | 300 | 19 | 0.60 | 80 |
| | Classrooms for evening classes and adults education | 500 | 19 | 0.60 | 80 |
| | Lecture halls | 500 | 19 | 0.60 | 80 |
| | Black, green wallboards and whiteboards | 500 | 19 | 0.70 | 80 |
| | Demonstration tables | 500 | 19 | 0.70 | 80 |
| | Art rooms | 500 | 19 | 0.60 | 80 |
| | Art rooms in art schools | 750 | 19 | 0.70 | 90 |
| | Technical drawing rooms | 750 | 16 | 0.70 | 80 |
| | Practical rooms and laboratories | 500 | 19 | 0.60 | 80 |
| | Handicraft rooms | 500 | 19 | 0.60 | 80 |
| | Teaching workshops | 500 | 19 | 0.60 | 80 |
| | Music practice rooms | 300 | 19 | 0.60 | 80 |
| | Computer practice rooms (menu driven) | 300 | 19 | 0.60 | 80 |
| | Language laboratories | 300 | 19 | 0.60 | 80 |
| | Preparation rooms and workshops | 500 | 22 | 0.60 | 80 |
| | Entrance halls | 200 | 22 | 0.40 | 80 |
| | Circulation areas, corridors | 100 | 25 | 0.40 | 80 |
| | Stairs | 150 | 25 | 0.40 | 80 |
| | Student common rooms and assembly halls | 200 | 22 | 0.40 | 80 |
| | Teachers rooms | 300 | 19 | 0.60 | 80 |
| | Library: bookshelves | 200 | 19 | 0.60 | 80 |
| | Library: reading areas | 500 | 19 | 0.60 | 80 |
| | Stock rooms for teaching materials | 100 | 25 | 0.40 | 80 |
| | Sports halls, gymnasiums, swimming pools (general use) | 300 | 22 | 0.60 | 80 |
| | School canteens | 200 | 22 | 0.40 | 80 |
| | Kitchens | 500 | 22 | 0.60 | 80 |

# 2. METHOD

## 2.1 Overview

### 2.1.1 Used material

The used material of the research includes:

- The book “Boys’ High School of Drama” edited by Vasileiadis Ilias in 2010 for information concerning the history of the school building and the possible, allowed interventions
- The master thesis “Restoration of the “Boys’ High School” of Drama - Assessment of its bearing capacity – Interventions” written by Konstantinos Paraschou in 2010 for the department of civil engineering of the Aristotle University of Thessaloniki. The retrieved information concerns:
  - The geometry and orientation of the building
  - The different types of constructions, their thicknesses and their boundary conditions
  - The different materials used in the constructions
  - Creation of the building’s thermal zones
- In-situ observations. The retrieved information concerns:
  - Equipment loads per area [$W.m^{-2}$]
  - Infiltration rate per area [$m^3.s^{-1}.m^{-2}$] at 4 Pa
  - Internal gains based on heat emitted from luminaires per area [$W.m^{-2}$]
  - Number of people per area
  - Hourly occupancy schedules for the year 2018-2019 for each one of the thermal zones
  - Hourly lighting schedules for each one of the thermal zones
  - Hourly equipment schedules for each one of the thermal zones
- Energy and daylight Greek and European standards. The retrieved information concerns:
  - School operating hours
  - Summer and winter temperature demands
  - Metabolic rates of the occupants
  - Maximum allowed thermal transmittance coefficients (U-values)
  - Transmittance, reflectance, absorptance typical values of solar radiation of materials

- Emissivity typical values of thermal radiation of materials
    - Recommendations of daylight provision through daylight openings
    - Different proposed levels of threshold DGP for glare protection
    - Lighting requirements for interiors (areas), tasks and activities
    - Infiltration schedules
- The EnergyPlus, the Masea, and the OpenStudio databases, as well as the IES Apache-Tables (EnergyPlus, 2017; IES Virtual Environment, 2012; MASEA, 2022; OpenStudio, 2020). The retrieved information concerns:
    - Properties of the different materials for the energy simulation such as roughness, thickness, conductivity, density, specific heat, thermal absorptance, solar absorptance, visible absorptance, U-value, Solar Heat Gain Coefficient and Visible Transmittance
- EnergyPlus weather data and location data from the web (EnergyPlus Weather Data, 2021)

All the above-mentioned material is necessary for the creation of accurate and realistic models for the conduction of dynamic energy and daylight simulations, whose results are according to the current energy and daylight demands of the Greek standards for school buildings. Furthermore, the accuracy and detail that is attempted will also give information on the capabilities of the Ladybug 0.0.69 and Honeybee 0.0.66 Legacy Plug-ins in handling such complicated models.

### 2.1.2 Approach

After the topic and the tools that it would be processed with were chosen, an in-situ visit was made for the acquisition of all the information that could be acquired for the set-up of the model, together with a study of the historical facts of the school building. Next, the relevant Greek and European standards were studied for input guidance and energy and daylight demand ranges and the thermal zones of the building were defined.

Then, the 3-D model of the existing situation was generated in Rhino. It was afterwards transferred to Grasshopper through the Ladybug 0.0.69 and Honeybee 0.0.66 Legacy Plug-ins. Specifically, in Grasshopper, all the different materials, constructions, and schedules were created and saved in the appropriate libraries. Then, all the different honeybee surfaces were created and grouped into the defined thermal zones. These were also assigned all the necessary attributes (surface types, boundary conditions, EnergyPlus constructions, Radiance materials, internal masses, thermal zone loads and schedules) (Honeybee Energy Modeling, 2016; Mackey, 2014).

As a next step, the honeybee zones were assigned to the OpenStudio simulation engine together with the weather file, the analysis period, the timestep of the simulation, the holiday days, the terrain type, the solar distribution type and the simulation outputs, as stated in the Ladybug Tools Forum (2021).

Then, the yearly energy simulation followed, and the results were post-processed in order to acquire the annual heating, cooling and electric light loads for each one of the thermal zones, as well as for the whole conditioned volume. Furthermore, the thermal comfort, and in specific, the percentage of the occupancy time that the conditions in the whole conditioned volume were considered comfortable, was calculated through the adaptive comfort calculator of the Ladybug 0.0.69 and Honeybee 0.0.66 Legacy Plug-ins (Ladybug Tools Forum, 2021). As already mentioned, since the adaptive comfort model is used only for free-running buildings, the results are used to give an impression of a relevant exploration and are considered inconsistent.

The daylight simulation came up next, and it was set-up, as stated in the Ladybug Tools Forum (2021), by assigning to the daylight simulation engine the honeybee zones, the weather file, a grid of sensors (every 1 m) for each one of the thermal zones and finally the right radiance and daysim parameters.

The annual daylight simulation took place, the chosen daylight metrics' results were post-processed and the spatial daylight autonomy (sDA), the hourly average illuminance and the hourly average uniformity were obtained for each thermal zone, for a no-shading scenario. A dynamic-shading scenario was applied to two selected thermal zones, and the daylight glare probability (DGP) was obtained for a defined point in each one of them, as well as the above-mentioned daylight metrics with the exception of the sDA, which is calculated only for no-shading scenarios (Ladybug Tools Forum, 2021).

After the assessment of the existing situation, a number of passive strategies for the improvement of the above results were implemented and a parametric model was built. These interventions concerned two types of wall insulation, two types of floor and roof insulation, three different window retrofit options, whose creation process can be found in GitHub (2022), two different types of interior shades and the addition of light shelves. Moreover, the colour of the walls was altered from yellow to white stucco.

The next step was to run annual daylight simulations for each one of the two selected thermal zones and get the daylight metrics concerning the sDA, the hourly average illuminance, the hourly average uniformity and the daylight glare probability (DGP) for a defined point in each thermal zone. All metrics were calculated for a dynamic-shading scenario, with the exception of the sDA which is calculated only for no-shading scenarios (Ladybug Tools Forum, 2021). The DGP also gave results for both dynamic shading and no-shading scenarios. These simulations had twelve iterations each, as the insulation alternatives were considered to not affect the daylight results. After the simulations were completed, an electric light schedule was produced for each iteration of each one of the two thermal zones, which replaced the corresponding ones in the energy model set-up. The control type of these schedules was the “Always on during active occupancy hours with auto dimming” with a target illuminance of 300 lx for the space, in contrast to the “Always on during active occupancy hours” that was used for the current state (Ladybug Tools Forum, 2021).

The parametric energy model ran next with the help of the OpenStudio simulation engine and an iterator, and forty-eight possible models were produced. The annual heating, cooling and electric light loads for the whole conditioned volume, as well as for the two selected thermal zones of each iteration were then obtained. What was also obtained, was the percentage of the occupancy time that the conditions were considered comfortable, for each of the forty-eight cases of the whole conditioned volume through the adaptive comfort calculator. Again, the results are used to give an impression of a relevant exploration and are considered inconsistent.

Finally, a csv file was created for all the forty-eight iterations of the parametric model which included all the different applied passive strategies and all the energy and daylight outcomes of the whole building and of each one of the two selected thermal zones. It was then uploaded to the Design Explorer space exploration online tool, the alternatives were visualized in a user-friendly way, and the different performances were compared based on quantitative metrics (Design Explorer, 2019).

## 2.2 Research Questions

The first research question that this thesis is dealing with, has to do with the ways certain thermal and visual performance indicators of the whole school building and of the two chosen thermal zones could be improved through the application of combinations of passive strategies that are parametrically assessed through dynamic energy and daylight simulations within the Grasshopper interface. Concerning the thermal part in particular, the thesis is trying to find the best combinations of passive strategies through which the annual heating, cooling and electric light loads for the whole building and the two selected thermal zones during the occupancy hours of a school year could be decreased and at the same time the thermal comfort inside the whole building could be increased. In addition to that, concerning the visual part, the aim is to increase the hourly average uniformity and the hourly average illuminance metrics in a year, as well as the spatial daylight autonomy (sDA), and to decrease the daylight glare probability (DGP) metric, both for the whole building and the two selected thermal zones.

The second research question that the thesis is dealing with, has to do with the assessment of the efficiency of the Ladybug 0.0.69 and Honeybee 0.0.66 Legacy Plug-ins of the Grasshopper interface concerning their performance during the energy and daylight simulations of a high-detail model, both during single simulations as well as during iterative ones.

## 2.3 Energy and Daylight Models Set-up

### 2.3.1 Construction of the energy and daylight model for the simulations of the existing situation

#### 2.3.1.1 Building documentation from existing literature

The “Boys High School” of Drama, Greece was built in the city of Drama during the second government of Venizelos, between 1928-1932, according to the “Construction of school buildings in the whole Greek state” program, through which many other school buildings (approximately 3000) were also built and multiple reforms in the educational sector took place. Those reforms were an attempt to improve and implement the attempts of previous governments (1913 and 1917). The high school building under study was built by the Technical Services of the Ministry of Education of Greece. Its main architect was Mr. G. Pantzaris, its service director was Mr. N. Balanos and its contractor Mr. I. Kalogirou (Marmaridou, 2013).

The school was built in the northwest end of the city, far, at the time, from the city center (Figure 4). Its exact location is: Latitude: 41° 09' 10.19" N and Longitude: 24° 08' 50.28" E. It is adjacent to the National Stadium of Drama on its north and it is built in neo-Byzantine style. It has a strongly rationalistic character, as its form reveals its function, and it combines it with classical principles. It is developed on two levels. The elevated, by 1.50 m, ground floor and the first floor, with an initial coverage area of 1534.80 m$^2$. It is covered by a ceramic tiled, wooden roof and has two basements with a depth of around 2.50 m and a semi-basement with a depth of around 1.75 m from the surrounding ground area. Its average height, from the ground to the level of the roof of the main entrance, is 12 m. It is characterized by absolute symmetry both concerning the North-South axis in top view, as well as the middle, vertical axis of the south and north facades (Figure 5). In April 2008 it was designated as a cultural heritage monument according to the suggestion of M. Zannos of the Directorate of Architectural Heritage of the Ministry of Culture on 5/2/2007. Today the building houses the 1st High School of the city of Drama (Marmaridou, 2013).


*Figure 4 Map depicting the position of the high school in Drama (source: Institute of Geology & Mineral Exploration)*

*Figure 5 Photograph of the main, south façade from the period 1928-32 (source: "Restoration of the "Boys' High School" of Drama - Assessment of its bearing capacity – Interventions", 2010)*

According to the initial plans, the floor plan is organized in a T-form (Figures 6,7). In specific, it is comprised of a central zone which consists of the entrance area with two offices (Principals' offices) on either side of the entrance doors, while a bit further there can be found the starts of the two west-east corridors that lead to the classrooms. Opposite the main entrance, when entering, one can see the main marble staircase (Figures 8,9), which branches off after the point that it provides entrance to the school's amphitheater, which is placed on a mezzanine floor, and leads to the first-floor level. Underneath the amphitheater there used to be a space for the physics and chemistry labs, but today it is used as a storage room, instead. The side parts of the floor plan recede from the plane of the main, south facade and protrude slightly towards the rear, thus completing the T-shape in top view. In each one of those side parts, there can be found a secondary staircase in the background (Figures 10,11), opposite the two side entrances, together with an office room and a classroom at each one of the two levels (Marmaridou, 2013).

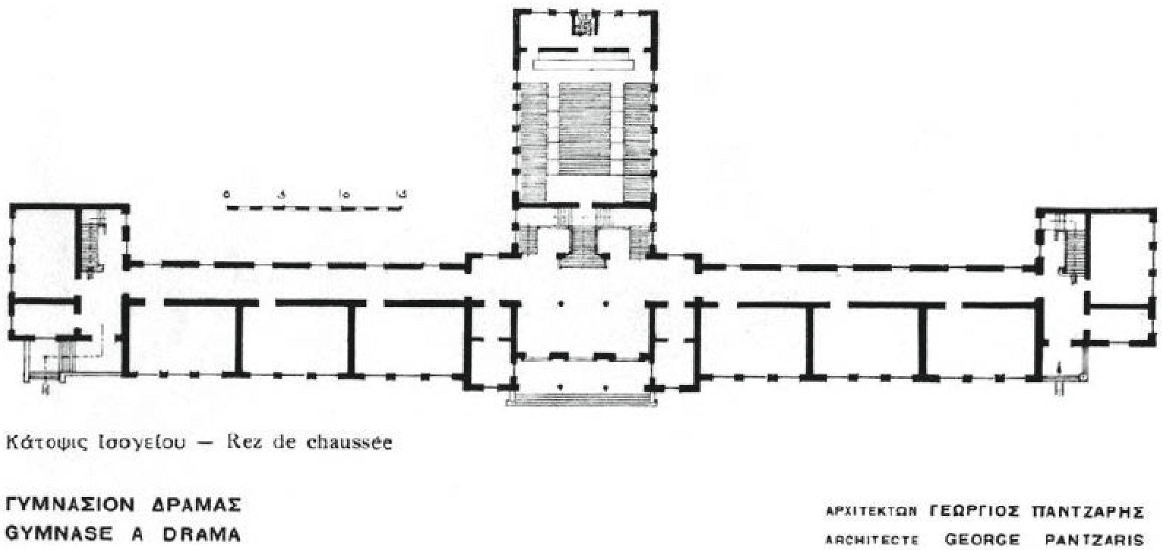


*Figure 6 Initial ground floor plan of the school (source: Pantzaris, 1928-32)*

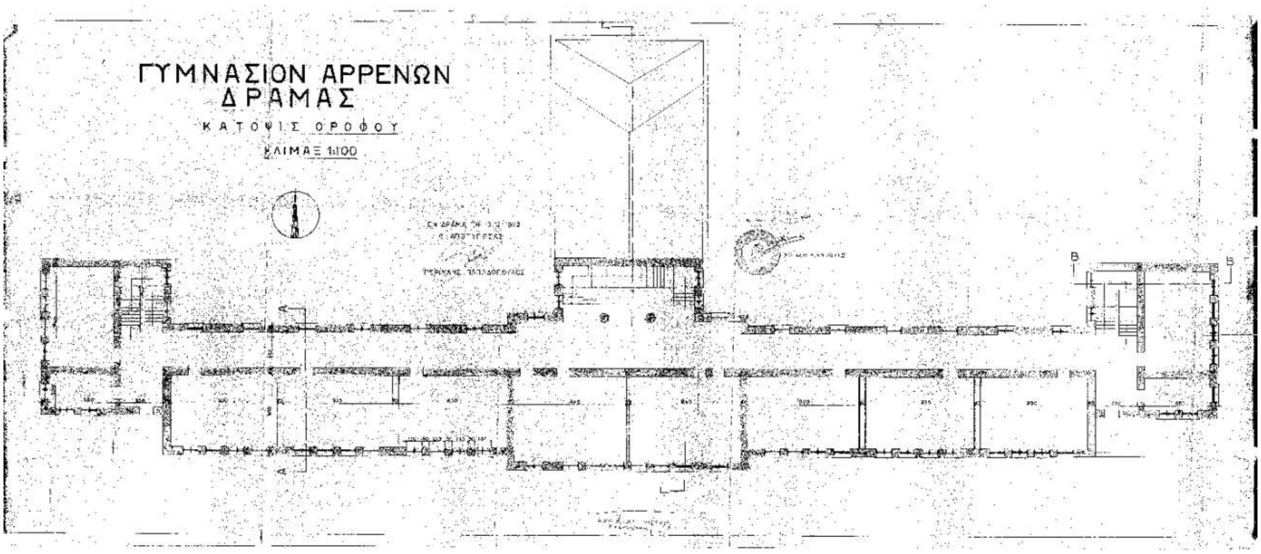


*Figure 7 Initial first floor plan of the school (source: Pantzaris, 1928-32)*

*Figures 8,9 Central entrance area and the marble main staircase of the school (Photos by the author, 2019)*

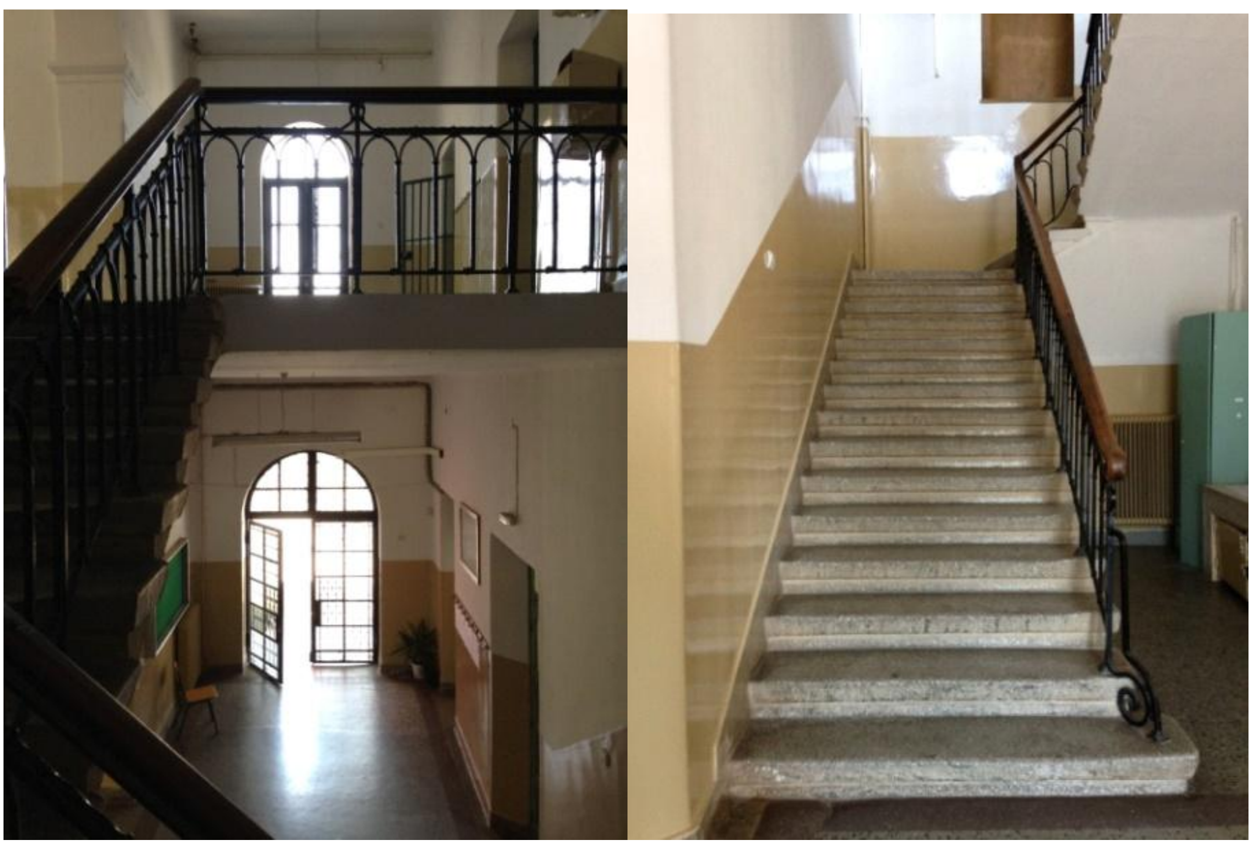

*Figures 10,11 Secondary entrance area and the secondary staircase of the west part of the school (Photos by the author, 2019)*

The west-east corridors are the ones that connect the three principal staircases of the building and give access to the classrooms, both on the ground floor and the first-floor levels (Figures 12,13).

*Figures 12,13 Ground floor and first floor north-facing corridors of the west part of the school (Photos by the author, 2019)*

There are six classrooms on the ground floor, (three on each side of the main entrance), with a south orientation. On the first floor there are currently ten classrooms that were initially eight, as stated in Marmaridou (2013), of various dimensions which are also facing south. The first classrooms on the left and right of the main entrance of the ground floor are today used as the teachers' office spaces.

In 1974, the school building was expanded with the construction of two new wings at the two extreme east and west parts of it, on the north-south axis, towards the rear part of the school. Thus, six classrooms were added to each wing, three per floor, as well as one room at the end of each new corridor for storage purposes. The new shape of the floor plan of the building was now in the form of the letter "E" (Figures 14,15,16) and the new coverage area amounted to 2180.8 m$^2$ (Marmaridou, 2013).

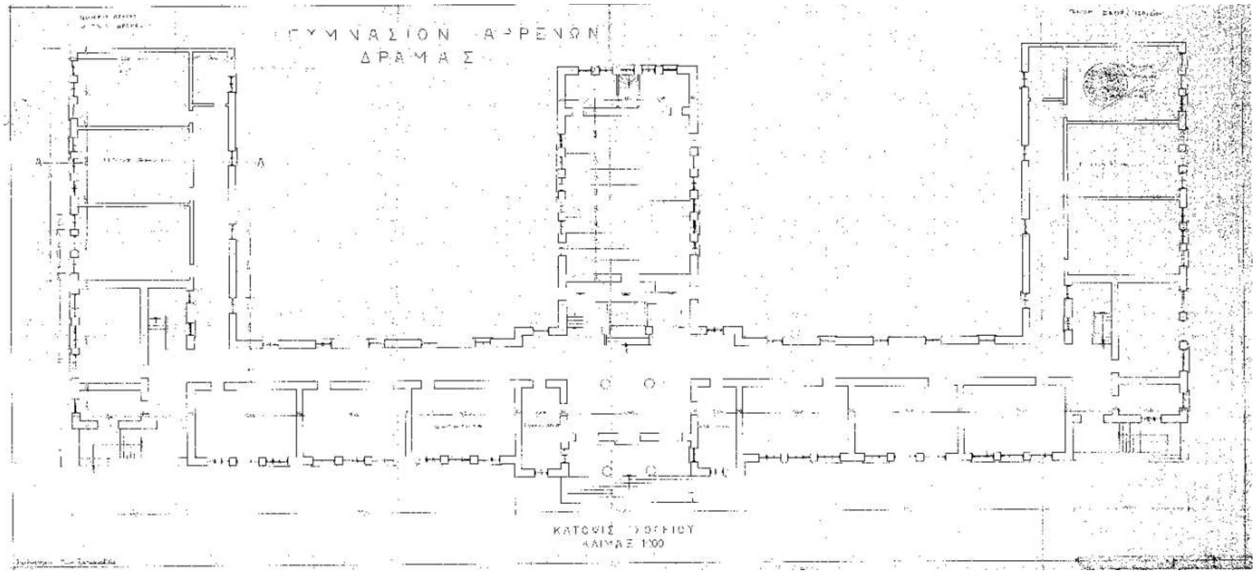


*Figure 14 Ground floor plan after the addition of the two wings (source: Dervisakis, 1975)*

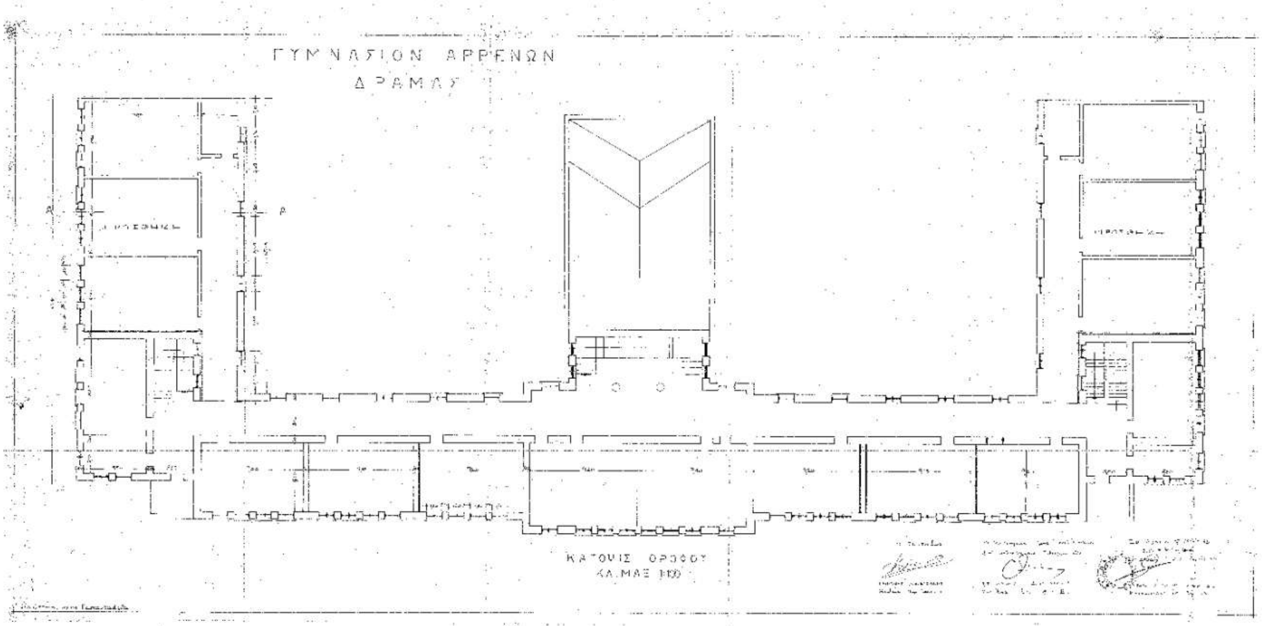


*Figure 15 First floor plan after the addition of the two wings (source: Dervisakis, 1975)*

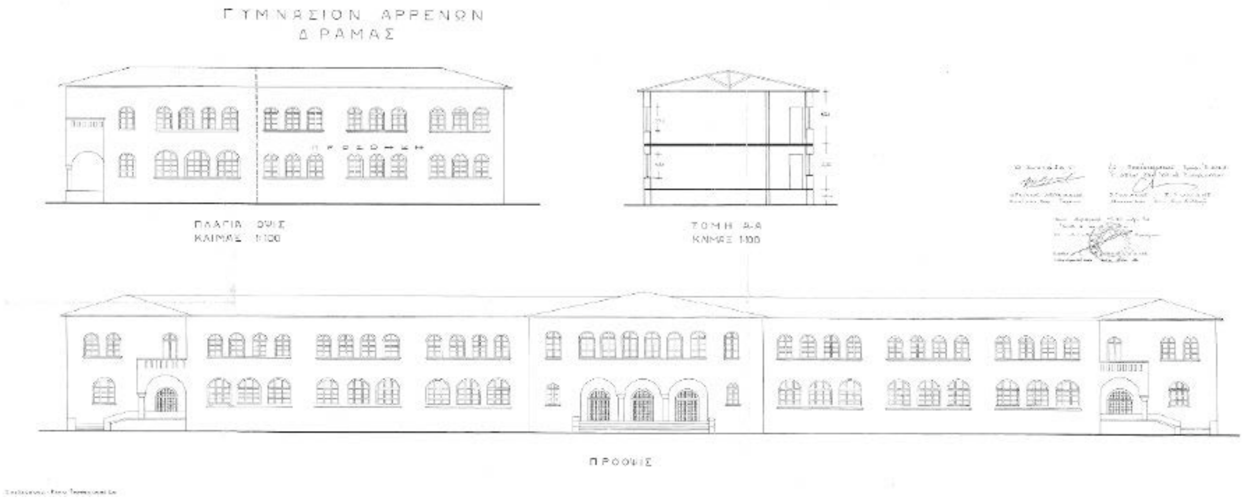


*East facade, section A-A and main south facade after the addition of the extensions (source: Dervisakis, 1975)*

The openings of the building are arched in their majority and provide the building with an adequate quantity of natural light. They have wooden frames, single glazing and are double casement with skylights. The classrooms of the ground floor of the initial school construction have three openings each (Figure 17), while the ones of the second floor, four, smaller in width each. The far east and west openings of the initial parts of the building that recede from the plane of the main, south façade are one in number for each office space of the ground floor and two for each office space of the first floor. Each of these offices has one more opening in their west or east sides. Moreover, in the central part of the south façade, over the arches of the ground floor, there are six openings in a row (Figure 18). Each of the classrooms that belong to the extension part of the school have two openings on the ground floor and three on the first floor. The windows of the corridors are located in the recesses of the "E" shape, and they are twenty-four for each floor with two of them being side exit doors. Finally, all the openings of the school's amphitheater are covered with plasterboards and are currently out of use.


*Figures 17,18 Ground floor south facing openings and first floor six windows in a row (Photos by the author, 2019)*

Concerning the materials that were used in the opaque constructions of the building, reinforced concrete was used in the structural elements, such as slabs (covered with cement mosaic), beams, arches and columns (covered with lime plaster). Load-baring natural stone masonry (covered with lime plaster) was applied in the majority of the exterior and the interior walls in three different widths. There is also brickwork from solid bricks with deep plaster grouting, also covered with lime plaster, as well as perforated-brick brickwork in three different widths, covered with the same type of plaster. Finally, most of the building is covered with a ceramic-tiled, wooden roof, except for the corridors of the extensions that have a flat, concrete-slab roof (Paraschou, 2010).

Most of the constructions of the building can be seen in Figures 19,20, while in the appendix, in chapter ”7.1 Constructions of the school building”, a more detailed approach of all the constructions with the materials used in each one of them and their boundary conditions can be found. There is also information on the different properties of the materials that are used in the energy and daylight simulations. These properties refer to the roughness, the thickness, the conductivity, the density, the specific heat, the thermal absorptance, the solar absorptance and the visible absorptance concerning the Energy Plus opaque materials, the U-value, the solar heat gain coefficient and the visible transmittance concerning the EnergyPlus window constructions and the reflectance, the transmittance, the emissivity, the thickness and the conductivity concerning the EnergyPlus shade materials (Big Ladder Software, 2021). For the radiance glass materials, red, green, and blue transmittance values are needed, for the radiance opaque materials, red, green and blue reflectance values, and for the radiance translucent (interior shade) materials, red, green and blue diffuse reflectance, specular reflection, diffuse transmission, specular transmission and roughness values

(Grasshopper Docs, 2020). Furthermore, there is a visualization of the boundary conditions of the different constructions in chapter “7.5 School building boundary conditions” of the Appendix.

The values of all the above properties are retrieved from different databases, such as the EnergyPlus database, the Masea database, and the OpenStudio database (EnergyPlus, 2017; MASEA, 2022; OpenStudio, 2020). For the U-values of the windows, since no information could be found in-situ, the suggestion of the T.O.T.E.E./2017 guide was used. So, according to T.O.T.E.E. (2017) and a calculation of the percentage of the wooden frame in the windows (30%), the U-value of 4.7 $W.m^{-2}.K^{-1}$ was used.

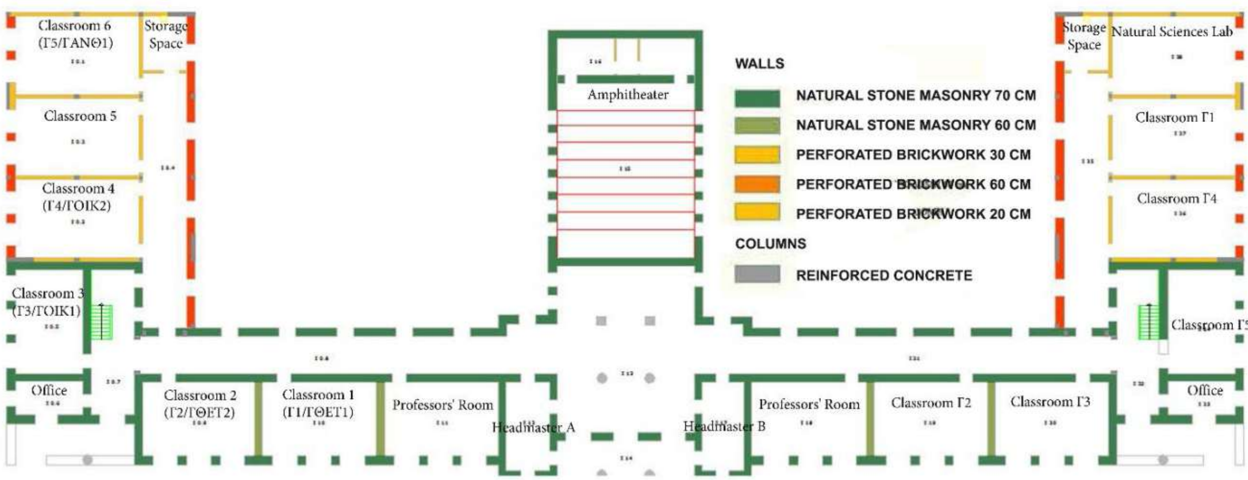


*Figure 19 Ground floor constructions (source: “Restoration of the “Boys’ High School” of Drama - Assessment of its bearing capacity – Interventions”, 2010, adapted by Marmaridou)*

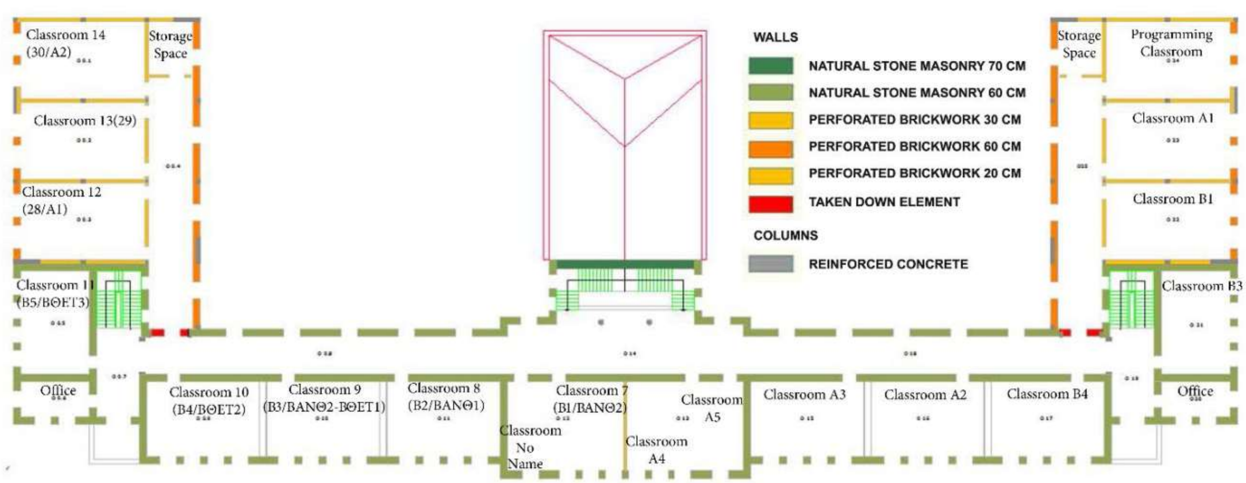


*Figure 20 First floor constructions (source: “Restoration of the “Boys’ High School” of Drama - Assessment of its bearing capacity – Interventions”, 2010, adapted by Marmaridou)*

### 2.3.1.2 Weather Data

The weather data that was used in the simulations comes from the EnergyPlus epw file for the city of Thessaloniki in northern Greece web (EnergyPlus Weather Data, 2021). This is the closest weather data that could be found to the one for the city of Drama and it gives information on:

- Latitude
- Location (Latitude 40°52 N and Longitude 22°971 E)
- dry bulb temperature
- dew point temperature
- relative humidity
- wind speed
- wind direction
- direct normal radiation
- diffuse horizontal radiation
- global horizontal radiation
- horizontal infrared radiation
- direct normal illuminance
- diffuse horizontal illuminance
- global horizontal illuminance
- total sky cover
- barometric pressure
- model year (2009)

### 2.3.1.3 Thermal zoning of the building

The building was separated into thermal zones according to a certain number of criteria. These criteria are stated in the T.O.T.E.E. (2017) guide and include the type of use of each zone, the orientation, the floor they belong to, whether it is conditioned or not, and the minimization of the number of thermal zones. Furthermore, the rules according to which an EnergyPlus model can be designed were taken into account. The final approach can be seen in the following figures (Figures 21,22).

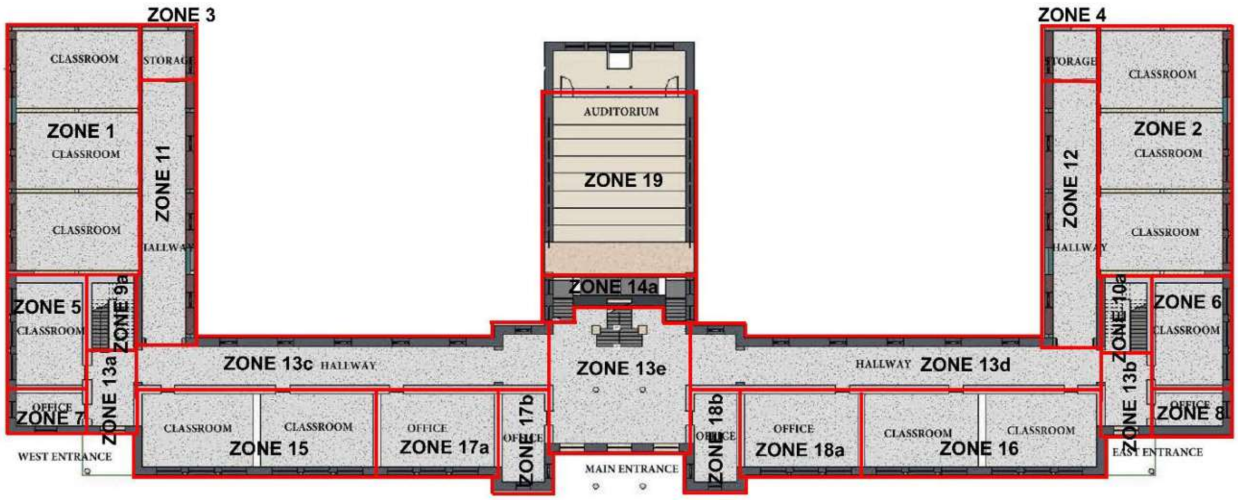


*Figure 21 Thermal zones of the ground floor*

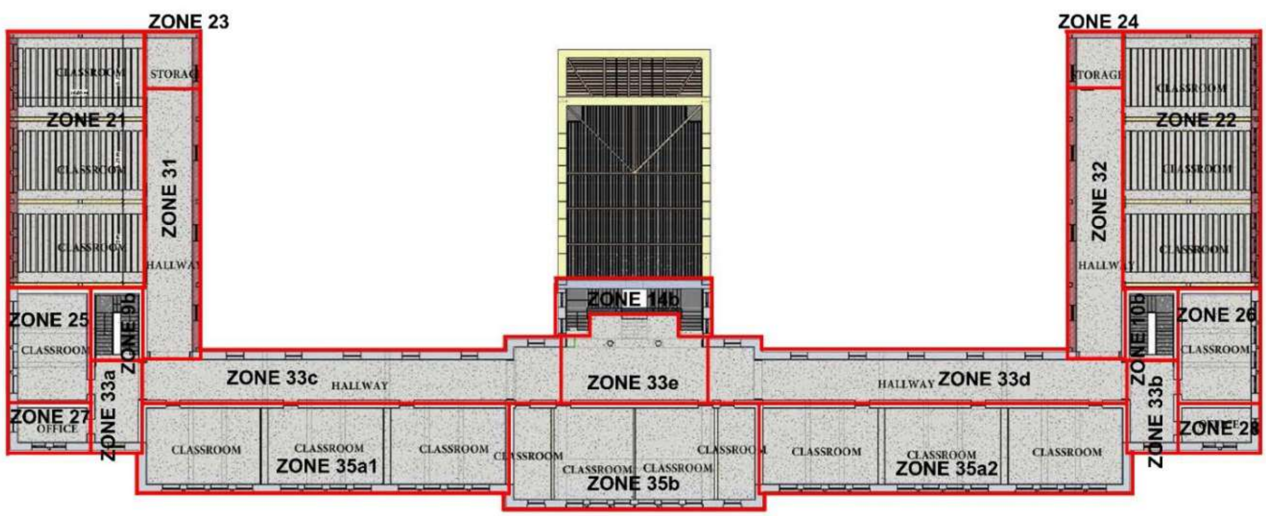


*Figure 22 Thermal zones of the first floor*

### 2.1.4 Greek and European Standard recommendations and material properties from existing databases

According to the specifications stated in the T.O.T.E.E. (2017) guide (Table 1), the secondary school buildings operate for 8 hours on weekdays and from the 9th of September till the 9th of May. The number of hours is used in the energy simulation for the heating and cooling schedules, and they range from 07:00 am to 15:00 pm, but for the days that the school is operating, what is used instead, is the days that are left after the holidays of the school year 2009 are subtracted, since that is the year that the weather file refers to during the simulation. They can be seen on Table 13.

Table 13 School holidays for the year 2009 in Greece (source: eortologio.net, 2013)

| **Holidays of the school year 2009** | | | |
|---|---|---|---|
| **January** | 1-7, 30 | **July** | 1-31 |
| **February** | - | **August** | 1-31 |
| **March** | 2, 24, 25 | **September** | 1-10 |
| **April** | 10-26 | **October** | 27, 28 |
| **May** | 1-5 | **November** | 17 |
| **June** | 8, 17-30 | **December** | 21-31 |

The summer and winter temperature demands are set according to the specifications mentioned in Table 2 and they are 20 $^{o}$C for the winter period and 26 $^{o}$C for the summer period. The heat that is released per user of a secondary school building is set to 80 W.m$^{-2}$, according to the suggestions of Table 3. This parameter is used in the calculations combined with the number of people per thermal zone of the school for the school year 2018-2019.

Concerning the maximum allowed thermal transmittance coefficients in the case of a radical renovation of a building that belongs to the climatic zone “D” of Greece, as stated in the T.O.T.E.E. (2017) guide, Table 14 shows the values for each one of the different structural elements that are met in the building studied. The information is derived from Table 4.

Table 14 Maximum allowed values of the thermal transmittance coefficient of the individual structural elements of the climatic zone “D” in case of radical renovation of an existing building (source: T.O.T.E.E., 2017)

| **Structural Element** | **Zone D maximum permissible coefficient of thermal transmittance U [$W.m^{-2}.K^{-1}$]** |
|---|---|
| **Outdoor horizontal or inclined surface in contact with exterior air (roof)** | 0.35 |
| **Exterior wall in contact with the exterior air** | 0.40 |
| **Floor in contact with the exterior air** | 0.35 |
| **Horizontal or inclined roof in contact with a closed unheated space** | 0.70 |
| **Wall in contact with a closed unheated space** | 0.70 |
| **Floor in contact with a closed unheated space** | 0.70 |
| **Wall in contact with the ground** | 0.70 |
| **Floor in contact with the ground** | 0.70 |
| **Window frame in contact with the exterior air** | 2.60 |

The daylight provision recommendations for the school building are retrieved from the EN 12464-1 European Standard and the Zumtobel Lighting Handbook and can be seen in Table 15. The sDA (spatial daylight autonomy) shows the minimum percentage of the selected area for which the target illuminance $E_T$ must be achieved for at least 50 % of the daylight occupancy hours (Daylighting Metrics Static vs. Dynamic Assessment, 2019).

Table 15 Lighting requirements for interiors (areas), tasks and activities (source: EN, 2011)

| | $E_m$ (average illuminance) | Measurement reference level | $U_o$ (Unformity) | sDA ($E_T$,%area) |
|---|---|---|---|---|
| **Classroom** | 300 | 0.80 | 0.60 | (300,50%) |
| **Lecture hall** | 500 | 0.80 | 0.60 | (500,50%) |
| **Computer practice rooms** | 300 | 0.80 | 0.60 | (300,50%) |
| **Entrance halls** | 200 | 0 | 0.40 | (200,50%) |
| **Circulation areas, corridors** | 100 | 0 | 0.40 | (100,50%) |
| **Stairs** | 150 | 0 | 0.40 | (150,50%) |
| **Teachers' rooms** | 300 | 0.80 | 0.60 | (300,50%) |
| **Stock rooms for materials** | 100 | 0.80 | 0.40 | (100,50%) |

### 2.3.1.5 In-situ observations

From the in-situ observations a lot of necessary information was obtained for the creation of the energy and daylight models of the school building. Table 16 shows different data and in specific, the areas and the values of different loads for each one of the thermal zones.

The number of people per area is defined by retrieving the actual number of people that were occupying each thermal zone of the west half of the building during the school year 2018-2019. For reasons of brevity the same numbers are used for the mirrored thermal zones of the east half of the school. The east half is occupied by classes for the first three years of high school, while the west half by classes for the last three. The equipment load per area [$W.m^{-2}$] is defined by retrieving the locations, types and number of the existing school equipment (Tables 17,18). The infiltration rate per area [$m^3.s^{-1}.m^{-2}$] at 4 Pa is retrieved from Honeybee's suggestions for leaky buildings after an approximation of the existing situation. Finally, the lighting density per area [$W.m^{-2}$] is defined by retrieving the actual number and power of the lamps of each thermal zone.

Table 16 Different load types' values for each thermal zone of the building

| Zone Name | Floor Area [$m^2$] | Max number of people | Equipment Load Per Area [$W.m^{-2}$] | Infiltration Rate Per Area [$m^3.s^{-1}.m^{-2}$] | Lighting Density Per Area [$W.m^{-2}$] | Number Of People Per Area [$ppl.m^{-2}$] |
|---|---|---|---|---|---|---|
| Zone 1/2 | 216.61 | 75 | 0.92 | 0.0006 | 11.97 | 0.362 |
| Zone 3/4 | 18.60 | 1 | 0 | 0.0006 | 3.87 | 0.054 |
| Zone 5/6 | 58.70 | 28 | 0 | 0.0006 | 3.68 | 0.477 |
| Zone 7/8 | 23.87 | 1 | 4.19 | 0.0006 | 3.02 | 0.042 |
| Zone 9a/10a | 21.32 | 15 | 0 | 0.0006 | 0 | 0.704 |
| Zone11/12 | 93.40 | 20 | 0 | 0.0006 | 2.31 | 0.214 |
| Zone13a/13b | 482.19 | 4 | 0 | 0.0006 | 3.47 | 0.128 |
| Zone13c/13d | 482.19 | 20 | 0 | 0.0006 | 1.58 | 0.146 |
| Zone13e | 482.19 | 12 | 0 | 0.0006 | 1.56 | 0.087 |
| Zone14a | 35.44 | 2 | 0 | 0.0006 | 2.03 | 0.056 |
| Zone 15/16 | 135.99 | 54 | 4.41 | 0.0006 | 3.18 | 0.397 |
| Zone 17a/18a | 65.68 | 13 | 4.57 | 0.0006 | 6.58 | 0.198 |
| Zone 17b/18b | 37.35 | 3 | 14.72 | 0.0006 | 3.86 | 0.080 |
| Zone 19 | 179.58 | 145 | 9.47 | 0.0006 | 16.04 | 0.807 |
| Zone 21/22 | 216.61 | 82 | 12.00 | 0.0006 | 7.98 | 0.379 |
| Zone 23/24 | 18.60 | 1 | 1 | 0.0006 | 3.87 | 0.054 |
| Zone 25/26 | 58.70 | 26 | 0 | 0.0006 | 2.45 | 0.443 |
| Zone 27/28 | 23.87 | 1 | 4.19 | 0.0006 | 3.02 | 0.042 |
| Zone 9b/10b | 21.32 | 5 | 0 | 0.0006 | 3.38 | 0.235 |
| Zone31/32 | 93.40 | 20 | 0 | 0.0006 | 2.31 | 0.214 |
| Zone33a/33b | 31.16 | 5 | 0 | 0.0006 | 3.47 | 0.160 |
| Zone33c/33d | 136.60 | 20 | 0 | 0.0006 | 1.58 | 0.146 |
| Zone33e | 80.89 | 10 | 0 | 0.0006 | 0 | 0.124 |
| Zone14b | 35.44 | 20 | 0 | 0.0006 | 1.02 | 0.564 |
| Zone35a1/35a2 | 201.66 | 86 | 4.46 | 0.0006 | 4.2 | 0.426 |
| Zone35b | 165.45 | 71 | 0 | 0.0006 | 2.39 | 0.429 |
| UnheatedZone1 | 229.30 | 4 | 78.50 | 0.0006 | 0.9 | 0.017 |
| UnheatedZone2 | 49.61 | 2 | 0 | 0.0006 | 1.45 | 0.040 |
| UnheatedZone3/4 | 23.73 | 2 | 51.21 | 0.0006 | 1.52 | 0.084 |
| UnheatedZone21/22Roof | 200.14 | 0 | 0 | 0.0006 | 0 | 0 |
| UnheatedZone25/26Roof | 58.70 | 0 | 0 | 0.0006 | 0 | 0 |
| UnheatedZone27/28Roof | 24.10 | 0 | 0 | 0.0006 | 0 | 0 |
| UnheatedZone9b/10bRoof | 21.32 | 0 | 0 | 0.0006 | 0 | 0 |
| UnheatedZone33a/33bRoof | 31.16 | 0 | 0 | 0.0006 | 0 | 0 |
| UnheatedZone33c/33dRoof | 136.60 | 0 | 0 | 0.0006 | 0 | 0 |
| UnheatedZone33eRoof | 80.90 | 0 | 0 | 0.0006 | 0 | 0 |
| UnheatedZone14bRoof | 35.44 | 0 | 0 | 0.0006 | 0 | 0 |
| UnheatedZone35a1/a2Roof | 201.66 | 0 | 0 | 0.0006 | 0 | 0 |
| UnheatedZone35bRoof | 21.24 | 0 | 0 | 0.0006 | 0 | 0 |
| UnheatedZone19Roof | 179.69 | 0 | 0 | 0.0006 | 0 | 0 |
| UnheatedZone2Roof | 49.61 | 0 | 0 | 0.0006 | 0 | 0 |

Table 17 Power Output per Appliance (source: qlabe.com, 2020)

| Appliance | Power Output per Appliance [W] |
|---|---|
| Printer | 50 |
| PC | 100 |
| Loudspeaker | 200 |
| Projector | 300 |

Table 18 Types, number and power of different equipment per thermal zone

| Zone Name | Appliances | Number of appliances | Watt |
|---|---|---|---|
| Zone 1/2 | PC | 2 | 200 |
| Zone 7/8 | PC | 1 | 100 |
| Zone 15/16 | Projector | 2 | 600 |
| Zone 17a/18a | PC | 3 | 300 |
| Zone 17b/18b | PC<br>Printer | 4<br>3 | 550 |
| Zone 19 | PC<br>Speaker<br>Projector | 2<br>6<br>1 | 1700 |
| Zone 21/22 | PC<br>Printer | 17<br>3 | 2600 |
| Zone 27/28 | PC | 1 | 100 |
| Zone35a1/35a2 | Projector | 3 | 900 |

Furthermore, in the appendix there is information about the hourly occupancy schedules that are retrieved from the actual school schedule for the year 2018-2019, between 08:00 am and 15:00 pm for each one of the thermal zones. The hourly activity occupancy schedules represent the metabolic rate of the occupants of the thermal zones when they are occupied, which is equal to 80 $W.m^{-2}$ per user (T.O.T.E.E., 2017). The hourly heating and cooling setpoint schedules for each one of the thermal zones have a minimum temperature value equal to 20 $^{o}C$ for the occupied hours of a cold period and equal to 16 $^{o}C$ for the unoccupied hours of a cold period, while for a hot period the maximum temperature value is set to 26 $^{o}C$ for the occupied hours and to 35 $^{o}C$ for the unoccupied hours. The hourly lighting schedules follow the hourly occupancy schedules for the assessment of the existing situation, considering that the lights are always on when a thermal zone is occupied. Finally, the hourly equipment schedules are defined by approximating the equipment's use frequencies which are approximated in this study according to logical deductions.

### 2.3.2 Energy and daylight simulations of the existing situation

After the accumulation and the application of the different data, the energy and daylight models were completed in the Grasshopper interface through the Ladybug 0.0.69 and Honeybee 0.0.66 Legacy Plug-ins. First, the energy model was completed by assigning the honeybee zones to the OpenStudio cross platform, (which uses the EnergyPlus energy simulation program), together with the weather file, the analysis period (full year), the timestep (hourly) of the simulation, the holiday days, the terrain type (suburbs), the solar distribution type (full interior and exterior with reflections) and the simulation outputs and then, the simulation was performed (Grasshopper Docs, 2020). It gave the results of the heating, cooling and electric light loads of the whole conditioned building, as well as of two selected thermal zones that represented one classroom and a teachers' office towards two different orientations (zone 6: classroom to the east, zone 17a: teachers' office to the south) and can be seen in Figure 21. The energy simulation, as already mentioned, uses an ideal air loads system. This means that the loads' results refer to the energy that needs to be removed or added to the zones by the system and not the values of electricity or fuel that it might take to remove or add this energy (Ladybug Tools Forum, 2021). Moreover, the adaptive comfort calculator of the Ladybug 0.0.69 and Honeybee 0.0.66 Legacy Plug-ins gave the percentage of thermal comfort during the occupancy hours for the whole conditioned building. This model calculates the occupants' thermal comfort levels for naturally ventilated buildings without any mechanical air-conditioning (Ladybug Tools Forum, 2021). It is based on the realization that the occupants of a building adapt to the exterior monthly mean temperature and can feel comfortable in buildings that maintain an interior temperature close to it, as long as the exterior is between 10 ºC and 33 ºC (Ladybug Tools Forum, 2021). In order to calculate the above results, the model used the hourly air temperature and the mean radiant temperature outcomes of the energy simulation for each one of the thermal zones, together with the hourly outdoor drybulb temperature values of the weather file of Thessaloniki. As already mentioned, since the adaptive comfort model is used only for free-running buildings, the results are only used to give an impression of a relevant exploration and are considered inconsistent.

Next the daylight simulation was executed, after assigning to the daylight simulation engine the honeybee zones, the weather file, a grid of sensors (every 1 m) for each one of the thermal zones and finally the right radiance and daysim parameters (Grasshopper Docs, 2020). The daylight metrics' results were post-processed and the spatial daylight autonomy, the hourly average illuminance and the hourly average uniformity values were obtained for each thermal zone, for a no-shading scenario. The dynamic-shading scenario that has already been mentioned, was applied to the two selected thermal zones, and gave results on the daylight glare probability for a defined point in each one of them, as well as on the above-mentioned metrics with the exception of the spatial daylight autonomy.

### 2.3.3 Construction of the energy and daylight models for the simulations of the improvement scenarios

For the improvement scenarios, different passive strategies were implemented, and a parametric model was built. For the energy improvement, these strategies included the suggestion of two different exterior insulation types for the exterior walls (Table 19), two other types of insulation for the floors and the ceilings (Table 20), change of the windows and choice between three different alternatives (Table 21), and finally, choice between two different interior shade types (Table 22), (the values were taken from ASHRAE's suggestions on Table 23). The insulation choices were made in a way that the U-value Standards' demands per type of construction are fulfilled. It is also considered that these interventions are capable of lowering the infiltration rate of the thermal zones and as a result the value of 0.00285 $m^3.s^{-1}.m^{-2}$ is applied to all of them, according to the ANSI/ASHRAE Standard (2010).

Table 19 FIBRANxps Etics GF exterior wall insulation properties for energy simulation (source: Fibran, 2021)

| | d [m] | λ [$W.m^{-1}.K^{-1}$] | c [$J.kg^{-1}.K^{-1}$] | ρ [$kg.m^{-3}$] | Thermal Absorp-tance | Solar Absorp-tance | Visible Absorp-tance | Roughness |
|---|---|---|---|---|---|---|---|---|
| **FIBRANxps Etics GF 80** | 0.08 | 0.034 | 1450 | 38 | 0.90 | 0.70 | 0.70 | Medium-Rough |
| **FIBRANxps Etics GF 160** | 0.16 | 0.034 | 1450 | 38 | 0.90 | 0.70 | 0.70 | Medium-Rough |

Table 20 FIBRANxps 400 floor and ceiling insulation properties for energy simulation (source: Fibran, 2021)

| | d [m] | λ [$W.m^{-1}.K^{-1}$] | c [$J.kg^{-1}.K^{-1}$] | ρ [$kg.m^{-3}$] | Thermal Absorp-tance | Solar Absorp-tance | Visible Absorp-tance | Roughness |
|---|---|---|---|---|---|---|---|---|
| **FIBRANxps 400 50** | 0.05 | 0.033 | 1450 | 38 | 0.90 | 0.70 | 0.70 | Medium-Rough |
| **FIBRANxps 400 100** | 0.1 | 0.034 | 1450 | 38 | 0.90 | 0.70 | 0.70 | Medium-Rough |

Table 21 Wooden-frame, double glazing window properties for energy simulation (source: NFRC Directory, 2021)

| Manufacturer Product code | Frame material | Glazing layers | Gap Fill | U-value [$W.m^{-2}.K^{-1}$] | SHGc | VT | Glass Coating |
|---|---|---|---|---|---|---|---|
| Marvin AAVFbcza0100000 | wood | 2 | Argon(90) / Air(10) | 1.59 | 0.54 | 0.62 | Low E1-0.068(3) |
| Double Glazing Clear Glass | wood | 2 | Air(100) | 2.67 | 0.70 | 0.79 | - |
| Marvin AAVFbasc0100000 | wood | 2 | Argon(90) / Air(10) | 1.30 | 0.32 | 0.55 | Low E2-0.042(2) / Low ERS-0.149(4) |

Table 22 ASHRAE draperies' properties for energy simulation (source: ASHRAE, 2001)

| Draperies | Reflectance | Transmittance | Emissivity | Thickness |
|---|---|---|---|---|
| **Open Weave Medium Color Draperies** | 0.25 | 0.60 | 0.9 | 0.001 |
| **Semi open Weave Light Color Draperies** | 0.40 | 0.45 | 0.9 | 0.001 |

Table 23 ASHRAE interior solar attenuation coefficients for single and insulating glass with draperies (source: ASHRAE, 2001)

| Glazing | Glass Trans-mission | Glazing SHGC (No Drapes) | IAC A | B | C | D | E | F | G | H | I | J |
|---|---|---|---|---|---|---|---|---|---|---|---|---|
| Single glass | | | | | | | | | | | | |
| 3 mm clear | 0.86 | 0.87 | 0.87 | 0.82 | 0.74 | 0.69 | 0.64 | 0.59 | 0.53 | 0.48 | 0.42 | 0.37 |
| 6 mm clear | 0.80 | 0.83 | 0.84 | 0.79 | 0.74 | 0.68 | 0.63 | 0.58 | 0.53 | 0.47 | 0.42 | 0.37 |
| 13 mm clear | 0.71 | 0.77 | 0.84 | 0.80 | 0.75 | 0.69 | 0.64 | 0.59 | 0.55 | 0.49 | 0.44 | 0.40 |
| 6 mm heat absorbing | 0.46 | 0.58 | 0.85 | 0.81 | 0.78 | 0.73 | 0.69 | 0.66 | 0.61 | 0.57 | 0.54 | 0.49 |
| 13 mm heat absorbing | 0.24 | 0.44 | 0.86 | 0.84 | 0.80 | 0.78 | 0.76 | 0.72 | 0.68 | 0.66 | 0.64 | 0.60 |
| Reflective coated | — | 0.52 | 0.95 | 0.90 | 0.85 | 0.82 | 0.77 | 0.72 | 0.68 | 0.63 | 0.60 | 0.55 |
| | — | 0.44 | 0.92 | 0.88 | 0.84 | 0.82 | 0.78 | 0.76 | 0.72 | 0.68 | 0.66 | 0.62 |
| | — | 0.35 | 0.90 | 0.88 | 0.85 | 0.83 | 0.80 | 0.75 | 0.73 | 0.70 | 0.68 | 0.65 |
| | — | 0.26 | 0.83 | 0.80 | 0.80 | 0.77 | 0.77 | 0.77 | 0.73 | 0.70 | 0.70 | 0.67 |
| Insulating glass, 6 mm air space | | | | | | | | | | | | |
| (3 mm out and 3 mm in) | 0.76 | 0.77 | 0.84 | 0.80 | 0.73 | 0.71 | 0.64 | 0.60 | 0.54 | 0.51 | 0.43 | 0.40 |
| Insulating glass 13 mm air space | | | | | | | | | | | | |
| Clear out and clear in | 0.64 | 0.72 | 0.80 | 0.75 | 0.70 | 0.67 | 0.63 | 0.58 | 0.54 | 0.51 | 0.45 | 0.42 |
| Heat absorbing out and clear in | 0.37 | 0.48 | 0.89 | 0.85 | 0.82 | 0.78 | 0.75 | 0.71 | 0.67 | 0.64 | 0.60 | 0.58 |
| Reflective coated | — | 0.35 | 0.95 | 0.93 | 0.93 | 0.90 | 0.85 | 0.80 | 0.78 | 0.73 | 0.70 | 0.70 |
| | — | 0.26 | 0.97 | 0.93 | 0.90 | 0.90 | 0.87 | 0.87 | 0.83 | 0.83 | 0.80 | 0.80 |
| | — | 0.17 | 0.95 | 0.95 | 0.90 | 0.90 | 0.85 | 0.85 | 0.80 | 0.80 | 0.75 | 0.75 |

**Interior Solar Attenuation (IAC)**

*Notes*:

1. Interior attenuation coefficients are for draped fabrics.
2. Other properties are for fabrics in flat orientation.
3. Use fabric reflectance and transmittance to obtain accurate IAC values.
4. Use openness and yarn reflectance or openness and fabric reflectance to obtain the various environmental characteristics, or to obtain approximate IAC values.

**Classification of Fabrics**

I = Open weave
II = Semiopen weave
III = Closed weave

D = Dark color
M = Medium color
L = Light color

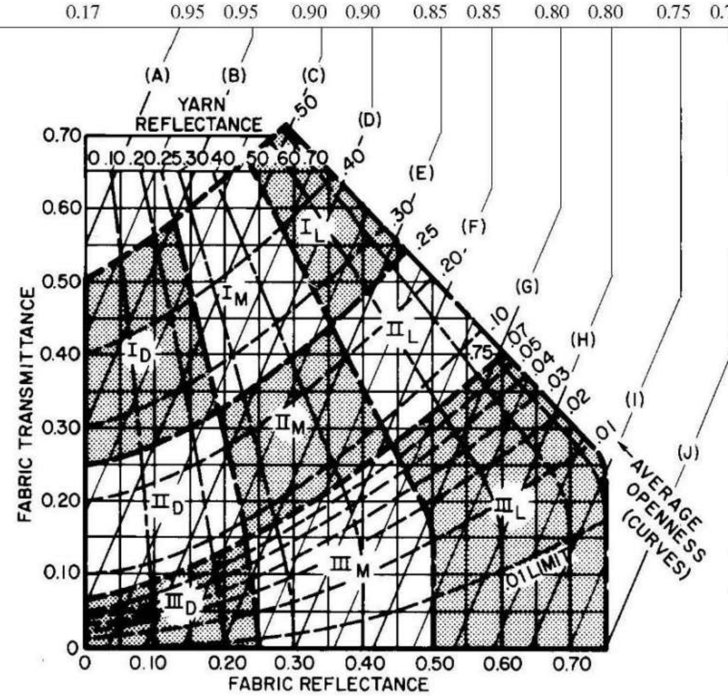

For the daylight improvement, the colour of the walls and the ceiling was altered inside the thermal zones from yellow to white stucco (Table 24) and the new radiance glass materials were created, according to the window choices mentioned above (Table 25). The radiance translucent materials for the two drapery options were also created (Table 26) and finally the addition of light shelves was examined (Table 27).

Table 24 White stucco properties for daylight simulation (source: github.com, 2021)

| White stucco | Red reflectance | Green reflectance | Blue reflectance |
|---|---|---|---|
| | 0.726 | 0.706 | 0.633 |

Table 25 Wooden-frame, double glazing window properties for daylight simulation (source: NFRC Directory, 2021)

| Manufacturer<br>Product code | Red transmittance | Green transmittance | Blue transmittance |
|---|---|---|---|
| Marvin<br>AAVFbcza0100000 | 0.62 | 0.62 | 0.62 |
| Double Glazing<br>Clear Glass | 0.79 | 0.79 | 0.79 |
| Marvin<br>AAVFbasc0100000 | 0.55 | 0.55 | 0.55 |

Table 26 Draperies' properties for daylight simulation (source: Ladybug Tools Forum, 2021)

| Draperies | Red diffusive reflectance | Green diffusive reflectance | Blue diffusive reflectance | Specular reflection | Diffusive transmis-sion | Specular transmis-sion | Rough-ness |
|---|---|---|---|---|---|---|---|
| **Open Weave Medium Color Draperies** | 0.500 | 0.500 | 0.500 | 0.005 | 0.2 | 0.02 | 0.2 |
| **Semi open Weave Light Color Draperies** | 0.680 | 0.680 | 0.680 | 0.01 | 0.26 | 0.03 | 0.2 |

Table 27 Light shelf properties for daylight simulation (source: spectraldb.com, 2021)

| Light Shelf | Diffuse reflectance for red | Diffuse reflectance for green | Diffuse reflectance for blue |
|---|---|---|---|
| | 0.726 | 0.706 | 0.633 |

### 2.3.4 Energy and daylight simulations of the improvement scenarios through an iterative method

The annual daylight simulations ran (for dynamic-shading scenarios) for each one of the two selected thermal zones and the daylight metrics concerning the spatial daylight autonomy, the hourly average illuminance, the hourly average uniformity, and the daylight glare probability for a defined point in each one of them were obtained. These simulations had twelve iterations each, as the parameters that affected the results were the three different window retrofit options, created according to GitHub (2022), the two different interior shade types and the addition of light shelves. After the simulations were completed, an electric light schedule was produced for each iteration of each one of the two zones. These schedules replaced the ones in the energy model set-up, which was then calculated with the new schedules. The lighting control type that was used, is the "Always on during active occupancy hours with auto dimming" control type of the Honeybee plug-in (Grasshopper Docs, 2020).

The next step was to run the parametric energy model with the help of the OpenStudio simulation engine and the Colibri iterator. Forty-eight possible models were produced. The annual heating, cooling and electric light loads for the whole conditioned volume, as well as for the two selected thermal zones of each iteration were then obtained. The percentage of the occupancy time that the conditions were considered comfortable for each of the forty-eight cases of the whole conditioned volume, was also obtained.

### 2.3.5 Visualization of the results

The outcomes of the current-state's energy and daylight simulations are given arithmetically and through graphs (tables, simple and stacked column charts).

The outcomes of the iterative energy and daylight simulations are also given through the above-mentioned methods (tables, simple and stacked column charts). Furthermore, they were combined in one csv file that includes all the forty-eight different scenarios, with the different applied passive strategies and all the energy and daylight outcomes of the whole building and of each one of the two selected thermal zones. They were then uploaded to Design Explorer, a space exploration online tool, as already mentioned. Through it, all the alternatives are visualized in a user-friendly way and the different performances are compared based on quantitative metrics.

# 3. RESULTS AND DISCUSSIONS

## 3.1 Current-state simulation results

### 3.1.1 Current-state energy simulation results

A number of representative energy and thermal comfort metrics were chosen in order to assess the energy and thermal comfort performance of the selected building volume in a year through energy simulations. These metrics include the heating, cooling and electric light loads, as well as the adaptive thermal comfort (only for an impression of a relevant exploration), and the results are explained in more detail in the next two subchapters.

#### 3.1.1.1 Heating, cooling, and electric light loads results

The energy simulation of the building model representing the current state of the school, gave results on the heating, cooling and electric light loads of the whole conditioned space and of each one of the defined thermal zones. Table 28 shows these results for the whole building, while Table 29 shows the heating, cooling and electric light loads of each thermal zone, respectively. As already mentioned, these results represent the energy that needs to be removed or added to a zone by an ideal system that does not include a coefficient of performance (COP), and not the values of electricity or fuel that it might take to add or remove this energy (Ladybug Tools Forum, 2021).

Table 28 Current-state energy simulation results of the whole building

| | |
|---|---|
| **Annual Heating Load [kWh.m$^{-2}$]** | 58.8 |
| **Annual Cooling Load [kWh.m$^{-2}$]** | 0.6 |
| **Annual Electric Light Load [kWh.m$^{-2}$]** | 2.8 |

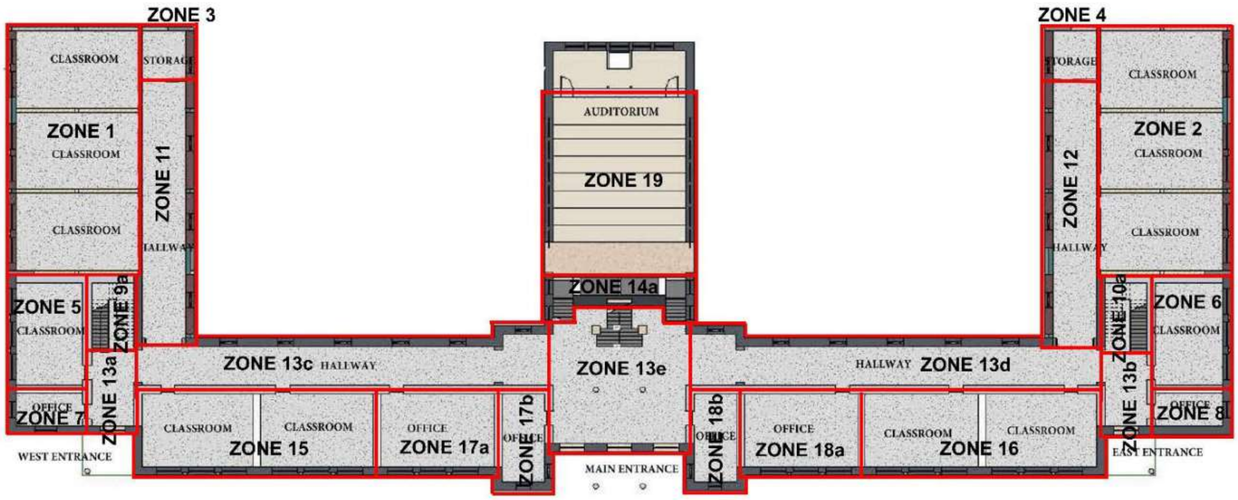


*Figure 23 Thermal zones of the ground floor*

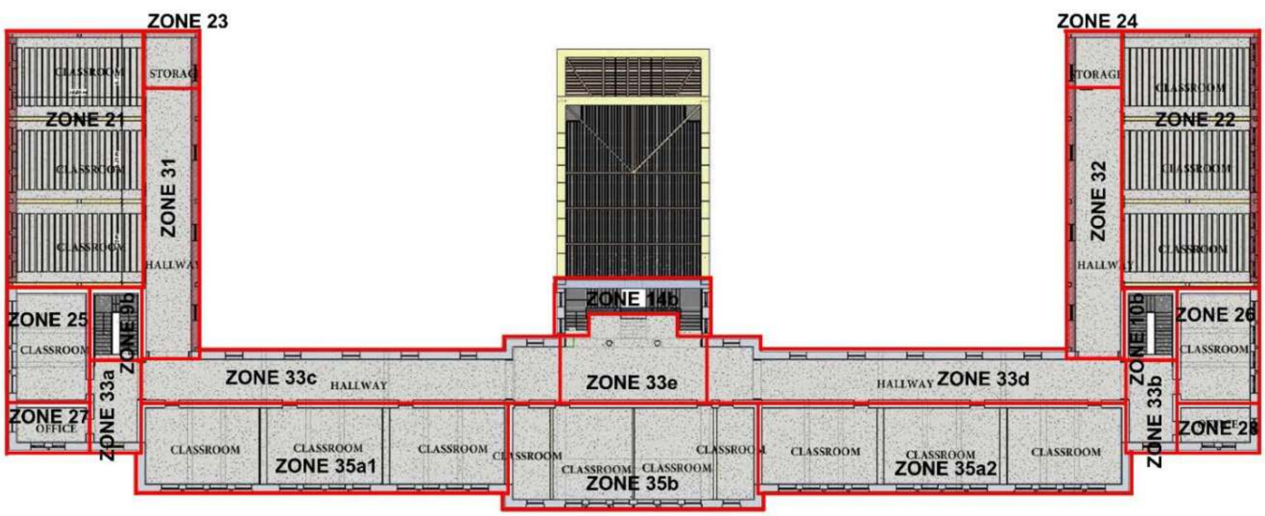


*Figure 24 Thermal zones of the first floor*

Table 29 Current-state annual heating, cooling and electric light loads' results per thermal zone

| Thermal Zone | Annual Heating Load [kWh.m-2] | Annual Cooling Load [kWh.m-2] | Annual Electric Light Load [kWh.m-2] |
|---|---|---|---|
| Zone1 | 27.3 | 0 | 5.8 |
| Zone2 | 26.7 | 0 | 5.6 |
| Zone3 | 119.8 | 0 | 0 |
| Zone4 | 120.1 | 0 | 0 |
| Zone5 | 35.9 | 0.1 | 2.7 |
| Zone6 | 35.6 | 0.2 | 2.7 |
| Zone7 | 94.6 | 0 | 1.7 |
| Zone8 | 93.4 | 0 | 1.6 |
| Zone9a | 6.7 | 0 | 1.9 |
| Zone10a | 7.1 | 0 | 1.9 |
| Zone11 | 40.6 | 0 | 2.6 |
| Zone12 | 37.6 | 0 | 2.6 |
| Zone13a | 11.7 | 0 | 4 |
| Zone13b | 12.3 | 0 | 4 |
| Zone13c | 47.9 | 0 | 1.8 |
| Zone13d | 51.4 | 0 | 1.8 |
| Zone13e | 21.2 | 0 | 1.8 |
| Zone14a | 71 | 0 | 2.3 |
| Zone15 | 23.9 | 0.1 | 2 |
| Zone16 | 23.8 | 0.1 | 2 |
| Zone17a | 18 | 0 | 3.2 |
| Zone18a | 18 | 0 | 3.2 |
| Zone17b | 33.9 | 0 | 2.2 |
| Zone18b | 34 | 0 | 2.2 |
| Zone19 | 78.1 | 0.2 | 0.9 |
| Zone21 | 59.1 | 1.3 | 4.2 |
| Zone22 | 58.8 | 1.3 | 4.2 |
| Zone23 | 248.6 | 0.7 | 0 |
| Zone24 | 249.4 | 0.7 | 0 |
| Zone25 | 64.1 | 2.4 | 2 |
| Zone26 | 63.8 | 2.3 | 1.9 |
| Zone27 | 153.3 | 1.7 | 1.7 |
| Zone28 | 152.5 | 1.7 | 1.6 |
| Zone9b | 21.8 | 1.2 | 3.9 |
| Zone10b | 22.4 | 1.1 | 3.9 |
| Zone31 | 169.8 | 0.5 | 2.6 |
| Zone32 | 160.4 | 0.3 | 2.6 |
| Zone33a | 30.6 | 1.4 | 4 |
| Zone33b | 30.8 | 1.6 | 4 |
| Zone33c | 107.5 | 0 | 1.8 |
| Zone33d | 115.7 | 0 | 1.8 |
| Zone33e | 62.8 | 0 | 0.5 |
| Zone14b | 179.7 | 0.2 | 1.2 |
| Zone35a1 | 35 | 2.7 | 2.5 |
| Zone35a2 | 34.7 | 2.4 | 2.5 |
| Zone35b | 54.5 | 1.5 | 1.63 |

The thermal zones that have a higher annual heating load than the average, are the zones with a higher area percentage towards the exterior air, like zones 3,4,7,8,27,28,14b and especially the ones that have in addition a ceiling towards the exterior air, like zones 23,24,31 and 32 (Table 29, Figures 23,24,25,26).

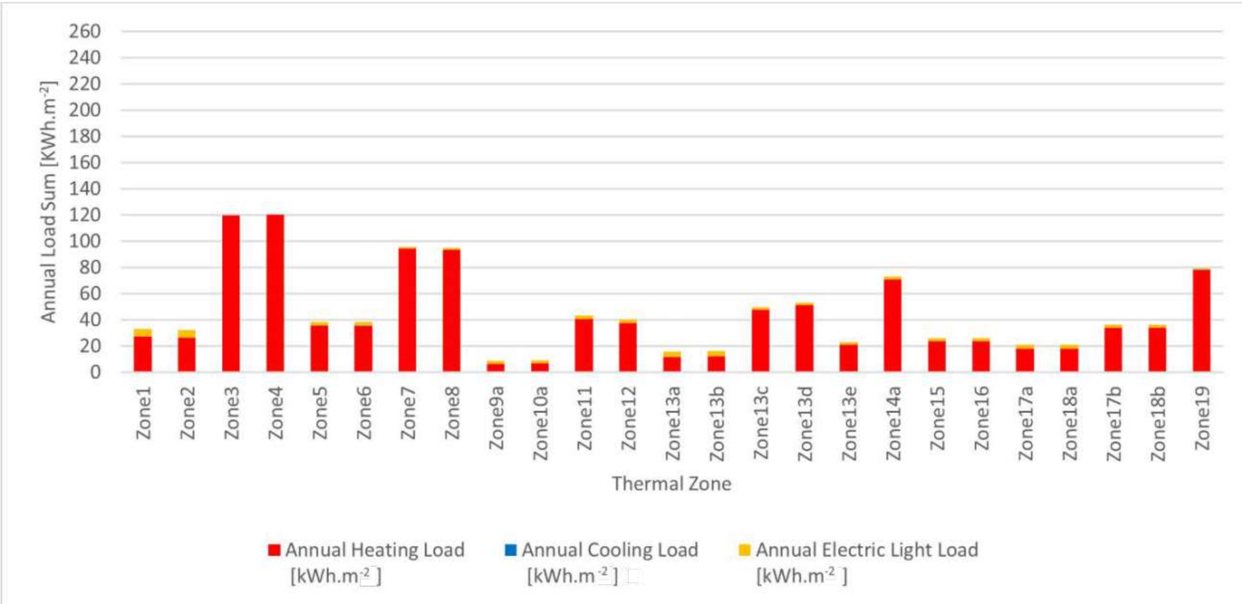


*Figure 25 Annual Load Sum of each Ground Floor Thermal Zone*

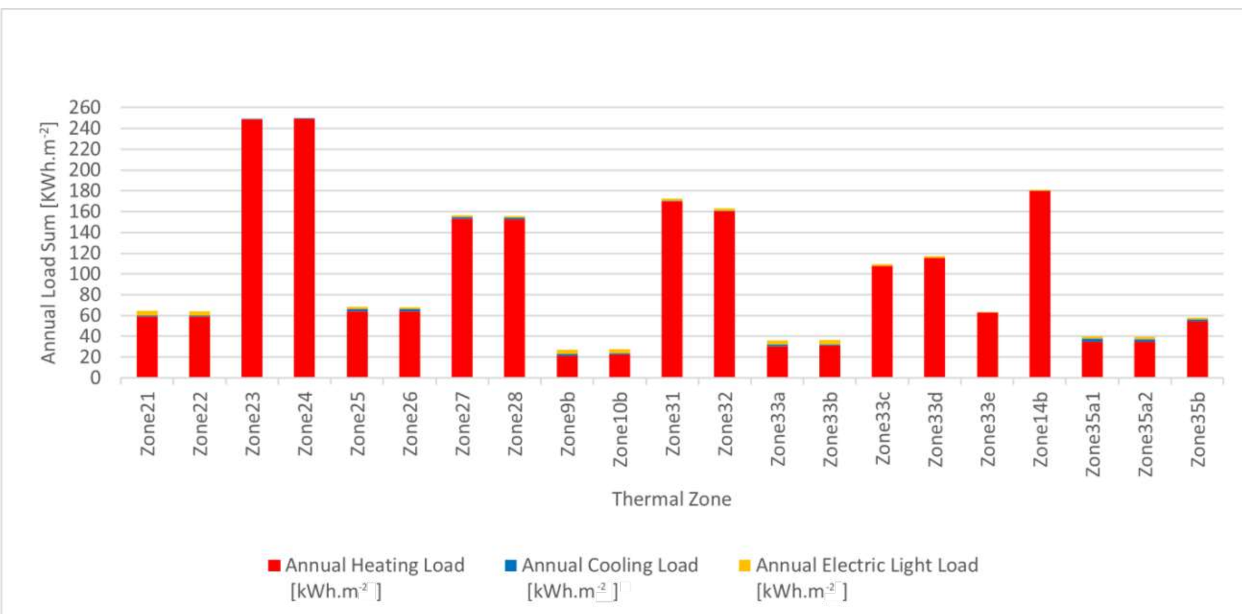


*Figure 26 Annual Load Sum of each First Floor Thermal Zone*

Also, the zones of the first floor have a higher average annual heating load than the ones of the ground floor by 55.9% (Table 30), again because they are more exposed to the exterior air.

Table 30 Current-state annual heating load per floor

| | |
|---|---|
| **Annual Heating Load – Ground Floor [kWh.m$^{-2}$]** | 43.6 |
| **Annual Heating Load – First Floor [kWh.m$^{-2}$]** | 98.8 |

The cooling load is in general low (Table 29), since the school is not operating during the warmer months, but what is observed again, is that the zones of the first floor have a higher average annual cooling load than the ones of the ground floor, because of their bigger exposure towards the exterior (Table 31).

Table 31 Current-state annual cooling load per floor

| | |
|---|---|
| **Annual Cooling Load – Ground Floor [kWh.m$^{-2}$]** | 0.03 |
| **Annual Cooling Load – First Floor [kWh.m$^{-2}$]** | 1.2 |

Finally, concerning the electric light load, the loads of the zones, as well as of the whole building, come from the application of the “Always on during active occupancy hours” lighting control type which represents the actual way the school building operates (Ladybug Tools Forum, 2021). This load seems to be higher for zones 1,21 and 2,22 which face the west and east respectively and are zones with a bigger depth compared to the rest (Table 29, Figures 23,24). Also, the entrance and stairs’ zones 13a,13b,33a,33b,9b and 10b, seem to have a higher electric light load compared to most of the other zones, due to the low visible transmittance of their openings (Table 29, Figures 23,24). The zones of the ground floor have a higher average annual electric light load than the ones of the first floor by only 4.5%, so the difference is not considered significant (Table 32).

Table 32 Current-state annual electric light load per floor

| | |
|---|---|
| **Annual Electric Light Load – Ground Floor [kWh.m$^{-}$** | 2.42 |
| **Annual Electric Light Load – First Floor [kWh.m$^{-2}$]** | 2.31 |

### 3.1.1.2 Thermal comfort results

The thermal comfort for the whole conditioned volume during the occupancy hours of a whole year is equal to 53.8 %. The results come from the "adaptive comfort model", as already mentioned, which calculates the occupants' thermal comfort levels for solely naturally ventilated buildings and are used in this study to give only an impression of a relevant exploration (Ladybug Tools Forum, 2021).

### 3.1.2 Current state daylight simulation results

A number of representative daylight metrics were chosen in order to assess the daylight performance of each thermal zone of the selected building volume in a year. These metrics include the spatial daylight autonomy (sDA), the hourly average illuminance percentage over a certain threshold value and the hourly average uniformity percentage over a certain threshold value in a year. They were calculated through grid (analysis) points that were set every 1 m for each thermal zone, while the daylight glare probability (DGP) was also calculated for a specific point in each chosen thermal zone.

The sDA and the DGP for specific points were given directly through the simulations. For the acquisition of the other two metrics though, post-processing was necessary. For the calculation of the hourly average illuminance percentage of each thermal zone that is over a certain threshold value in a year, first the average illuminance value was calculated for each thermal zone from the values of their grid points for every hour and then the calculation of the percentage of these hourly-averaged values that is over the corresponding threshold value, followed. The same method was applied for the calculation of the hourly average uniformity percentage of each thermal zone that is over a certain threshold value in a year. The calculated daylight metrics are explained in more detail in the next subchapter.

### 3.1.2.1 sDA, illuminance, uniformity and point glare values results

Each thermal zone, according to its use, has a different minimum target illuminance ($E_T$) threshold for achieving its spatial daylight autonomy (sDA). This threshold is at 100 lx for circulation areas, corridors, and storage rooms, at 150 lx for stairs, at 300 lx for classrooms, computer practice rooms and teachers' rooms and at 500 lx for lecture halls (EN, 2011). The sDA represents the percentage of the analysis points that meet or exceed the target Illuminance $E_T$ for at least 50% of the daylight occupancy hours (Daylighting Metrics Static vs. Dynamic Assessment, 2019). As Table 33 shows, this is valid for each one of the thermal zones.

Going on to the hourly average illuminance percentage that is over a certain threshold value in a year, again, the thresholds vary according to the use of the space as mentioned above. The threshold is 100 lx for circulation areas, corridors, and storage rooms, 150 lx for stairs, 300 lx for classrooms, computer practice rooms and teachers' rooms and 500 lx for lecture halls (EN, 2011). As Table 33 shows, almost all thermal zones have their average illuminance over their threshold value for over 90% of the occupancy hours, with the exception of a few ones. The exceptions are the east and west staircases (9a,10a,9b,10b) which are not well naturally lit, although their demands are not as high. This happens due to the low visible transmittance values of the entrance doors opposite the stairs.

Table 33 Current-state sDA [%], hourly average illuminance [%] and hourly average uniformity [%] simulation results per thermal zone in a year

| Thermal Zone | sDA [%] no-shading scenarios | Hourly Average Illuminance [%] no-shading scenarios | Hourly Average Uniformity [%] no-shading scenarios |
|---|---|---|---|
| Zone1 | 100 (>=300 [lux]) | 97.1 (>=300 [lux]) | 0 |
| Zone2 | 100 (>=300 [lux]) | 98.4 (>=300 [lux]) | 0 |
| Zone3 | 100 (>=100 [lux]) | - | - |
| Zone4 | 100 (>=100 [lux]) | - | - |
| Zone5 | 100 (>=300 [lux]) | 99 (>=300 [lux]) | 13.5 |
| Zone6 | 100 (>=300 [lux]) | 99.4 (>=300 [lux]) | 3.8 |
| Zone7 | 100 (>=300 [lux]) | 99.3 (>=300 [lux]) | 0 |
| Zone8 | 100 (>=300 [lux]) | 99.4 (>=300 [lux]) | 0 |
| Zone9a | 100 (>=150 [lux]) | 66.1 (>=150 [lux]) | 100 |
| Zone10a | 100 (>=150 [lux]) | 81.7 (>=150 [lux]) | 100 |
| Zone11 | 100 (>=100 [lux]) | 98.8 (>=100 [lux]) | 0 |
| Zone12 | 99.2 (>=100 [lux]) | 98.5 (>=100 [lux]) | 0 |
| Zone13a | 100 (>=100 [lux]) | 99.7 (>=100 [lux]) | 0 |
| Zone13b | 100 (>=100 [lux]) | 99.7 (>=100 [lux]) | 0 |
| Zone13c | 100 (>=100 [lux]) | 99.4 (>=100 [lux]) | 8.9 |
| Zone13d | 100 (>=100 [lux]) | 99.4 (>=100 [lux]) | 13.7 |
| Zone13e | 100 (>=100 [lux]) | 99.2 (>=100 [lux]) | 6 |
| Zone14a | 100 (>=150 [lux]) | 97.4 (>=150 [lux]) | 83.7 |
| Zone15 | 100 (>=300 [lux]) | 99.2 (>=300 [lux]) | 0 |
| Zone16 | 100 (>=300 [lux]) | 99.2 (>=300 [lux]) | 0 |
| Zone17a | 100 (>=300 [lux]) | 99.3 (>=300 [lux]) | 0 |
| Zone18a | 100 (>=300 [lux]) | 99.3 (>=300 [lux]) | 0 |
| Zone17b | 100 (>=300 [lux]) | 94 (>=300 [lux]) | 0 |
| Zone18b | 100 (>=300 [lux]) | 94 (>=300 [lux]) | 0 |
| Zone19 | 100 (>=500 [lux]) | 95.9 (>=500 [lux]) | 37.8 |
| Zone21 | 100 (>=300 [lux]) | 96.8 (>=300 [lux]) | 0 |
| Zone22 | 100 (>=300 [lux]) | 98.3 (>=300 [lux]) | 12.6 |
| Zone23 | 100 (>=100 [lux]) | - | - |
| Zone24 | 100 (>=100 [lux]) | - | - |
| Zone25 | 100 (>=300 [lux]) | 98.9 (>=300 [lux]) | 38 |
| Zone26 | 100 (>=300 [lux]) | 99.3 (>=300 [lux]) | 17 |
| Zone27 | 100 (>=300 [lux]) | 99.3 (>=300 [lux]) | 0 |
| Zone28 | 100 (>=300 [lux]) | 99.3 (>=300 [lux]) | 0 |
| Zone9b | 100 (>=150 [lux]) | 76.2 (>=150 [lux]) | 100 |
| Zone10b | 100 (>=150 [lux]) | 86.8 (>=150 [lux]) | 100 |
| Zone31 | 100 (>=100 [lux]) | 99.5 (>=100 [lux]) | 0 |
| Zone32 | 100 (>=100 [lux]) | 99.4 (>=100 [lux]) | 1 |
| Zone33a | 100 (>=100 [lux]) | 99.5 (>=100 [lux]) | 0 |
| Zone33b | 100 (>=100 [lux]) | 99.4 (>=100 [lux]) | 1.9 |
| Zone33c | 100 (>=100 [lux]) | 99.7 (>=100 [lux]) | 50.4 |
| Zone33d | 100 (>=100 [lux]) | 99.7 (>=100 [lux]) | 62.6 |
| Zone33e | 100 (>=100 [lux]) | 98.9 (>=100 [lux]) | 100 |
| Zone14b | 100 (>=150 [lux]) | 99.7 (>=150 [lux]) | 52.4 |
| Zone35a1 | 100 (>=300 [lux]) | 99 (>=300 [lux]) | 0 |
| Zone35a2 | 100 (>=300 [lux]) | 99 (>=300 [lux]) | 0 |
| Zone35b | 100 (>=300 [lux]) | 98.1 (>=300 [lux]) | 0 |

The hourly average uniformity percentages in a year that are over certain thresholds according to the use of the spaces, can also be seen on Table 33 and on Figures 27 and 28. The threshold is 0.4 for entrance halls, corridors, stairs, and storage rooms, and 0.6 for classrooms, lecture halls, computer practice rooms and teachers' offices (EN, 2011). The uniformity of most thermal zones is very low, mainly because they have openings on their one side only. The thermal zones with higher uniformities are the ones that represent the staircases of the building which have low average illuminances (zones 9a,10a,9b,10b,14a,14b). Finally, the thermal zones that represent the first-floor corridor towards the north (zones 33c,33d), some classrooms with a smaller depth (zones 25,26), and the amphitheater (zone 19) that has openings on both sides, also have slightly higher uniformities.

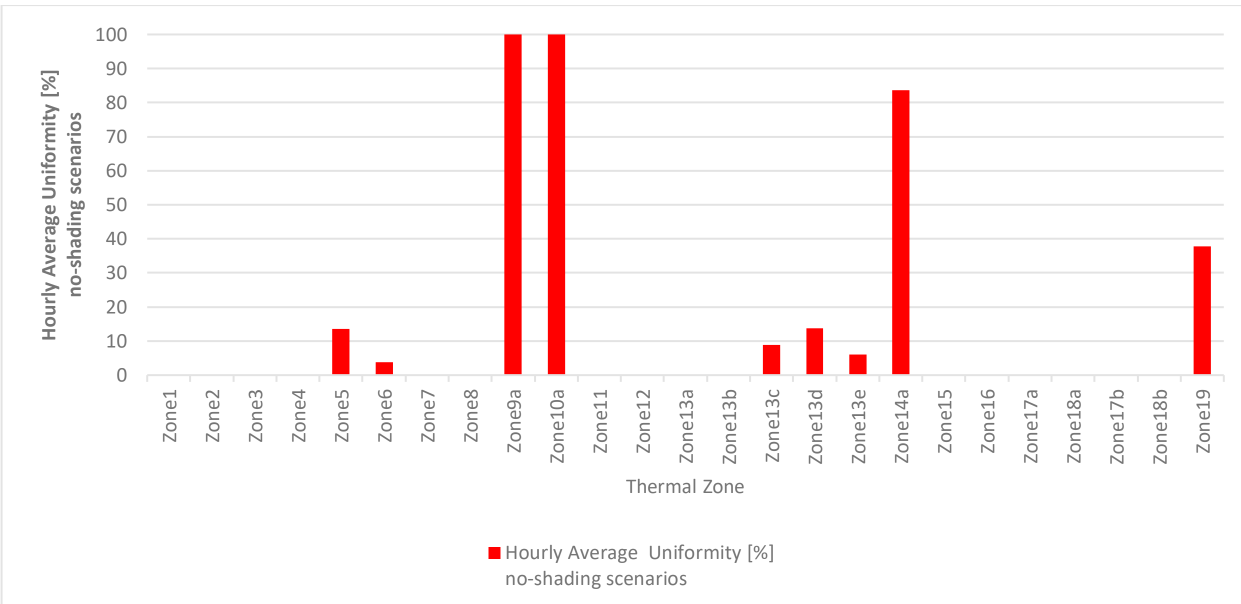


*Figure 27 Hourly Average Uniformity Percentage of each Ground Floor Thermal Zone in a Year*

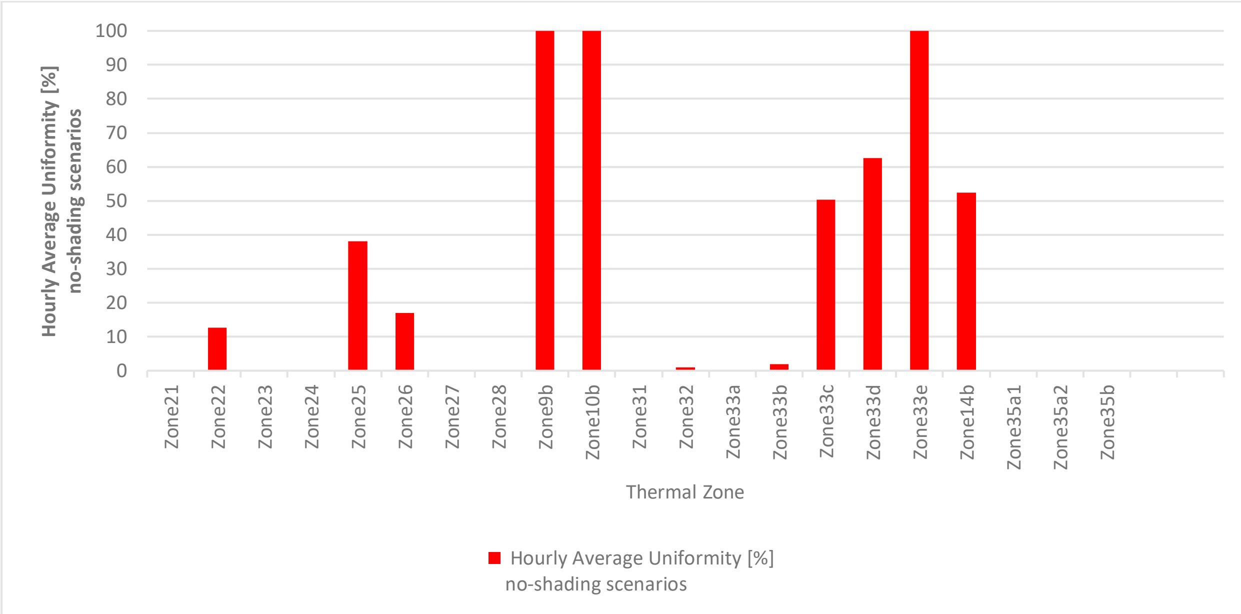


*Figure 28 Hourly Average Uniformity Percentage of each First Floor Thermal Zone in a Year*

It has to be noted here, that Grasshopper calculates the sDA only for no-shading scenarios (Ladybug Tools Forum, 2021). As a result, the sDA, refers to values without the effect of dynamic shading. The hourly average illuminance percentage and the hourly average uniformity percentage metrics mentioned above are also calculated for no-shading scenarios.

Still, the hourly average illuminance percentage and the hourly uniformity percentage metrics, together with the DGP for a specific point, were also calculated for dynamic-shading scenarios for each one of the two selected thermal zones. Those are zone 6 facing the east and zone 17a facing the south, both on the ground floor (Figure 23). Only two thermal zones were selected for these metrics with dynamic shading, due to the fact that the calculation time demanded for such a simulation is very high. For the shading, semi-open weave draperies of a medium color were chosen, according to suggestions stated in CE Center (2022). The results for the two zones can be seen on Tables 34,35,36.

Table 34 shows the hourly average illuminance percentage that is over the threshold value of 300 lx for dynamic-shading scenarios of the two selected thermal zones. We can see that these results are slightly different compared to the corresponding ones of the no-shading scenarios of the two zones. This is due to the use of the daysim simulation engine instead of the radiance one. Still, the differences are so slight that they can be ignored and the conclusion that is reached is that the hourly average illuminance [%] over the defined threshold value for both zones is not affected by the application of interior shading.

Table 34 Hourly average illuminance [%] over 300 lx for dynamic-shading scenarios of the two selected thermal zones in a year

| | |
|---|---|
| **Zone 6** | 99.4 |
| **Zone 17a** | 99.5 |

Table 35 shows the hourly uniformity percentages that are over the threshold value of 0.6 for dynamic-shading scenarios of the two selected thermal zones. It is observed that the hourly uniformity percentage over 0.6 of zone 6 slightly rises once shading is applied, due to the decrease of the hourly average illuminance values. On the contrary, the one of zone 17a remains to the value of 0 (comparison to corresponding results of Table 33).

Table 35 Hourly uniformity [%] over 0.6 for dynamic-shading scenarios of the two selected thermal zones in a year

| | |
|---|---|
| **Zone 6** | 6.1 |
| **Zone 17a** | 0 |

Finally, Table 36 shows the DGP [% of occupancy hours >=0.35 (Perceptible Glare)] for dynamic-shading and no-shading scenarios of the two selected thermal zones which is calculated for a specific, vulnerable to the sunlight, point of each one of the two zones (EN 17037, 2018). For the dynamic-shading scenarios, both values are below the 5 % threshold of the total time of occupation of a space. For the no-shading scenarios, it is observed that zone 17a's point DGP exceeds the threshold by far, reaching the value of 18 %. On the contrary, zone 6 maintains its point DGP below 5 %.

Table 36 DGP [% occupancy hours >=0.35 (Perceptible Glare)] for dynamic-shading and no-shading scenarios of the two selected thermal zones

| | **Dynamic-shading DGP** | **No shading DGP** |
|---|---|---|
| **Zone 6** | 1.4 | 1.7 |
| **Zone 17a** | 0.4 | 18 |

Figure 29 is the energy balance diagram of the current state of the school building, and it summarizes the sources of heat entering and leaving the thermal zones. The heat entering each thermal zone includes heat from people, heat from computers/appliances (equipment), heat from the lighting installations, solar heat through the windows, and heat from the heating system that is used. The heat losses of each thermal zone are the result of the cooling of their space. Finally, depending on the conditions, heat gains or losses can come from conduction through the building envelope, both from the opaque and the transparent building elements, but it can also be the result of natural ventilation, as well as the result of infiltration, which is the air flowing into the thermal zones through cracks in the walls that cannot be controlled. Everything above zero is heat entering the zone, and everything below zero is heat leaving the zone and these two must always be equal. That is achieved through the storage part of the diagram which is the energy that is stored in the building's mass (Hydra, 2020).

It is observed that there is a comparably high percentage of heat coming from the heating system, especially between November and March. That is because there is a demand for it due to the high percentages of heat losses that the combination of opaque conduction, glazing conduction and infiltration gives.

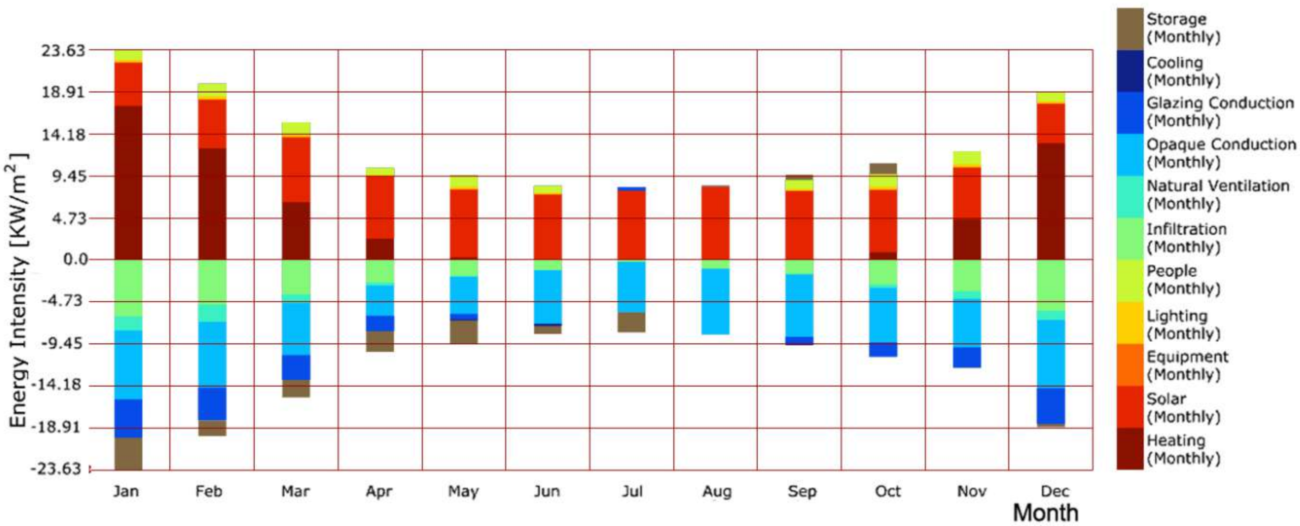


*Figure 29 Energy Balance Diagram*

## 3.2 Improvement-scenarios' simulation results

### 3.2.1 Energy simulation results of different improvement scenarios

As already mentioned, the different improvement techniques summed up to forty-eight different scenarios. The results of the energy and thermal comfort metrics of the energy simulation can be found on Table 37 "Iterative energy simulation results of the parametric, improved model for the whole conditioned volume".

In the next chapters the different scenarios will be arranged in reference to the different values of their different loads' results, as well as of the different percentages of thermal comfort results.

Table 37 Iterative energy simulation results of the parametric, improved model for the whole conditioned volume

| | Wall Insulation Thickness [m] | Floor/Ceiling Insulation Thickness [m] | Window U-value [W.m$^{-2}$.K$^{-1}$] | Interior Shade Transmittance | Light Shelf (0=yes) (1=no) | Heating Load [kWh.m$^{-2}$] | Cooling Load [kWh.m$^{-2}$] | Electric Light Load [kWh.m$^{-2}$] | Percent of Time Comfortable [%] |
|---|---|---|---|---|---|---|---|---|---|
| Scenario 1 | 0.08 | 0.05 | 1.59 | 0.6 | 0 | 21.2 | 0.9 | 2.7 | 77.1 |
| Scenario 2 | 0.16 | 0.05 | 1.59 | 0.6 | 0 | 19.1 | 1 | 2.7 | 77.2 |
| Scenario 3 | 0.08 | 0.1 | 1.59 | 0.6 | 0 | 20.2 | 1 | 2.7 | 76.5 |
| Scenario 4 | 0.16 | 0.1 | 1.59 | 0.6 | 0 | 18.1 | 1.1 | 2.7 | 76.4 |
| Scenario 5 | 0.08 | 0.05 | 2.67 | 0.6 | 0 | 21.3 | 1.4 | 2.7 | 74.7 |
| Scenario 6 | 0.16 | 0.05 | 2.67 | 0.6 | 0 | 19.2 | 1.5 | 2.7 | 74.6 |
| Scenario 7 | 0.08 | 0.1 | 2.67 | 0.6 | 0 | 20.4 | 1.6 | 2.7 | 74.3 |
| Scenario 8 | 0.16 | 0.1 | 2.67 | 0.6 | 0 | 18.3 | 1.7 | 2.7 | 73.9 |
| Scenario 9 | 0.08 | 0.05 | 1.3 | 0.6 | 0 | 22.8 | 0.6 | 2.8 | 78.9 |
| Scenario 10 | 0.16 | 0.05 | 1.3 | 0.6 | 0 | 20.7 | 0.6 | 2.8 | 79.5 |
| Scenario 11 | 0.08 | 0.1 | 1.3 | 0.6 | 0 | 21.8 | 0.6 | 2.8 | 78.9 |
| Scenario 12 | 0.16 | 0.1 | 1.3 | 0.6 | 0 | 19.7 | 0.7 | 2.8 | 79.3 |
| Scenario 13 | 0.08 | 0.05 | 1.59 | 0.45 | 0 | 21.2 | 0.9 | 2.7 | 77.1 |
| Scenario 14 | 0.16 | 0.05 | 1.59 | 0.45 | 0 | 19.2 | 1 | 2.7 | 77.3 |
| Scenario 15 | 0.08 | 0.1 | 1.59 | 0.45 | 0 | 20.3 | 1 | 2.7 | 76.5 |
| Scenario 16 | 0.16 | 0.1 | 1.59 | 0.45 | 0 | 18.2 | 1.1 | 2.7 | 76.4 |
| Scenario 17 | 0.08 | 0.05 | 2.67 | 0.45 | 0 | 21.4 | 1.4 | 2.7 | 75 |
| Scenario 18 | 0.16 | 0.05 | 2.67 | 0.45 | 0 | 19.3 | 1.5 | 2.7 | 74.7 |
| Scenario 19 | 0.08 | 0.1 | 2.67 | 0.45 | 0 | 20.4 | 1.6 | 2.7 | 74.4 |
| Scenario 20 | 0.16 | 0.1 | 2.67 | 0.45 | 0 | 18.4 | 1.7 | 2.7 | 74.1 |
| Scenario 21 | 0.08 | 0.05 | 1.3 | 0.45 | 0 | 22.8 | 0.6 | 2.8 | 78.9 |
| Scenario 22 | 0.16 | 0.05 | 1.3 | 0.45 | 0 | 20.8 | 0.6 | 2.8 | 79.5 |
| Scenario 23 | 0.08 | 0.1 | 1.3 | 0.45 | 0 | 21.8 | 0.6 | 2.8 | 78.9 |
| Scenario 24 | 0.16 | 0.1 | 1.3 | 0.45 | 0 | 19.7 | 0.7 | 2.8 | 79.3 |
| Scenario 25 | 0.08 | 0.05 | 1.59 | 0.6 | 1 | 21.2 | 0.9 | 2.7 | 77.1 |
| Scenario 26 | 0.16 | 0.05 | 1.59 | 0.6 | 1 | 19.1 | 1 | 2.7 | 77.2 |
| Scenario 27 | 0.08 | 0.1 | 1.59 | 0.6 | 1 | 20.2 | 1 | 2.7 | 76.5 |
| Scenario 28 | 0.16 | 0.1 | 1.59 | 0.6 | 1 | 18.1 | 1.1 | 2.7 | 76.4 |
| Scenario 29 | 0.08 | 0.05 | 2.67 | 0.6 | 1 | 21.3 | 1.4 | 2.7 | 74.7 |
| Scenario 30 | 0.16 | 0.05 | 2.67 | 0.6 | 1 | 19.2 | 1.5 | 2.7 | 74.6 |
| Scenario 31 | 0.08 | 0.1 | 2.67 | 0.6 | 1 | 20.4 | 1.6 | 2.7 | 74.3 |
| Scenario 32 | 0.16 | 0.1 | 2.67 | 0.6 | 1 | 18.3 | 1.7 | 2.7 | 73.9 |
| Scenario 33 | 0.08 | 0.05 | 1.3 | 0.6 | 1 | 22.8 | 0.6 | 2.8 | 78.9 |
| Scenario 34 | 0.16 | 0.05 | 1.3 | 0.6 | 1 | 20.7 | 0.6 | 2.8 | 79.5 |
| Scenario 35 | 0.08 | 0.1 | 1.3 | 0.6 | 1 | 21.8 | 0.6 | 2.8 | 78.9 |
| Scenario 36 | 0.16 | 0.1 | 1.3 | 0.6 | 1 | 19.7 | 0.7 | 2.8 | 79.3 |
| Scenario 37 | 0.08 | 0.05 | 1.59 | 0.45 | 1 | 21.2 | 0.9 | 2.7 | 77.1 |
| Scenario 38 | 0.16 | 0.05 | 1.59 | 0.45 | 1 | 19.2 | 1 | 2.7 | 77.3 |
| Scenario 39 | 0.08 | 0.1 | 1.59 | 0.45 | 1 | 20.3 | 1 | 2.7 | 76.5 |
| Scenario 40 | 0.16 | 0.1 | 1.59 | 0.45 | 1 | 18.2 | 1.1 | 2.7 | 74.4 |
| Scenario 41 | 0.08 | 0.05 | 2.67 | 0.45 | 1 | 21.4 | 1.4 | 2.7 | 74.9 |
| Scenario 42 | 0.16 | 0.05 | 2.67 | 0.45 | 1 | 19.3 | 1.5 | 2.7 | 74.8 |
| Scenario 43 | 0.08 | 0.1 | 2.67 | 0.45 | 1 | 20.4 | 1.6 | 2.7 | 74.5 |
| Scenario 44 | 0.16 | 0.1 | 2.67 | 0.45 | 1 | 18.4 | 1.7 | 2.7 | 74.1 |
| Scenario 45 | 0.08 | 0.05 | 1.3 | 0.45 | 1 | 22.8 | 0.6 | 2.8 | 78.9 |
| Scenario 46 | 0.16 | 0.05 | 1.3 | 0.45 | 1 | 20.8 | 0.6 | 2.8 | 79.5 |
| Scenario 47 | 0.08 | 0.1 | 1.3 | 0.45 | 1 | 21.8 | 0.6 | 2.8 | 78.9 |
| Scenario 48 | 0.16 | 0.1 | 1.3 | 0.45 | 1 | 19.7 | 0.7 | 2.8 | 79.3 |
| Current State | - | - | 4.7 | 0.36 | 1 | 58.8 | 0.6 | 2.8 | 53.8 |

### 3.2.1.1 Heating, cooling and electric light loads results

Figure 30 and Table 38 show all the combinations of the different retrofit options that give the annual heating load results from the lowest to the highest value. As it can be observed on Table 38, the addition of a light shelf does not affect the annual heating load when the rest of the retrofit options remain the same. Scenarios 4 and 28 give the lowest heating load results which are both equal to 18.1 $kWh.m^{-2}$, while the highest heating load results are observed in scenarios 9,33,21,45 and they are all equal to 22.8 $kWh.m^{-2}$. As we go through the scenarios, it can be seen that the combination of a thicker wall insulation and a thicker floor/ceiling insulation, together with a window U-value equal to 1.59 $W.m^{-2}.K^{-1}$, according to the NFRC directory (2021), and a higher interior shade transmittance gives the best performance concerning the heating load. In the case of the worst performance, the combination of a thinner wall insulation and a thinner floor/ceiling insulation, together with a window U-value equal to 1.30 $W.m^{-2}.K^{-1}$ is observed. In these cases, the two interior shade transmittance alternatives that are given, do not affect the result.

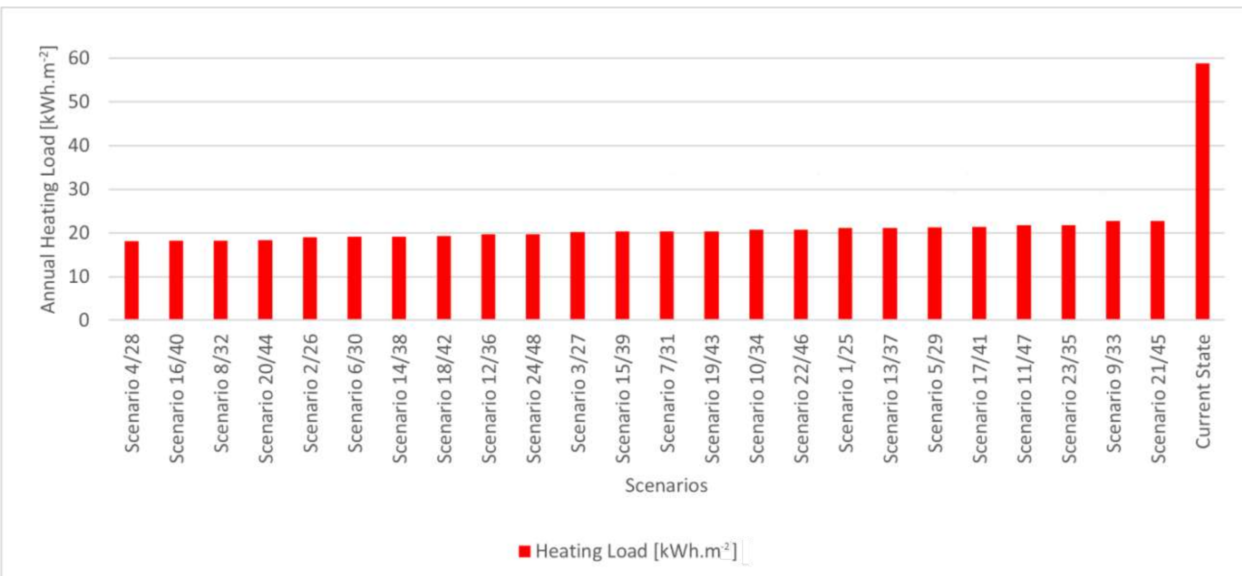


*Figure 30 Annual Heating Load per Scenario [$kWh.m^{-2}$]*

Table 38 Iterative energy simulation results of the parametric, improved model for the whole conditioned volume from the lowest to the highest value of the annual heating load results

| | Wall Insulation Thickness [m] | Floor/Ceiling Insulation Thickness [m] | Window U-value [$W.m^{-2}.K^{-1}$] | Interior Shade Transmittance | Light Shelf (0=yes) (1=no) | Heating Load [$kWh.m^{-2}$] |
|---|---|---|---|---|---|---|
| Scenario 4/28 | 0.16 | 0.1 | 1.59 | 0.6 | 0/1 | 18.1 |
| Scenario 16/40 | 0.16 | 0.1 | 1.59 | 0.45 | 0/1 | 18.2 |
| Scenario 8/32 | 0.16 | 0.1 | 2.67 | 0.6 | 0/1 | 18.3 |
| Scenario 20/44 | 0.16 | 0.1 | 2.67 | 0.45 | 0/1 | 18.4 |
| Scenario 2/26 | 0.16 | 0.05 | 1.59 | 0.6 | 0/1 | 19.1 |
| Scenario 6/30 | 0.16 | 0.05 | 2.67 | 0.6 | 0/1 | 19.2 |
| Scenario 14/38 | 0.16 | 0.05 | 1.59 | 0.45 | 0/1 | 19.2 |
| Scenario 18/42 | 0.16 | 0.05 | 2.67 | 0.45 | 0/1 | 19.3 |
| Scenario 12/36 | 0.16 | 0.1 | 1.3 | 0.6 | 0/1 | 19.7 |
| Scenario 24/48 | 0.16 | 0.1 | 1.3 | 0.45 | 0/1 | 19.7 |
| Scenario 3/27 | 0.08 | 0.1 | 1.59 | 0.6 | 0/1 | 20.2 |
| Scenario 15/39 | 0.08 | 0.1 | 1.59 | 0.45 | 0/1 | 20.3 |
| Scenario 7/31 | 0.08 | 0.1 | 2.67 | 0.6 | 0/1 | 20.4 |
| Scenario 19/43 | 0.08 | 0.1 | 2.67 | 0.45 | 0/1 | 20.4 |
| Scenario 10/34 | 0.16 | 0.05 | 1.3 | 0.6 | 0/1 | 20.7 |
| Scenario 22/46 | 0.16 | 0.05 | 1.3 | 0.45 | 0/1 | 20.8 |
| Scenario 1/25 | 0.08 | 0.05 | 1.59 | 0.6 | 0/1 | 21.2 |
| Scenario 13/37 | 0.08 | 0.05 | 1.59 | 0.45 | 0/1 | 21.2 |
| Scenario 5/29 | 0.08 | 0.05 | 2.67 | 0.6 | 0/1 | 21.3 |
| Scenario 17/41 | 0.08 | 0.05 | 2.67 | 0.45 | 0/1 | 21.4 |
| Scenario 11/47 | 0.08 | 0.1 | 1.3 | 0.45 | 0/1 | 21.8 |
| Scenario 23/35 | 0.08 | 0.1 | 1.3 | 0.6 | 0/1 | 21.8 |
| Scenario 9/33 | 0.08 | 0.05 | 1.3 | 0.6 | 0/1 | 22.8 |
| Scenario 21/45 | 0.08 | 0.05 | 1.3 | 0.45 | 0/1 | 22.8 |
| Current State | - | - | 4.7 | 0.36 | 1 | 58.8 |

Table 39 shows the highest and the lowest annual heating load results for the two chosen thermal zones (zones 6 and 17a). Thermal zone 6 is located on the ground floor and it is facing towards the east. As it can be seen on Table 39, scenarios 4,14,16,27,29 and 39 give the lowest annual heating load results which are all equal to 21.0 $kWh.m^{-2}$. This means that they are higher than the lowest annual heating load of the whole conditioned volume by 16.0 %. The highest annual heating load results are observed in scenarios 9,11,22,24,34,36,46 and 48 and they are all equal to 22.6 $kWh.m^{-2}$ which is lower than the highest annual heating load of the whole conditioned volume by 0.9 %. The best performances in this case are given through the combination of a thicker wall insulation and a window U-value equal to 1.59 $W.m^{-2}.K^{-1}$, while the floor/ceiling insulation thickness, the interior energy transmittance value and the existence of a light shelf do not affect the result. The worst performances are given through the combination of a thinner wall insulation and a window U-value equal to 1.30 $W.m^{-2}.K^{-1}$, while the floor/ceiling insulation thickness, the interior shade transmittance value and the existence of a light shelf do not affect the result.

Thermal zone 17a is located on the ground floor and it is facing towards the south. As it can be seen on Table 39, scenarios 8,20,32 and 44 give the lowest annual heating load results which are all equal to 9.6 kWh.m$^{-2}$. This means that they are lower than the lowest annual heating load of the whole conditioned volume by 47.0 %. The highest annual heating load results are observed in scenarios 21 and 45 and they are both equal to 11.6 kWh.m$^{-2}$ which is lower than the highest annual heating load of the whole conditioned volume by 49.1 %. The best performances in this case are given through the combination of a thicker wall insulation, a thicker floor/ceiling insulation and a window U-value equal to 2.67 W.m$^{-2}$.K$^{-1}$, while the interior shade transmittance value and the existence of a light shelf do not affect the result. The worst performances are given through the combination of a thinner wall insulation, a thinner floor/ceiling insulation, a window U-value equal to 1.30 W.m$^{-2}$.K$^{-1}$, and a lower interior shade transmittance, while the existence of a light shelf does not affect the result.

Table 39 Iterative energy simulation results of the parametric, improved model for thermal zones 6 and 17a. The lowest and the highest values of the annual heating load of each thermal zone are given

| | | Wall Insulation Thickness [m] | Floor/Ceiling Insulation Thickness [m] | Window U-value [W.m$^{-2}$.K$^{-1}$] | Interior Shade Transmittance | Light Shelf (0=yes) (1=no) | Annual Heating Load [kWh.m$^{-2}$] |
|---|---|---|---|---|---|---|---|
| Zone 6 lowest | Scenario 4 | 0.16 | 0.1 | 1.59 | 0.6 | 0 | 21 |
| | Scenario 14 | 0.16 | 0.05 | 1.59 | 0.45 | 0 | 21 |
| | Scenario 16 | 0.16 | 0.1 | 1.59 | 0.45 | 0 | 21 |
| | Scenario 27 | 0.16 | 0.05 | 1.59 | 0.6 | 1 | 21 |
| | Scenario 29 | 0.16 | 0.1 | 1.59 | 0.6 | 1 | 21 |
| | Scenario 39 | 0.16 | 0.05 | 1.59 | 0.45 | 1 | 21 |
| Zone 6 highest | Scenario 9 | 0.08 | 0.05 | 1.3 | 0.6 | 0 | 22.6 |
| | Scenario 11 | 0.08 | 0.1 | 1.3 | 0.6 | 0 | 22.6 |
| | Scenario 22 | 0.08 | 0.05 | 1.3 | 0.45 | 0 | 22.6 |
| | Scenario 24 | 0.08 | 0.1 | 1.3 | 0.45 | 0 | 22.6 |
| | Scenario 34 | 0.08 | 0.05 | 1.3 | 0.6 | 1 | 22.6 |
| | Scenario 36 | 0.08 | 0.1 | 1.3 | 0.6 | 1 | 22.6 |
| | Scenario 46 | 0.08 | 0.05 | 1.3 | 0.45 | 1 | 22.6 |
| | Scenario 48 | 0.08 | 0.1 | 1.3 | 0.45 | 1 | 22.6 |
| Zone6 Current State | | | | 4.7 | 0.36 | 1 | 35.6 |
| Zone 17a lowest | Scenario 8 | 0.16 | 0.1 | 2.67 | 0.6 | 0 | 9.6 |
| | Scenario 20 | 0.16 | 0.1 | 2.67 | 0.45 | 0 | 9.6 |
| | Scenario 32 | 0.16 | 0.1 | 2.67 | 0.6 | 1 | 9.6 |
| | Scenario 44 | 0.16 | 0.1 | 2.67 | 0.45 | 1 | 9.6 |
| Zone 17a highest | Scenario 21 | 0.08 | 0.05 | 1.3 | 0.45 | 0 | 11.6 |
| | Scenario 45 | 0.08 | 0.05 | 1.3 | 0.45 | 1 | 11.6 |
| Zone17a Current State | | | | 4.7 | 0.36 | 1 | 18 |

Figure 31 shows the reduction percentage of the annual heating load of each one of the scenarios studied in comparison to the annual heating load of the current state of the building. The best-performing scenarios (scenarios 4 and 28) have an annual heating load 69.2 % smaller than the current state's, while the worst-performing ones (scenarios 9,33,21,45) have an annual heating load 61.2 % smaller than the current state's.

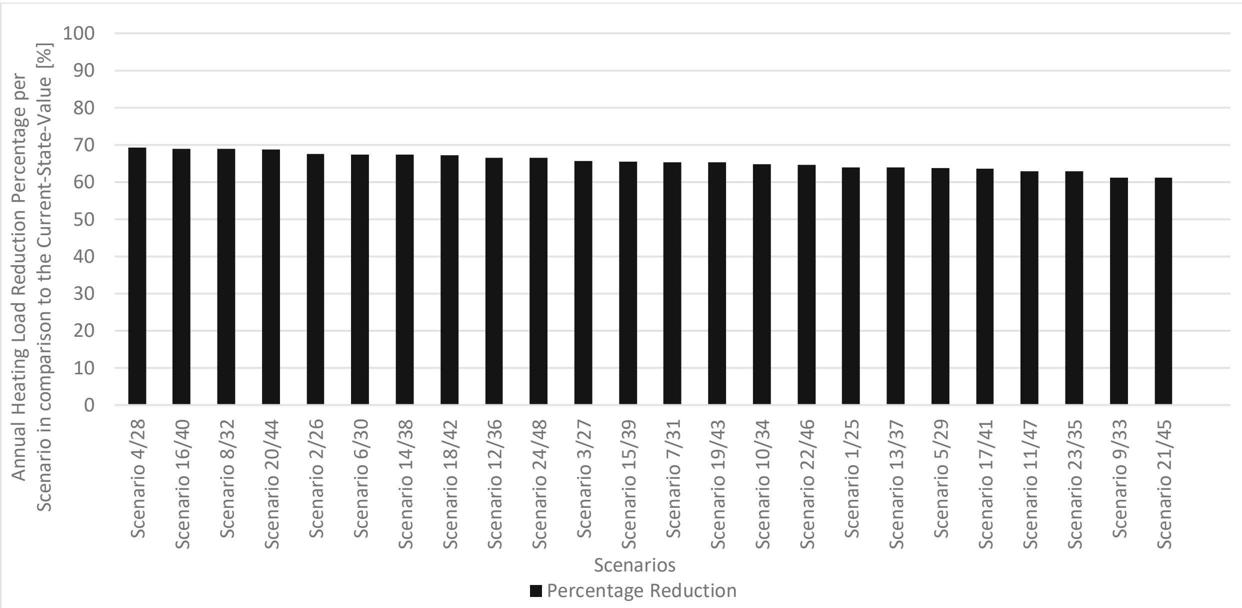


*Figure 31 Annual Heating Load Reduction Percentage per Scenario in comparison to the Current-State-Value [%]*

Figure 32 shows the reduction percentage of the annual heating load of each one of the extreme scenarios of the two chosen thermal zones above (6 and 17a) in comparison to the annual heating load of the current state of each one of the two thermal zones, respectively. The best-performing scenarios of thermal zone 6 (scenarios 4,14,16,27,29 and 39) have an annual heating load 41.0 % smaller than the current state's, while the worst-performing ones (scenarios 9,11,22,24,34,36,46 and 48) have an annual heating load 36.5 % smaller than the current state's. The best-performing scenarios of thermal zone 17a (scenarios 8,20,32 and 44) have an annual heating load 46.7 % smaller than the current state's, while the worst-performing ones (scenarios 21 and 45) have an annual heating load 35.6 % smaller than the current state's.

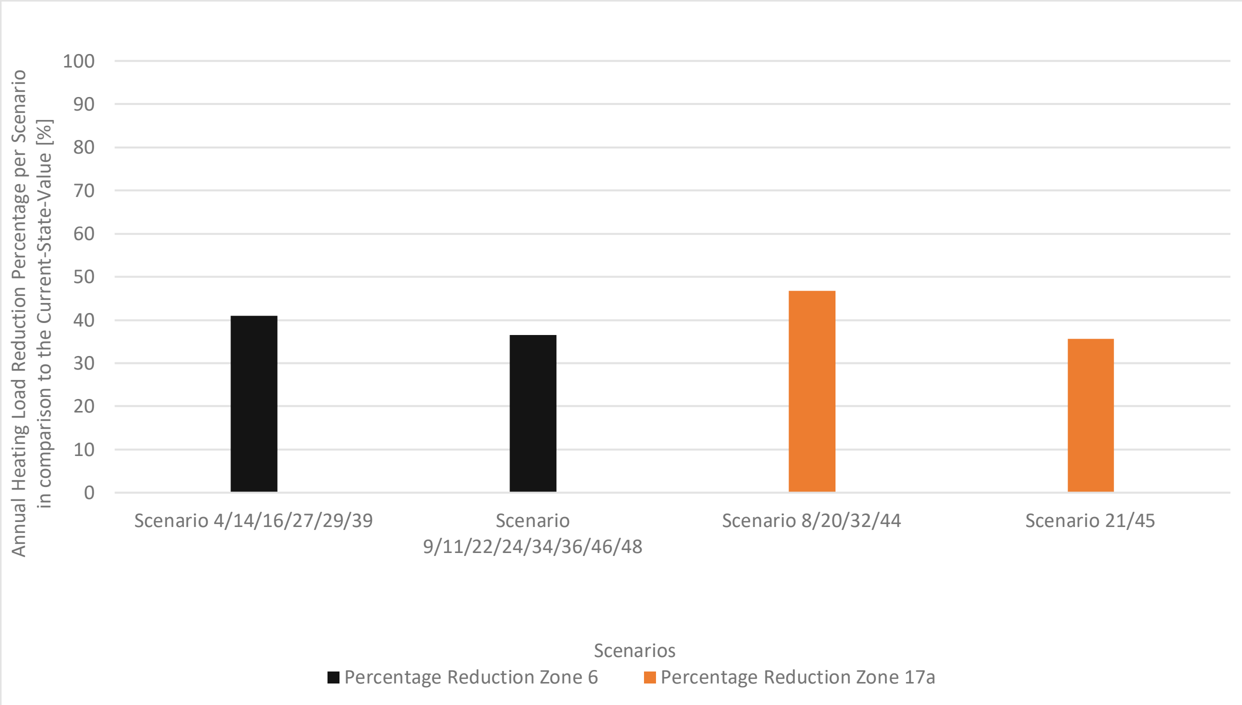


*Figure 32 Annual Heating Load Reduction Percentage per Extreme Scenario of thermal zones 6 and 17a in comparison to the Current-State-Value [%]*

Moving on to the analysis of the annual cooling load separately (Figure 33, Table 40), it is observed that scenarios 10,34,22,46,11,47,23,35,9,33,21 and 45 give the lowest cooling load results which are all equal to 0.6 kWh.m$^{-2}$, while the highest cooling load results are observed in scenarios 8,32,20 and 44 and they are all equal to 1.7 kWh.m$^{-2}$. In this case, it can be observed as we go through the scenarios, that the parameter that mainly impacts the result is the window U-value. The lower the window U-value, the lower the cooling load. Still, the cooling load is in all scenarios low in comparison to the heating load and the value differences are not significant, as the school does not operate during the warmer months (second half of June, July, August, first half of September).

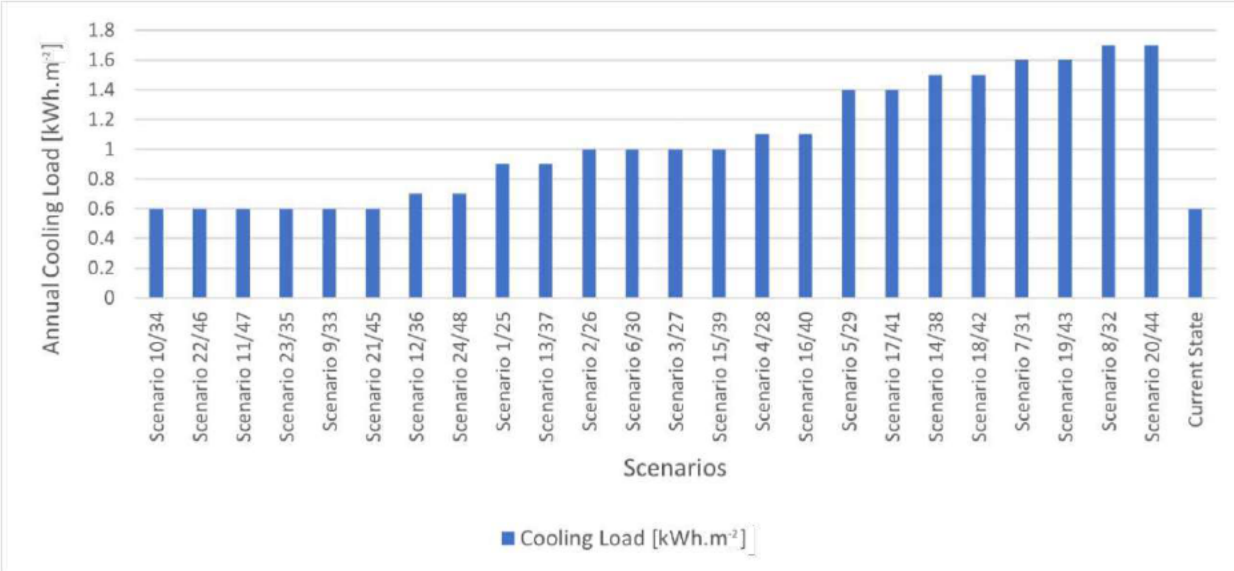


*Figure 33 Annual Cooling Load per Scenario [kWh.m$^{-2}$]*

Table 40 Iterative energy simulation results of the parametric, improved model for the whole conditioned volume from the lowest to the highest value of the annual cooling load results

| | Wall Insulation Thickness [m] | Floor/Ceiling Insulation Thickness [m] | Window U-value [W.m$^{-2}$.K$^{-1}$] | Interior Shade Transmittance | Light Shelf (0=yes) (1=no) | Cooling Load [kWh.m$^{-2}$] |
|---|---|---|---|---|---|---|
| Scenario 10/34 | 0.16 | 0.05 | 1.3 | 0.6 | 0/1 | 0.6 |
| Scenario 22/46 | 0.16 | 0.05 | 1.3 | 0.45 | 0/1 | 0.6 |
| Scenario 11/47 | 0.08 | 0.1 | 1.3 | 0.6 | 0/1 | 0.6 |
| Scenario 23/35 | 0.08 | 0.1 | 1.3 | 0.45 | 0/1 | 0.6 |
| Scenario 9/33 | 0.08 | 0.05 | 1.3 | 0.6 | 0/1 | 0.6 |
| Scenario 21/45 | 0.08 | 0.05 | 1.3 | 0.45 | 0/1 | 0.6 |
| Scenario 12/36 | 0.16 | 0.1 | 1.3 | 0.6 | 0/1 | 0.7 |
| Scenario 24/48 | 0.16 | 0.1 | 1.3 | 0.45 | 0/1 | 0.7 |
| Scenario 1/25 | 0.08 | 0.05 | 1.59 | 0.6 | 0/1 | 0.9 |
| Scenario 13/37 | 0.08 | 0.05 | 1.59 | 0.45 | 0/1 | 0.9 |
| Scenario 2/26 | 0.16 | 0.05 | 1.59 | 0.6 | 0/1 | 1 |
| Scenario 14/38 | 0.16 | 0.05 | 1.59 | 0.45 | 0/1 | 1 |
| Scenario 3/27 | 0.08 | 0.1 | 1.59 | 0.6 | 0/1 | 1 |
| Scenario 15/39 | 0.08 | 0.1 | 1.59 | 0.45 | 0/1 | 1 |
| Scenario 4/28 | 0.16 | 0.1 | 1.59 | 0.6 | 0/1 | 1.1 |
| Scenario 16/40 | 0.16 | 0.1 | 1.59 | 0.45 | 0/1 | 1.1 |
| Scenario 5/29 | 0.08 | 0.05 | 2.67 | 0.6 | 0/1 | 1.4 |
| Scenario 17/41 | 0.08 | 0.05 | 2.67 | 0.45 | 0/1 | 1.4 |
| Scenario 6/30 | 0.16 | 0.05 | 2.67 | 0.6 | 0/1 | 1.5 |
| Scenario 18/42 | 0.16 | 0.05 | 2.67 | 0.45 | 0/1 | 1.5 |
| Scenario 7/31 | 0.08 | 0.1 | 2.67 | 0.6 | 0/1 | 1.6 |
| Scenario 19/43 | 0.08 | 0.1 | 2.67 | 0.45 | 0/1 | 1.6 |
| Scenario 8/32 | 0.16 | 0.1 | 2.67 | 0.6 | 0/1 | 1.7 |
| Scenario 20/44 | 0.16 | 0.1 | 2.67 | 0.45 | 0/1 | 1.7 |
| Current State | - | - | 4.7 | 0.36 | 1 | 0.6 |

Table 41 shows the highest and the lowest annual cooling load results for the two chosen thermal zones (zones 6 and 17a). As it can be seen on Table 41, scenarios 9,10,22 and 23 give the lowest annual cooling load results for thermal zone 6 which are all equal to 0.2 $kWh.m^{-2}$. The highest annual cooling load results are observed in scenarios 7,8,20,21,32,33,34,35,44,45,46 and 47 and they are all equal to 1.2 $kWh.m^{-2}$. The best performances in this case are given through the combination of a thinner floor/ceiling insulation, a window U-value equal to 1.30 $W.m^{-2}.K^{-1}$, and the addition of light shelves on the windows, while the wall insulation thickness and the interior shade transmittance value do not affect the result. In the case of the worst performances, no specific parameter seems to individually affect the result. Once again though, the value differences are not significant.

As it can be seen on Table 41, scenarios 9,10,11,12,21,22,23,24,33,34,35,36,45,46,47 and 48 give the lowest annual cooling load results for thermal zone 17a which are all equal to 0.2 $kWh.m^{-2}$. The highest annual cooling load results are observed in scenarios 7,8,19,20,31,32,43 and 44 and they are all equal to 1.8 $kWh.m^{-2}$.The best performances in this case seem to be affected by a window U-value equal to 1.30 $W.m^{-2}.K^{-1}$, while the wall insulation thickness, the floor/ceiling insulation thickness, the interior shade transmittance value and the existence of a light shelf do not affect the result. The worst performances are given through the combination of a thicker floor/ceiling insulation and a window U-value equal to 2.67 $W.m^{-2}.K^{-1}$, while the wall insulation thickness, the interior shade transmittance value and the existence of light shelves does not affect the result.

Table 41 Iterative energy simulation results of the parametric, improved model for thermal zones 6 and 17a. The lowest and the highest values of the annual cooling load of each thermal zone are given

| | | Wall Insulation Thickness [m] | Floor/Ceiling Insulation Thickness [m] | Window U-value [W.m$^{-2}$.K$^{-1}$] | Interior Shade Transmittance | Light Shelf (0=yes) (1=no) | Annual Cooling Load [kWh.m$^{-2}$] |
|---|---|---|---|---|---|---|---|
| Zone 6 lowest | Scenario 9 | 0.08 | 0.05 | 1.3 | 0.6 | 0 | 0.2 |
| | Scenario 10 | 0.16 | 0.05 | 1.3 | 0.6 | 0 | 0.2 |
| | Scenario 22 | 0.08 | 0.05 | 1.3 | 0.45 | 0 | 0.2 |
| | Scenario 23 | 0.16 | 0.05 | 1.3 | 0.45 | 0 | 0.2 |
| Zone 6 highest | Scenario 7 | 0.08 | 0.1 | 2.67 | 0.6 | 0 | 1.2 |
| | Scenario 8 | 0.16 | 0.1 | 2.67 | 0.6 | 0 | 1.2 |
| | Scenario 20 | 0.08 | 0.1 | 2.67 | 0.45 | 0 | 1.2 |
| | Scenario 21 | 0.16 | 0.1 | 2.67 | 0.45 | 0 | 1.2 |
| | Scenario 32 | 0.08 | 0.1 | 2.67 | 0.6 | 1 | 1.2 |
| | Scenario 33 | 0.16 | 0.1 | 2.67 | 0.6 | 1 | 1.2 |
| | Scenario 34 | 0.08 | 0.05 | 1.3 | 0.6 | 1 | 1.2 |
| | Scenario 35 | 0.16 | 0.05 | 1.3 | 0.6 | 1 | 1.2 |
| | Scenario 44 | 0.08 | 0.1 | 2.67 | 0.45 | 1 | 1.2 |
| | Scenario 45 | 0.16 | 0.1 | 2.67 | 0.45 | 1 | 1.2 |
| | Scenario 46 | 0.08 | 0.05 | 1.3 | 0.45 | 1 | 1.2 |
| | Scenario 47 | 0.16 | 0.05 | 1.3 | 0.45 | 1 | 1.2 |
| Zone6 Current State | | - | - | 4.7 | 0.36 | 1 | 0.2 |
| Zone 17a lowest | Scenario 9 | 0.08 | 0.05 | 1.3 | 0.6 | 0 | 0.2 |
| | Scenario 10 | 0.16 | 0.05 | 1.3 | 0.6 | 0 | 0.2 |
| | Scenario 11 | 0.08 | 0.1 | 1.3 | 0.6 | 0 | 0.2 |
| | Scenario 12 | 0.16 | 0.1 | 1.3 | 0.6 | 0 | 0.2 |
| | Scenario 21 | 0.08 | 0.05 | 1.3 | 0.45 | 0 | 0.2 |
| | Scenario 22 | 0.16 | 0.05 | 1.3 | 0.45 | 0 | 0.2 |
| | Scenario 23 | 0.08 | 0.1 | 1.3 | 0.45 | 0 | 0.2 |
| | Scenario 24 | 0.16 | 0.1 | 1.3 | 0.45 | 0 | 0.2 |
| | Scenario 33 | 0.08 | 0.05 | 1.3 | 0.6 | 1 | 0.2 |
| | Scenario 34 | 0.16 | 0.05 | 1.3 | 0.6 | 1 | 0.2 |
| | Scenario 35 | 0.08 | 0.1 | 1.3 | 0.6 | 1 | 0.2 |
| | Scenario 36 | 0.16 | 0.1 | 1.3 | 0.6 | 1 | 0.2 |
| | Scenario 45 | 0.08 | 0.05 | 1.3 | 0.45 | 1 | 0.2 |
| | Scenario 46 | 0.16 | 0.05 | 1.3 | 0.45 | 1 | 0.2 |
| | Scenario 47 | 0.08 | 0.1 | 1.3 | 0.45 | 1 | 0.2 |
| | Scenario 48 | 0.16 | 0.1 | 1.3 | 0.45 | 1 | 0.2 |
| Zone 17a highest | Scenario 7 | 0.08 | 0.1 | 2.67 | 0.6 | 0 | 1.8 |
| | Scenario 8 | 0.16 | 0.1 | 2.67 | 0.6 | 0 | 1.8 |
| | Scenario 19 | 0.08 | 0.1 | 2.67 | 0.45 | 0 | 1.8 |
| | Scenario 20 | 0.16 | 0.1 | 2.67 | 0.45 | 0 | 1.8 |
| | Scenario 31 | 0.08 | 0.1 | 2.67 | 0.6 | 1 | 1.8 |
| | Scenario 32 | 0.16 | 0.1 | 2.67 | 0.6 | 1 | 1.8 |
| | Scenario 43 | 0.08 | 0.1 | 2.67 | 0.45 | 1 | 1.8 |
| | Scenario 44 | 0.16 | 0.1 | 2.67 | 0.45 | 1 | 1.8 |
| Zone17a Current State | | - | - | 4.7 | 0.36 | 1 | 0 |

The reduction percentage of the annual cooling load of each one of the studied scenarios in comparison to the annual cooling load of the current state both for the whole conditioned volume and the two selected thermal zones will not be analyzed here since the value differences are very small, as Tables 43 and 44 show. Instead, it will be taken into account at the analysis of the annual load sum that will be examined later.

Moving on to the analysis of the annual electric light load (Figure 34, Table 42), it is observed that the different scenarios give results either equal to 2.7 $kWh.m^{-2}$ or 2.8 $kWh.m^{-2}$ which are either 0.1 $kWh.m^{-2}$ smaller the electric light load of the current state or equal to it, respectively. The electric light load of the current state of the whole studied building volume comes from the application of the "Always on during active occupancy hours" lighting control type which represents the actual way the school building operates (Ladybug Tools Forum, 2021). The only way to obtain lower electric light loads for the different improved scenarios was by producing more efficient electric light schedules through daylight simulations that ran through the Daysim simulation engine. These simulations though, ran only for the two selected thermal zones (thermal zone 6 and 17a), because of the time demanded for each one of them. They used the "Always on during active occupancy hours with auto dimming" lighting control type with a target illuminance of 300 lx for each space (Ladybug Tools Forum, 2021). As a result, in this study only these two thermal zones have improved electric light schedules which replaced the ones in the energy model set-up and their impact is not so significant on the electric light load of the different scenarios of the whole studied building volume as Figure 34 and Table 42 show.

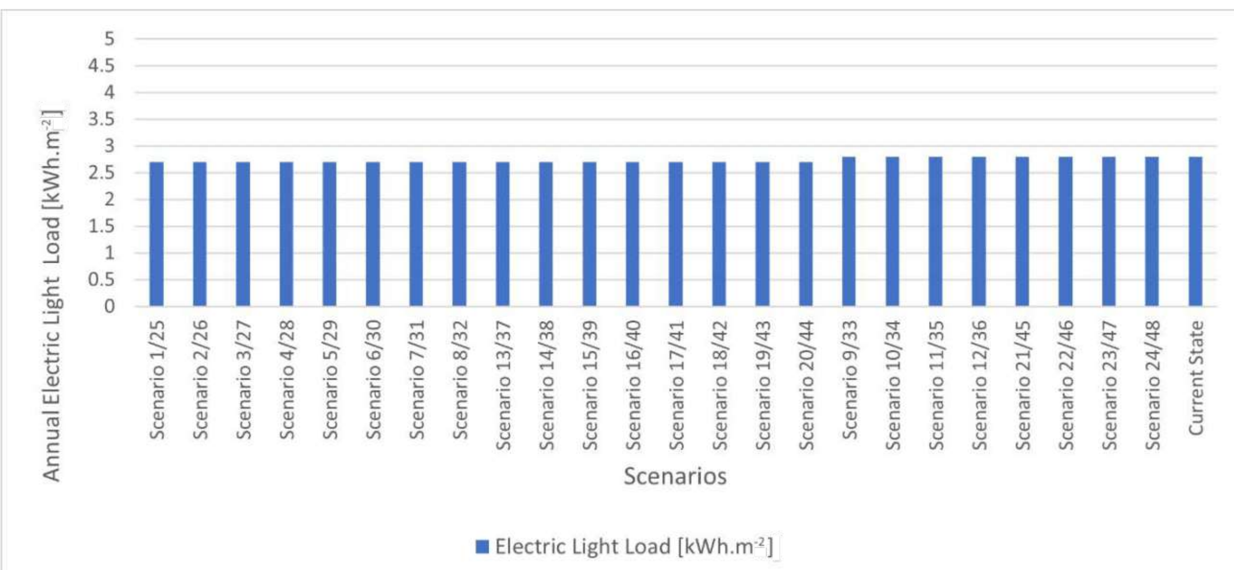


*Figure 34 Annual Electric Light Load per Scenario [$kWh.m^{-2}$]*

Table 42 Iterative energy simulation results of the parametric, improved model for the whole conditioned volume from the lowest to the highest value of the annual electric light load results

| | Wall Insulation Thickness [m] | Floor/Ceiling Insulation Thickness [m] | Window U-value [$W.m^{-2}.K^{-1}$] | Interior Shade Transmittance | Light Shelf (0=yes) (1=no) | Electric Light Load [$kWh.m^{-2}$] |
|---|---|---|---|---|---|---|
| Scenario 1/25 | 0.08 | 0.05 | 1.59 | 0.6 | 0/1 | 2.7 |
| Scenario 2/26 | 0.16 | 0.05 | 1.59 | 0.6 | 0/1 | 2.7 |
| Scenario 3/27 | 0.08 | 0.1 | 1.59 | 0.6 | 0/1 | 2.7 |
| Scenario 4/28 | 0.16 | 0.1 | 1.59 | 0.6 | 0/1 | 2.7 |
| Scenario 5/29 | 0.08 | 0.05 | 2.67 | 0.6 | 0/1 | 2.7 |
| Scenario 6/30 | 0.16 | 0.05 | 2.67 | 0.6 | 0/1 | 2.7 |
| Scenario 7/31 | 0.08 | 0.1 | 2.67 | 0.6 | 0/1 | 2.7 |
| Scenario 8/32 | 0.16 | 0.1 | 2.67 | 0.6 | 0/1 | 2.7 |
| Scenario 13/37 | 0.08 | 0.05 | 1.59 | 0.45 | 0/1 | 2.7 |
| Scenario 14/38 | 0.16 | 0.05 | 1.59 | 0.45 | 0/1 | 2.7 |
| Scenario 15/39 | 0.08 | 0.1 | 1.59 | 0.45 | 0/1 | 2.7 |
| Scenario 16/40 | 0.16 | 0.1 | 1.59 | 0.45 | 0/1 | 2.7 |
| Scenario 17/41 | 0.08 | 0.05 | 2.67 | 0.45 | 0/1 | 2.7 |
| Scenario 18/42 | 0.16 | 0.05 | 2.67 | 0.45 | 0/1 | 2.7 |
| Scenario 19/43 | 0.08 | 0.1 | 2.67 | 0.45 | 0/1 | 2.7 |
| Scenario 20/44 | 0.16 | 0.1 | 2.67 | 0.45 | 0/1 | 2.7 |
| Scenario 9/33 | 0.08 | 0.05 | 1.3 | 0.6 | 0/1 | 2.8 |
| Scenario 10/34 | 0.16 | 0.05 | 1.3 | 0.6 | 0/1 | 2.8 |
| Scenario 11/35 | 0.08 | 0.1 | 1.3 | 0.6 | 0/1 | 2.8 |
| Scenario 12/36 | 0.16 | 0.1 | 1.3 | 0.6 | 0/1 | 2.8 |
| Scenario 21/45 | 0.08 | 0.05 | 1.3 | 0.45 | 0/1 | 2.8 |
| Scenario 22/46 | 0.16 | 0.05 | 1.3 | 0.45 | 0/1 | 2.8 |
| Scenario 23/47 | 0.08 | 0.1 | 1.3 | 0.45 | 0/1 | 2.8 |
| Scenario 24/48 | 0.16 | 0.1 | 1.3 | 0.45 | 0/1 | 2.8 |
| Current | - | - | 4.7 | 0.36 | 1 | 2.8 |

When these two thermal zones are examined individually though, the electric light load is more significantly decreased for each one of their different scenarios in comparison to their current state's load value. The electric light load is either 0.8 $kWh.m^{-2}$ or 0.9 $kWh.m^{-2}$ for thermal zone 6 in comparison to the 2.7 $kWh.m^{-2}$ of its current state and either 1.4 $kWh.m^{-2}$ or 1.5 $kWh.m^{-2}$ for thermal zone 17a in comparison to the 3.2 $kWh.m^{-2}$ of its current state, as Table 43 shows.

Table 43 Iterative energy simulation results of the parametric, improved model for thermal zones 6 and 17a. The lowest and the highest values of the annual electric light load of each thermal zone are given

| | | Wall Insulation Thickness [m] | Floor/Ceiling Insulation Thickness [m] | Window U-value [$W.m^{-2}.K^{-1}$] | Interior Shade Transmittance | Light Shelf (0=yes) (1=no) | Annual Electric Light Load [$kWh.m^{-2}$] |
|---|---|---|---|---|---|---|---|
| Zone 6 lowest | Scenario 12 | 0.16 | 0.1 | 1.3 | 0.6 | 0 | 0.8 |
| | Scenario 14/38 | 0.16 | 0.05 | 1.59 | 0.45 | 0/1 | 0.8 |
| | Scenario 3/27 | 0.16 | 0.05 | 1.59 | 0.6 | 0/1 | 0.8 |
| | Scenario 1 | 0.08 | 0.05 | 1.59 | 0.6 | 0 | 0.8 |
| | Scenario 13 | 0.08 | 0.05 | 1.59 | 0.45 | 0 | 0.8 |
| | Scenario 4/28 | 0.16 | 0.1 | 1.59 | 0.6 | 0/1 | 0.8 |
| | Scenario 16/40 | 0.16 | 0.1 | 1.59 | 0.45 | 0/1 | 0.8 |
| | Scenario 5/29 | 0.16 | 0.1 | 1.59 | 0.6 | 0/1 | 0.8 |
| | Scenario 2/26 | 0.16 | 0.05 | 1.59 | 0.6 | 0 | 0.8 |
| | Scenario 15/39 | 0.08 | 0.1 | 1.59 | 0.45 | 0/1 | 0.8 |
| | Scenario 17/41 | 0.16 | 0.05 | 2.67 | 0.45 | 0/1 | 0.8 |
| | Scenario 43 | 0.16 | 0.05 | 2.67 | 0.45 | 1 | 0.8 |
| | Scenario 6/30 | 0.16 | 0.05 | 2.67 | 0.6 | 0/1 | 0.8 |
| | Scenario 18/42 | 0.08 | 0.05 | 2.67 | 0.45 | 0/1 | 0.8 |
| | Scenario 8/32 | 0.16 | 0.1 | 2.67 | 0.6 | 0 | 0.8 |
| | Scenario 21/45 | 0.16 | 0.1 | 2.67 | 0.45 | 0/1 | 0.8 |
| | Scenario 33 | 0.16 | 0.1 | 2.67 | 0.6 | 1 | 0.8 |
| | Scenario 7/31 | 0.08 | 0.1 | 2.67 | 0.6 | 0/1 | 0.8 |
| | Scenario 20 | 0.08 | 0.1 | 2.67 | 0.45 | 0 | 0.8 |
| Zone 6 highest | Scenario 10 | 0.16 | 0.05 | 1.3 | 0.6 | 0.9 | 0.9 |
| | Scenario 23 | 0.16 | 0.05 | 1.3 | 0.45 | 0.9 | 0.9 |
| | Scenario 22 | 0.08 | 0.05 | 1.3 | 0.45 | 0.9 | 0.9 |
| | Scenario 9 | 0.08 | 0.05 | 1.3 | 0.6 | 0.9 | 0.9 |
| | Scenario 25 | 0.16 | 0.1 | 1.3 | 0.45 | 0.9 | 0.9 |
| | Scenario 37 | 0.16 | 0.1 | 1.3 | 0.6 | 0.9 | 0.9 |
| | Iteration 48 | 0.16 | 0.1 | 1.3 | 0.45 | 0.9 | 0.9 |
| | Scenario 11/35 | 0.08 | 0.1 | 1.3 | 0.6 | 0/1 | 0.9 |
| | Scenario 24 | 0.08 | 0.1 | 1.3 | 0.45 | 0.9 | 0.9 |
| | Scenario 36 | 0.08 | 0.1 | 1.3 | 0.6 | 0.9 | 0.9 |
| | Scenario 46 | 0.08 | 0.1 | 1.3 | 0.45 | 0.9 | 0.9 |
| Zone6 Current State | - | - | - | 4.7 | 0.36 | 1 | 2.7 |
| Zone 17a lowest | Scenario 41 | 0.08 | 0.05 | 2.67 | 0.45 | 1 | 1.4 |
| | Scenario 42 | 0.16 | 0.05 | 2.67 | 0.45 | 1 | 1.4 |
| | Scenario 43 | 0.08 | 0.1 | 2.67 | 0.45 | 1 | 1.4 |
| | Scenario 44 | 0.16 | 0.1 | 2.67 | 0.45 | 1 | 1.4 |
| Zone 17a highest | Scenario 1/25 | 0.08 | 0.05 | 1.59 | 0.6 | 0/1 | 1.5 |
| | Scenario 2/26 | 0.16 | 0.05 | 1.59 | 0.6 | 0/1 | 1.5 |
| | Scenario 3/27 | 0.08 | 0.1 | 1.59 | 0.6 | 0/1 | 1.5 |
| | Scenario 4/28 | 0.16 | 0.1 | 1.59 | 0.6 | 0/1 | 1.5 |
| | Scenario 5/29 | 0.08 | 0.05 | 2.67 | 0.6 | 0/1 | 1.5 |
| | Scenario 6/30 | 0.16 | 0.05 | 2.67 | 0.6 | 0/1 | 1.5 |
| | Scenario 7/31 | 0.08 | 0.1 | 2.67 | 0.6 | 0/1 | 1.5 |
| | Scenario 8/32 | 0.16 | 0.1 | 2.67 | 0.6 | 0/1 | 1.5 |
| | Scenario 9/33 | 0.08 | 0.05 | 1.3 | 0.6 | 0/1 | 1.5 |
| | Scenario 10/34 | 0.16 | 0.05 | 1.3 | 0.6 | 0/1 | 1.5 |

| | | | | | | | |
|---|---|---|---|---|---|---|---|
| | Scenario 11/35 | 0.08 | 0.1 | 1.3 | 0.6 | 0/1 | 1.5 |
| | Scenario 12/36 | 0.16 | 0.1 | 1.3 | 0.6 | 0/1 | 1.5 |
| | Scenario 13/37 | 0.08 | 0.05 | 1.59 | 0.45 | 0/1 | 1.5 |
| | Scenario 14/38 | 0.16 | 0.05 | 1.59 | 0.45 | 0/1 | 1.5 |
| | Scenario 15/39 | 0.08 | 0.1 | 1.59 | 0.45 | 0/1 | 1.5 |
| | Scenario 16/40 | 0.16 | 0.1 | 1.59 | 0.45 | 0/1 | 1.5 |
| | Scenario 17 | 0.08 | 0.05 | 2.67 | 0.45 | 0 | 1.5 |
| | Scenario 18 | 0.16 | 0.05 | 2.67 | 0.45 | 0 | 1.5 |
| | Scenario 19 | 0.08 | 0.1 | 2.67 | 0.45 | 0 | 1.5 |
| | Scenario 20 | 0.16 | 0.1 | 2.67 | 0.45 | 0 | 1.5 |
| | Scenario 21/45 | 0.08 | 0.05 | 1.3 | 0.45 | 0/1 | 1.5 |
| | Scenario 22/46 | 0.16 | 0.05 | 1.3 | 0.45 | 0/1 | 1.5 |
| | Scenario 23/47 | 0.08 | 0.1 | 1.3 | 0.45 | 0/1 | 1.5 |
| | Scenario 24/48 | 0.16 | 0.1 | 1.3 | 0.45 | 0/1 | 1.5 |
| Zone17a Current State | - | - | - | 4.7 | 0.36 | 1 | 3.2 |

The reduction percentage of the annual electric light load of each one of the studied scenarios in comparison to the annual electric light load of the current state both for the whole conditioned volume and the two thermal zones under study will also not be analyzed here since the value differences are very small in comparison to the value differences of the sum of the different loads. Instead, it will be taken into account at the analysis of the annual load sum that will be examined next.

Figure 35 and Table 44 show all the combinations of the different retrofit options that give the annual load sum results from the lowest to the highest value. As it can be observed on Table 44, the addition of a light shelf does not affect the annual load sum when the rest of the retrofit options remain the same. Scenarios 4 and 28 give the lowest annual load sum results which are both equal to 21.9 $kWh.m^{-2}$. The highest annual load sum results are observed in scenarios 9,33,21,45 and they are all equal to 26.2 $kWh.m^{-2}$. As we go through the scenarios, it can be seen that the combination of a thicker wall insulation and a thicker floor/ceiling insulation, together with a window U-value equal to 1.59 $W.m^{-2}.K^{-1}$, and a higher interior shade transmittance gives the best performance. In the case of the worst performance, the combination of a thinner wall insulation and a thinner floor/ceiling insulation, together with a window U-value equal to 1.30 $W.m^{-2}.K^{-1}$, is observed. In these cases, the two interior shade transmittance alternatives that are given, do not affect the result.

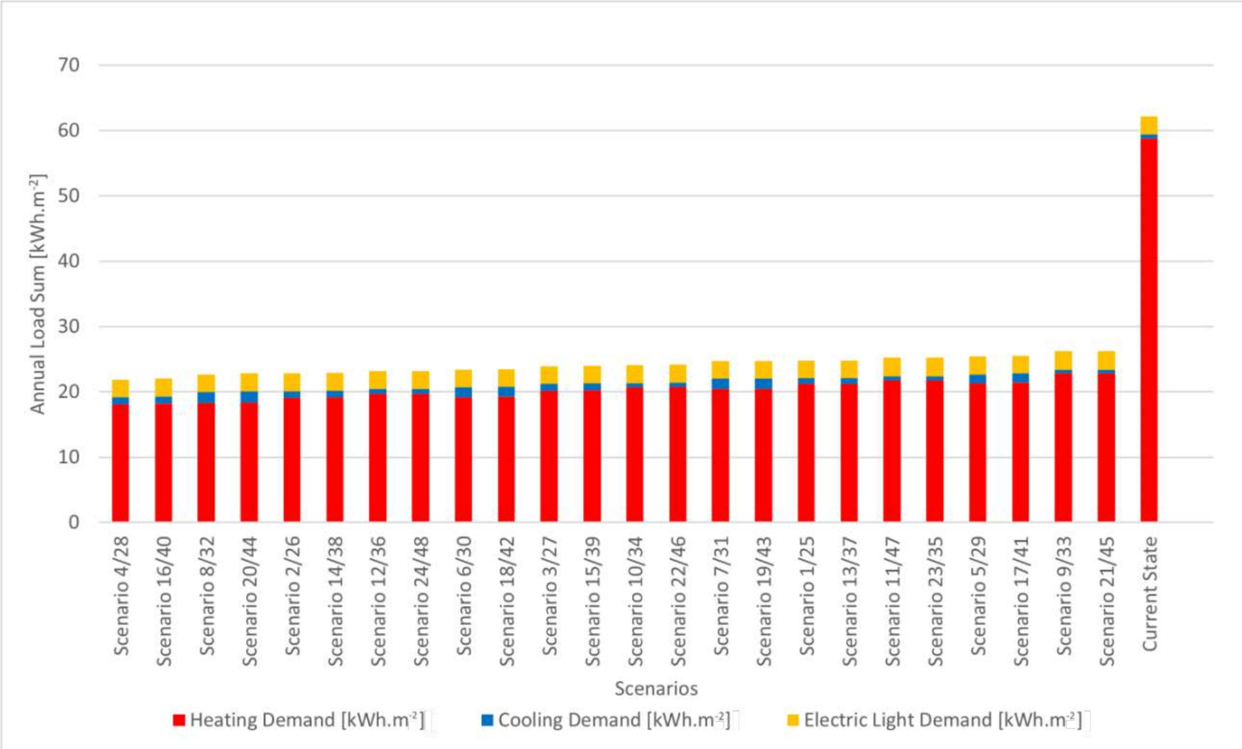


*Figure 35 Annual Load Sum per Scenario for the whole conditioned volume [kWh.m$^{-2}$]*

Table 44 Iterative energy simulation results of the parametric, improved model for the whole conditioned volume from the lowest to the highest value of the annual load sum results

| | Wall Insulation Thickness [m] | Floor/Ceiling Insulation Thickness [m] | Window U-value [W.m$^{-2}$.K$^{-1}$] | Interior Shade Transmittance | Light Shelf (0=yes) (1=no) | Annual Heating Load [kWh.m$^{-2}$] | Annual Cooling Load [kWh.m$^{-2}$] | Annual Electric Light Load [kWh.m$^{-2}$] | Annual Load Sum [kWh.m$^{-2}$] |
|---|---|---|---|---|---|---|---|---|---|
| Scenario 4/28 | 0.16 | 0.1 | 1.59 | 0.6 | 0/1 | 18.1 | 1.1 | 2.7 | 21.9 |
| Scenario 16/40 | 0.16 | 0.1 | 1.59 | 0.45 | 0/1 | 18.2 | 1.1 | 2.7 | 22 |
| Scenario 8/32 | 0.16 | 0.1 | 2.67 | 0.6 | 0/1 | 18.3 | 1.7 | 2.7 | 22.7 |
| Scenario 20/44 | 0.16 | 0.1 | 2.67 | 0.45 | 0/1 | 18.4 | 1.7 | 2.7 | 22.8 |
| Scenario 2/26 | 0.16 | 0.05 | 1.59 | 0.6 | 0/1 | 19.1 | 1 | 2.7 | 22.8 |
| Scenario 14/38 | 0.16 | 0.05 | 1.59 | 0.45 | 0/1 | 19.2 | 1 | 2.7 | 22.9 |
| Scenario 12/36 | 0.16 | 0.1 | 1.3 | 0.6 | 0/1 | 19.7 | 0.7 | 2.8 | 23.2 |
| Scenario 24/48 | 0.16 | 0.1 | 1.3 | 0.45 | 0/1 | 19.7 | 0.7 | 2.8 | 23.2 |
| Scenario 6/30 | 0.16 | 0.05 | 2.67 | 0.6 | 0/1 | 19.2 | 1.5 | 2.7 | 23.4 |
| Scenario 18/42 | 0.16 | 0.05 | 2.67 | 0.45 | 0/1 | 19.3 | 1.5 | 2.7 | 23.5 |
| Scenario 3/27 | 0.08 | 0.1 | 1.59 | 0.6 | 0/1 | 20.2 | 1 | 2.7 | 23.9 |
| Scenario 15/39 | 0.08 | 0.1 | 1.59 | 0.45 | 0/1 | 20.3 | 1 | 2.7 | 24 |
| Scenario 10/34 | 0.16 | 0.05 | 1.3 | 0.6 | 0/1 | 20.7 | 0.6 | 2.8 | 24.1 |
| Scenario 22/46 | 0.16 | 0.05 | 1.3 | 0.45 | 0/1 | 20.8 | 0.6 | 2.8 | 24.2 |
| Scenario 7/31 | 0.08 | 0.1 | 2.67 | 0.6 | 0/1 | 20.4 | 1.6 | 2.7 | 24.7 |
| Scenario 19/43 | 0.08 | 0.1 | 2.67 | 0.45 | 0/1 | 20.4 | 1.6 | 2.7 | 24.7 |
| Scenario 1/25 | 0.08 | 0.05 | 1.59 | 0.6 | 0/1 | 21.2 | 0.9 | 2.7 | 24.8 |
| Scenario 13/37 | 0.08 | 0.05 | 1.59 | 0.45 | 0/1 | 21.2 | 0.9 | 2.7 | 24.8 |
| Scenario 11/47 | 0.08 | 0.1 | 1.3 | 0.45 | 0/1 | 21.8 | 0.6 | 2.8 | 25.2 |
| Scenario 23/35 | 0.08 | 0.1 | 1.3 | 0.6 | 0/1 | 21.8 | 0.6 | 2.8 | 25.2 |
| Scenario 5/29 | 0.08 | 0.05 | 2.67 | 0.6 | 0/1 | 21.3 | 1.4 | 2.7 | 25.4 |
| Scenario 17/41 | 0.08 | 0.05 | 2.67 | 0.45 | 0/1 | 21.4 | 1.4 | 2.7 | 25.5 |
| Scenario 9/33 | 0.08 | 0.05 | 1.3 | 0.6 | 0/1 | 22.8 | 0.6 | 2.8 | 26.2 |
| Scenario 21/45 | 0.08 | 0.05 | 1.3 | 0.45 | 0/1 | 22.8 | 0.6 | 2.8 | 26.2 |
| Current State | - | - | 4.7 | 0.36 | 0/1 | 58.8 | 0.6 | 2.8 | 62.2 |

Table 45 shows the highest and the lowest annual load sum results for the two chosen thermal zones (zones 6 and 17a). As it can be seen on Table 45, scenarios 14, 27 and 39 give the lowest annual load sum results which are all equal to 22.4 $kWh.m^{-2}$. This means that they are higher than the lowest annual load sum of the whole conditioned volume by 2.3 %. The highest annual load sum results are observed in scenarios 34 and 46 and they are both equal to 24.7 $kWh.m^{-2}$ which is lower than the highest annual load sum of the whole conditioned volume by 5.7 %. The best performances in this case are given through the combination of a thicker wall insulation and a window U-value equal to 1.59 $W.m^{-2}.K^{-1}$, while the floor/ceiling insulation thickness, the interior shade transmittance value and the existence of a light shelf do not affect the result. The worst performances are given through the combination of a thinner wall insulation, a window U-value equal to 1.30 $W.m^{-2}.K^{-1}$, and the absence of a light shelf, while the floor/ceiling insulation thickness and the interior shade transmittance value do not affect the result.

Concerning thermal zone 17a, as it can be seen on Table 45, scenarios 2 and 26 give the lowest annual load sum results which are both equal to 11.9 $kWh.m^{-2}$. This means that they are lower than the lowest annual load sum of the whole conditioned volume by 45.7 %. The highest annual load sum results are observed in scenarios 21 and 45 and they are both equal to 13.3 $kWh.m^{-2}$ which is lower than the highest annual load sum of the whole conditioned volume by 49.2 %. The best performances in this case are given through the combination of a thicker wall insulation, a window U-value equal to 1.59 $W.m^{-2}.K^{-1}$, and a higher interior shade transmittance, while the floor/ceiling insulation thickness and the existence of a light shelf, do not affect the result. The worst performances are given through the combination of a thinner wall insulation, a window U-value equal to 1.30 $W.m^{-2}.K^{-1}$, and a lower interior shade transmittance, while the floor/ceiling insulation thickness and the existence of light shelves do not affect the result.

Table 45 Iterative energy simulation results of the parametric, improved model for thermal zones 6 and 17a from the lowest to the highest value of the annual load sum results

| | | Wall Insulation Thickness [m] | Floor/Ceiling Insulation Thickness [m] | Window U-value [W.m$^{-2}$.K$^{-1}$] | Interior Shade Transmittance | Light Shelf (0=yes) (1=no) | Annual Load Sum [kWh.m$^{-2}$] |
|---|---|---|---|---|---|---|---|
| Zone 6 lowest | Scenario 14 | 0.16 | 0.05 | 1.59 | 0.45 | 0 | 22.4 |
| | Scenario 27 | 0.16 | 0.05 | 1.59 | 0.6 | 1 | 22.4 |
| | Scenario 39 | 0.16 | 0.05 | 1.59 | 0.45 | 1 | 22.4 |
| Zone 6 highest | Scenario 34 | 0.08 | 0.05 | 1.3 | 0.6 | 1 | 24.7 |
| | Scenario 46 | 0.08 | 0.05 | 1.3 | 0.45 | 1 | 24.7 |
| Zone6 Current State | | | | | | | 38.5 |
| Zone 17a lowest | Scenario 2 | 0.16 | 0.05 | 1.59 | 0.6 | 0 | 11.9 |
| | Scenario 26 | 0.16 | 0.05 | 1.59 | 0.6 | 1 | 11.9 |
| Zone 17a highest | Scenario 21 | 0.08 | 0.05 | 1.3 | 0.45 | 0 | 13.3 |
| | Scenario 45 | 0.08 | 0.05 | 1.3 | 0.45 | 1 | 13.3 |
| Zone17a Current State | | | | | | | 21.2 |

Figure 36 shows the reduction percentage of the annual load sum of each one of the studied scenarios in comparison to the annual load sum of the current state of the building. The best-performing scenarios (scenarios 4 and 28) have an annual load sum 64.8 % smaller than the current state's, while the worst-performing ones (scenarios 9,33,21,45) have an annual load sum 57.9 % smaller than the current state's.

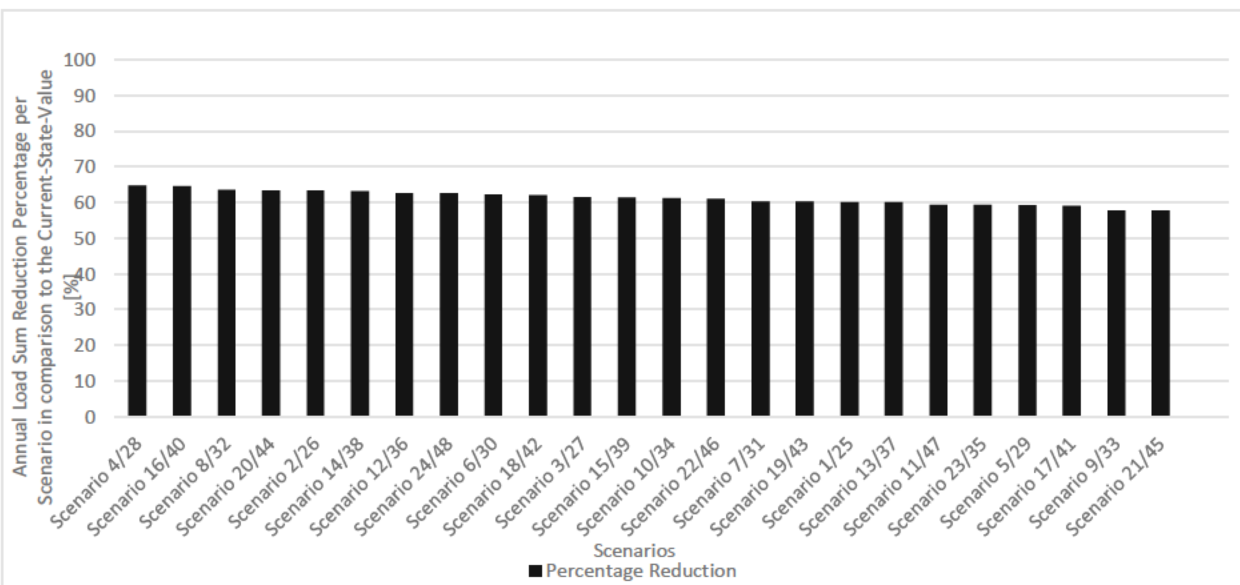


*Figure 36 Annual Load Sum Reduction Percentage per Scenario in comparison to the Current-State-Value [%]*

Figure 37 shows the reduction percentage of the annual load sum of each one of the extreme scenarios above of the two chosen thermal zones (6 and 17a) in comparison to the annual load sum of the current state of each one of the two thermal zones. The best-performing scenarios of thermal zone 6 (scenarios 14,27 and 39) have an annual load sum 41.8 % smaller than the zone's current state, while the worst-performing ones (scenarios 34 and 46) have an annual load sum 35.8 % smaller than its current state's. The best-performing scenarios of thermal zone 17a (scenarios 2 and 26) have an annual load sum 43.9 % smaller than its current state's, while the worst-performing ones (scenarios 21 and 45) have an annual load sum 46.7 % smaller than its current state's.

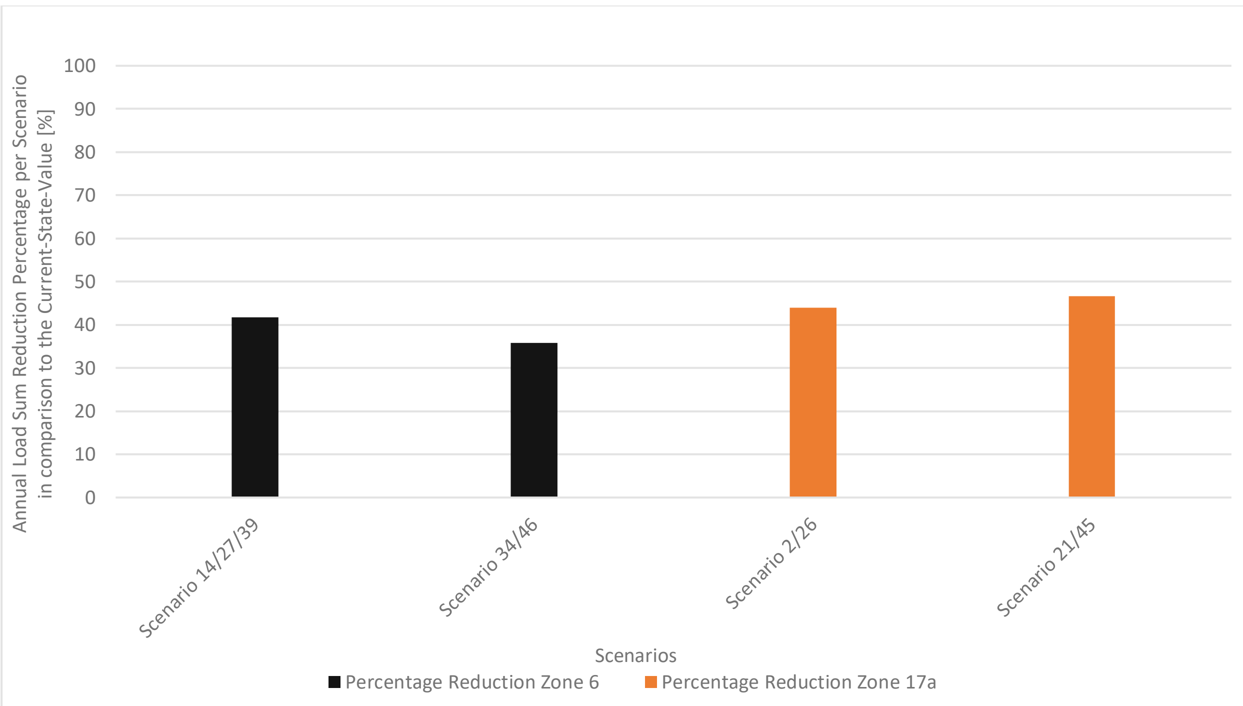


*Figure 37 Annual Load Sum Reduction Percentage per Extreme Scenario of thermal zones 6 and 17a in comparison to the Current-State-Value [%]*

As it can be seen above, the parametric analysis of each thermal zone separately can give information on how to further improve the annual load sum results for the whole conditioned volume by using the best-performing parameters for each one of the thermal zones. Only a sample of two thermal zones is used in this study, because the time needed to perform each thermal zone's parametric simulation with the existing tools and means is long, as already stated.

Furthermore, as mentioned before, all these are the results of an ideal air loads system which gives the energy that needs to be removed or added to a thermal zone or a conditioned volume and does not include a coefficient of performance (COP) (Ladybug Tools Forum, 2021).

#### 3.2.1.2 Thermal comfort results

Figure 38 and Table 46 show all the combinations of the different retrofit options that give the percentage of annual thermal comfort from the lowest to the highest value. As it can be observed on Table 46, scenarios 8 and 32 give the lowest percentage of annual thermal comfort and they are both equal to 73.9 %. The highest percentage of annual thermal comfort is observed in scenarios 10,22,34 and 46 and it is equal to 79.5 %. As we go through the scenarios, it can be seen that the combination of a thicker wall insulation and a thinner floor/ceiling insulation, together with a U-value equal window to 1.30 $W.m^{-2}.K^{-1}$, according to the NFRC directory (2021), and a lower interior shade transmittance gives the best performance. In the case of the worst performance, the combination of a thicker wall insulation and a thicker floor/ceiling insulation, together with a window U-value equal to 2.67 $W.m^{-2}.K^{-1}$, and a higher interior shade transmittance is observed. In these cases, the presence of light shelves, does not affect the result. The parameter that mostly affects these outcomes though, is the U-value of the windows. In specific, the lower the U-value, the higher the thermal comfort as Table 46 and Table A-58 of the Appendix show.

As mentioned before, these results come from the "adaptive comfort model" which calculates the occupants' thermal comfort levels for solely naturally ventilated, free-running buildings. Since the building in this study is not free-running, the results are used to give only an impression of a relevant exploration.

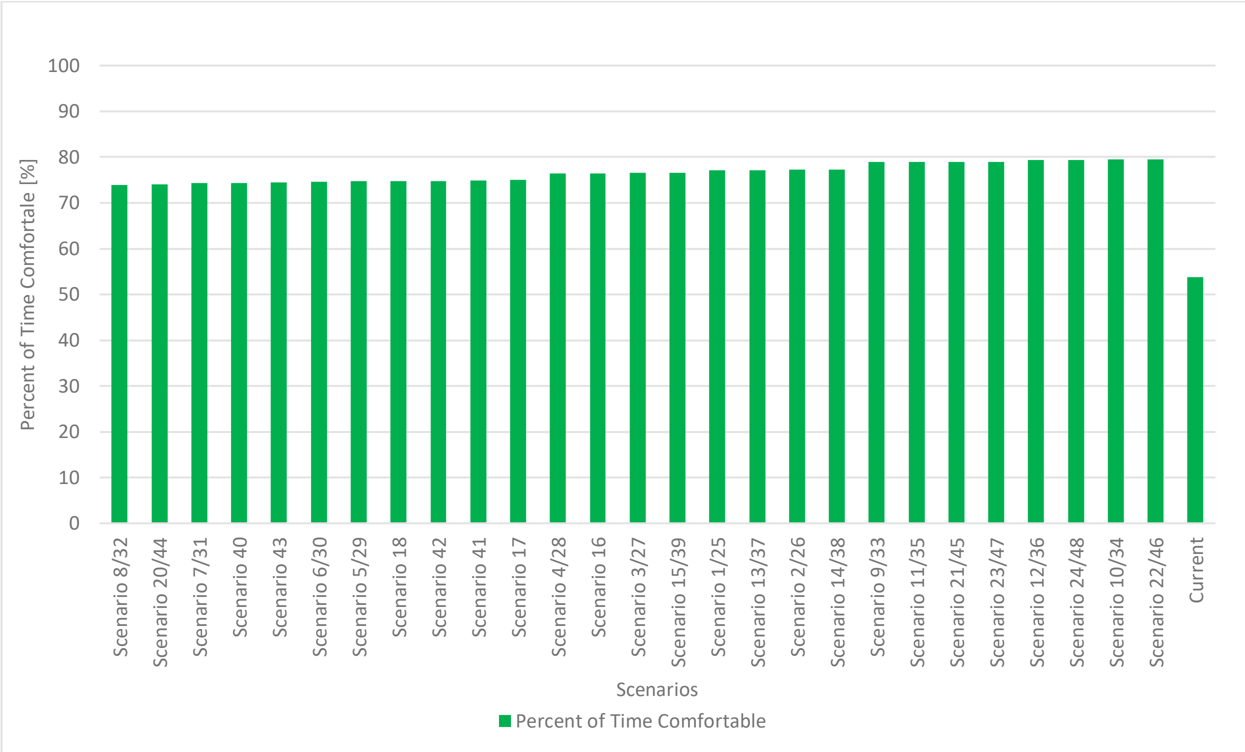


*Figure 38 Percentage of annual thermal comfort per scenario for the whole conditioned volume [%]*

Table 46 Iterative energy simulation results of the parametric, improved model for the whole conditioned volume from the lowest to the highest percentage of annual thermal comfort

| | Wall Insulation Thickness [m] | Floor/Ceiling Insulation Thickness [m] | Window U-value [W.m$^{-2}$.K$^{-1}$] | Interior Shade Transmittance | Light Shelf (0=yes) (1=no) | Percent of Time Comfortable [%] |
|---|---|---|---|---|---|---|
| Scenario 8/32 | 0.16 | 0.1 | 2.67 | 0.6 | 0/1 | 73.9 |
| Scenario 20/44 | 0.16 | 0.1 | 2.67 | 0.45 | 0/1 | 74.1 |
| Scenario 7/31 | 0.08 | 0.1 | 2.67 | 0.6 | 0/1 | 74.3 |
| Scenario 40 | 0.16 | 0.1 | 1.59 | 0.45 | 1 | 74.4 |
| Scenario 43 | 0.08 | 0.1 | 2.67 | 0.45 | 1 | 74.5 |
| Scenario 6/30 | 0.16 | 0.05 | 2.67 | 0.6 | 0/1 | 74.6 |
| Scenario 5/29 | 0.08 | 0.05 | 2.67 | 0.6 | 0/1 | 74.7 |
| Scenario 18 | 0.16 | 0.05 | 2.67 | 0.45 | 0 | 74.7 |
| Scenario 42 | 0.16 | 0.05 | 2.67 | 0.45 | 1 | 74.8 |
| Scenario 41 | 0.08 | 0.05 | 2.67 | 0.45 | 1 | 74.9 |
| Scenario 17 | 0.08 | 0.05 | 2.67 | 0.45 | 0 | 75 |
| Scenario 4/28 | 0.16 | 0.1 | 1.59 | 0.6 | 0/1 | 76.4 |
| Scenario 16 | 0.16 | 0.1 | 1.59 | 0.45 | 0 | 76.4 |
| Scenario 3/27 | 0.08 | 0.1 | 1.59 | 0.6 | 0/1 | 76.5 |
| Scenario 15/39 | 0.08 | 0.1 | 1.59 | 0.45 | 0/1 | 76.5 |
| Scenario 1/25 | 0.08 | 0.05 | 1.59 | 0.6 | 0/1 | 77.1 |
| Scenario 13/37 | 0.08 | 0.05 | 1.59 | 0.45 | 0/1 | 77.1 |
| Scenario 2/26 | 0.16 | 0.05 | 1.59 | 0.6 | 0/1 | 77.2 |
| Scenario 14/38 | 0.16 | 0.05 | 1.59 | 0.45 | 0/1 | 77.3 |
| Scenario 9/33 | 0.08 | 0.05 | 1.3 | 0.6 | 0/1 | 78.9 |
| Scenario 11/35 | 0.08 | 0.1 | 1.3 | 0.6 | 0/1 | 78.9 |
| Scenario 21/45 | 0.08 | 0.05 | 1.3 | 0.45 | 0/1 | 78.9 |
| Scenario 23/47 | 0.08 | 0.1 | 1.3 | 0.45 | 0/1 | 78.9 |
| Scenario 12/36 | 0.16 | 0.1 | 1.3 | 0.6 | 0/1 | 79.3 |
| Scenario 24/48 | 0.16 | 0.1 | 1.3 | 0.45 | 0/1 | 79.3 |
| Scenario 10/34 | 0.16 | 0.05 | 1.3 | 0.6 | 0/1 | 79.5 |
| Scenario 22/46 | 0.16 | 0.05 | 1.3 | 0.45 | 0/1 | 79.5 |
| Current State | - | - | 4.7 | 0.36 | 1 | 53.8 |

Figure 39 shows the increase percentage of the annual thermal comfort of each one of the studied scenarios in comparison to the annual thermal comfort of the current state of the building. The best-performing scenarios (scenarios 10,22,34 and 46) have an annual thermal comfort 47.8 % higher than the current state's, while the worst-performing ones (scenarios 8 and 32) have an annual thermal comfort 37.4 % higher than the current state's. All in all, the increase is significant for the whole studied volume, but as mentioned before they only represent an impression of a relevant exploration.

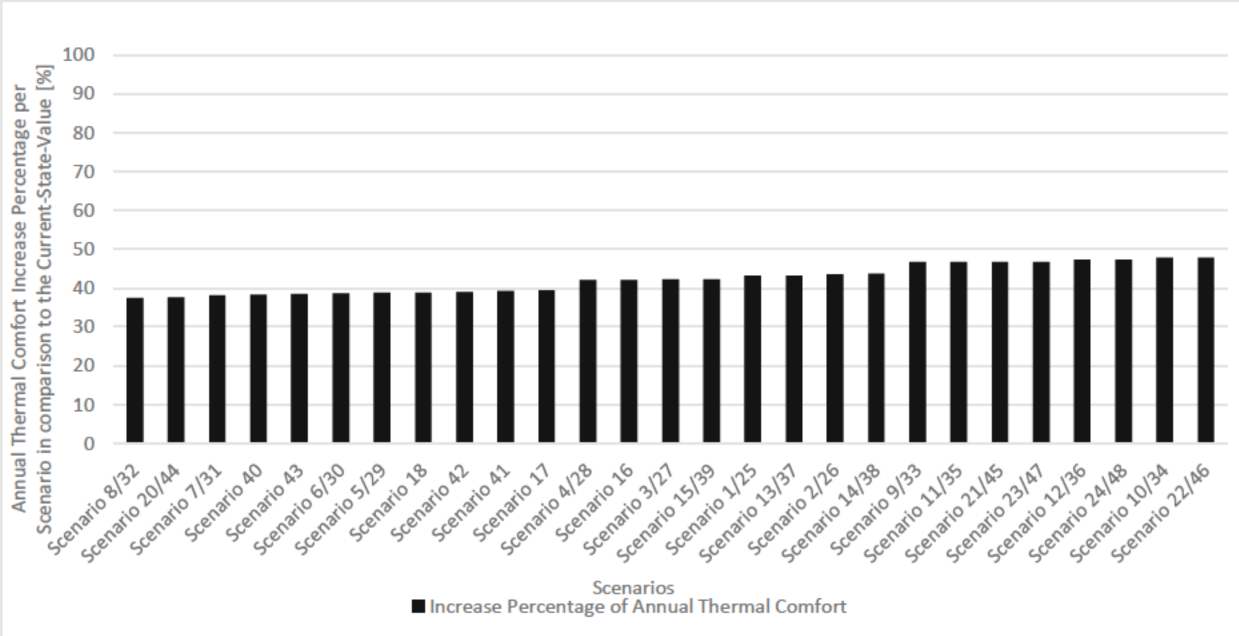


*Figure 39 Annual Thermal Comfort Increase Percentage per Scenario in comparison to the Current-State-Value [%]*

### 3.2.2 Daylight simulation results of different improvement scenarios

The different optimization techniques that were applied to the daylight simulations, summed up to twelve different combinations since it was considered that the insulation alternatives do not affect the daylight results. These results can be found in the two following tables (Tables 47,48). As it can be seen, the study was performed only for the two selected thermal zones (zones 6,17a), and in specific, for a grid of points (analysis points) that was set every 1 m in each one of them. This was due to the fact that the process for calculating the chosen daylight metrics with the application of dynamic shading could only be realized through the daysim simulation engine which proved to be extremely time-demanding, as already mentioned. All metrics were calculated for a dynamic-shading scenario, with the exception of the sDA which is calculated only for no-shading scenarios through these tools (Ladybug Tools Forum, 2021). The DGP also gave results for both dynamic shading and no-shading scenarios.

Table 47 Iterative daylight simulation results of the parametric, improved model for thermal zone 6

| | Window U-value [W.m$^{-2}$.K$^{-1}$] | Interior Shade Transmit-tance | Light Shelf (0=yes) (1=no) | sDA [%] (>300 [lx]) | Hourly Average Illuminance [%] (>=300 [lx]) | Hourly Uniformity [%] (>=0.6) | DGP [%] occupancy hours >=0.35 (dynamic shading) | DGP [%] occupancy hours >=0.35 (no-shading) |
|---|---|---|---|---|---|---|---|---|
| Scenario 1 | 1.59 | 0.6 | 0 | 100 | 98.2 | 7.5 | 0 | 0 |
| Scenario 2 | 1.59 | 0.6 | 1 | 100 | 98.5 | 1.8 | 0 | 0 |
| Scenario 3 | 1.59 | 0.45 | 0 | 100 | 98.2 | 7.6 | 0 | 0 |
| Scenario 4 | 1.59 | 0.45 | 1 | 100 | 98.5 | 1.8 | 0 | 0 |
| Scenario 5 | 2.67 | 0.6 | 0 | 100 | 98.7 | 7.3 | 0 | 0.1 |
| Scenario 6 | 2.67 | 0.6 | 1 | 100 | 99 | 1.9 | 0 | 0 |
| Scenario 7 | 2.67 | 0.45 | 0 | 100 | 98.7 | 7.3 | 0 | 0.1 |
| Scenario 8 | 2.67 | 0.45 | 1 | 100 | 99 | 1.7 | 0 | 0 |
| Scenario 9 | 1.3 | 0.6 | 0 | 100 | 98 | 7.7 | 0 | 0 |
| Scenario 10 | 1.3 | 0.6 | 1 | 100 | 98.2 | 2.3 | 0 | 0 |
| Scenario 11 | 1.3 | 0.45 | 0 | 100 | 97.7 | 7.5 | 0 | 0 |
| Scenario 12 | 1.3 | 0.45 | 1 | 100 | 98.2 | 2.3 | 0 | 0 |
| Current state | 4.7 | 0.36 | 1 | 100 | 99.4 | 6.1 | 1.4 | 1.7 |

Table 48 Iterative daylight simulation results of the parametric, improved model for thermal zone 17a

| | Window U-value [W.m$^{-2}$.K$^{-1}$] | Interior Shade Transmit-tance | Light Shelf (0=yes) (1=no) | sDA [%] (>300 [lx]) | Hourly Average Illuminance [%] (>=300 [lx]) | Hourly Uniformity [%] (>=0.6) | DGP [%] occupancy hours >=0.35 (Dynamic shading) | DGP [%] occupancy hours >=0.35 (no-shading) |
|---|---|---|---|---|---|---|---|---|
| Scenario 1 | 1.59 | 0.6 | 0 | 100 | 86.9 | 0 | 0 | 11.5 |
| Scenario 2 | 1.59 | 0.6 | 1 | 100 | 98.2 | 0 | 0 | 11 |
| Scenario 3 | 1.59 | 0.45 | 0 | 100 | 86.9 | 0 | 0 | 11.5 |
| Scenario 4 | 1.59 | 0.45 | 1 | 100 | 98.2 | 0 | 0 | 11 |
| Scenario 5 | 2.67 | 0.6 | 0 | 100 | 99 | 0 | 0.1 | 14 |
| Scenario 6 | 2.67 | 0.6 | 1 | 100 | 98.8 | 0 | 0.1 | 13.4 |
| Scenario 7 | 2.67 | 0.45 | 0 | 100 | 98.9 | 0 | 0.1 | 14 |
| Scenario 8 | 2.67 | 0.45 | 1 | 100 | 98.8 | 0 | 0 | 13 |
| Scenario 9 | 1.3 | 0.6 | 0 | 100 | 88.1 | 0 | 0 | 10.1 |
| Scenario 10 | 1.3 | 0.6 | 1 | 100 | 88.5 | 0 | 0 | 9.4 |
| Scenario 11 | 1.3 | 0.45 | 0 | 100 | 88.1 | 0 | 0.1 | 10.1 |
| Scenario 12 | 1.3 | 0.45 | 1 | 100 | 88.5 | 0 | 0 | 9.4 |
| Current state | 4.7 | 0.36 | 1 | 100 | 99.5 | 0 | 0.4 | 18 |

#### 3.2.2.1 Spatial daylight autonomy, hourly average illuminance, hourly average uniformity and point glare values results

The two selected thermal zones are a classroom and a teachers' office space. Both of those types of space-use have a minimum target illuminance ($E_T$) threshold equal to 300 lx for achieving their spatial daylight autonomy (sDA) (EN, 2018). As Tables 47 and 48 show, each iteration out of the twelve performed ones of each thermal zone, and in extension each of the forty-eight ones, has an sDA equal to 100 %. This means that 100 % of the defined analysis points meet or exceed the target Illuminance $E_T$ of 300 lx for at least 50 % of the daylight occupancy hours (Daylighting Metrics Static vs. Dynamic Assessment, 2019).

Going on to the hourly average illuminance percentage that is over a certain threshold value in a year, again, the threshold is defined to 300 lx for both types of space use, according to the Standards. As Tables 47 and 48 show, the hourly average illuminance percentages range from 97.7 % to 99 % for thermal zone 6 and from 86.9 % to 99 % for thermal zone 17a. It can be observed that the hourly average illuminance percentage alternatives of thermal zone 6 slightly dropped from the current state's 99.4 % value, while the ones of thermal zone 17a as well, compared to the current state's 99.3 %. The drop mainly happened due to the new windows' glazing properties, and in specific, their red, green, and blue transmittance values, but still, the percentages remain high.

The hourly uniformity percentages in a year that are over the threshold of 0.6 which is the threshold both for classrooms and teachers' office spaces, are shown once again on Tables 47 and 48 for thermal zones 6 and 17a, respectively. As it can be seen, the hourly uniformity of thermal zone 6 ranges from 1.7 % to 7.7 %. The iterations with higher hourly uniformity percentages are the ones where a light shelf is used. Compared to the current state's 6.1 %, we reach the conclusion that in order to not fall a lot below it, because of the rest of the interventions, the light shelves have to be applied. On the contrary, every iteration of thermal zone 17a ends up having a 0 % hourly uniformity. This means that neither of the daylight interventions were enough to raise this zone's hourly uniformity percentage which remains the same as the current state's.

Last, but not least, Tables 47 and 48 also show the DGP [% of occupancy hours >=0.35 (Perceptible Glare)] for zones 6 and 17a, respectively (EN, 2018). Both dynamic-shading and no-shading scenarios are examined in each zone. The DGP is calculated for the same, vulnerable to the sunlight point of each one of the two zones, as in the current state's simulations. All the DGP percentages of zone 6 range from 0 % to 0.1 %, and as a result are below the 5 % threshold and also lower than the current state's results both for the dynamic and the no-shading scenarios. The results of each iteration of zone 17a are all well below the 5 % threshold for the no-shading scenarios, while they range from 9.4 % to 14 % for the dynamic-shading scenarios. This means that the point DGP values of the no-shading scenarios of zone 17a exceed the threshold of 5 %, but they are now lower compared to the current state's 18 %.

### 3.2.3 Design Explorer

The results of the energy and the daylight optimization scenarios were all combined in one csv file that includes all the forty-eight iterations, with the different applied passive strategies and all the energy and daylight outcomes of the whole building and of each one of the two selected thermal zones. They were then uploaded to Design Explorer, a space exploration online tool, through which all the alternatives can be visualized in a user-friendly way and the different performances can be compared based on quantitative metrics. The relevant link is given below:

https://tt-acm.github.io/DesignExplorer/?ID=aHR0cHM6Ly9kcml2ZS5nb29nbGUuY29tL2RyaXZlL2ZvbGRlcnMvMWpxZ3NnVVA4SHZ4bXpUSFRpWGNVSVJfbmpxQU9uZ1c2P3VzcD1zaGFyaW5n

## 3.3 Efficiency of the Ladybug 0.0.69 and Honeybee 0.0.66 Legacy Plug-ins of the Grasshopper-Rhino interface

The assessment of the efficiency of the tools used for this study is also part of its focus, as already mentioned. A 16 GB RAM laptop and a 16 GB RAM desktop were used for the simulations of the high-detail model of the current state. Concerning the energy simulation part, for which the laptop was used, the calculation time lasted a couple of hours, and it took place through the EnergyPlus simulation engine. The interface faced only little lagging issues, but the process was all in all flowing easily.

Going on to the current state's daylight simulations, the calculation time for the simulation that used the Radiance engine for the no-shading scenarios was similar to that of the energy part and took place through the laptop. When the Daysim engine was used, which was necessary for the application of the dynamic shading scenarios and for the calculation of the point daylight glare probability (DGP), the calculation time rose significantly. As a result, the daylight metrics that were calculated with the second simulation engine, were only calculated for two selected thermal zones. Moreover, the use of the desktop was necessary for those demanding calculations and the post-processing of the results demanded a lot of time as well, because the interface had to cope with serious lagging issues.

After the assessment of the existing situation, several passive strategies for the improvement of the above results were implemented and a high-detail parametric model was built with forty-eight alternatives in total. The process for building it was also very demanding, concerning apart from the necessary research, some more serious lagging issues.

The annual daylight simulations ran for dynamic-shading scenarios (except for the sDA that is calculated for no-shading scenarios, as stated in Ladybug Tools Forum (2021)) through the Daysim simulation engine only for each one of the two selected thermal zones, because of the high time demands. These simulations had twelve iterations each, as the insulation alternatives were considered to not affect the daylight results. The desktop was used, and the calculation time lasted about a week. Again, serious lagging issues appeared, and the interface crashed multiple times until the completion of the simulations.

Finally, the parametric energy model ran with the help of the EnergyPlus simulation engine and an iterator, and forty-eight possible models were produced, but they only took a couple of days to run through the desktop. This happened because solely the first calculation was more demanding, as it was the one that produced an hourly csv file for a whole year, while the rest of the 47 ones took place through the use of the Colibri iterator, which is another Rhino-Grasshopper plug-in, that speeded up the process by producing only the final annual requested results.

All in all, the calculation process was quite challenging and demanding, as the existing means were not powerful enough for such detailed building models. Moreover, the plug-ins sometimes faced coding issues that had to be manually resolved due to the fact that at that point in time they were still under an intensive process of development and corrections. Currently, the more recent release of these plug-ins under the name “Ladybug Tools” is considered to be more stable (Ladybug Tools Forum, 2021).

# 4. CONCLUSION

## 4.1 Outcomes of the study

The thermal and visual assessment and improvement of the "Boys' high school" building in the city of Drama in northern Greece through building performance simulations with the help of the Ladybug 0.0.69 and Honeybee 0.0.66 Legacy Plug-ins of the Grasshopper-Rhino interface was completed successfully, but with certain challenges and delays. The nature of these challenges had to do with the insufficiency of the means used for the creation and simulation of such detailed building models, as well as with coding issues of the plug-ins that had to be resolved.

The simulations of the current state of the building gave results both on its energy and its daylight performance. An ideal air loads system was used for the energy demands or in other words, a system that does not include a coefficient of performance (COP) and can only give information about the heat removed or added to a zone by the system and not about the values of electricity or fuel that it takes to add or remove this heat (Ladybug Tools Forum, 2021).

According to the results, the annual heating load of the whole conditioned volume is equal to 58.8 $kWh.m^{-2}$ and is considered high, as the building is not well insulated, the windows are old and not performing well and the infiltration rate is in general high, leading to heat losses. Concerning the individual thermal zones, the ones that have a higher heating load than the average, are those with a higher area percentage towards the exterior air or unheated spaces and as a result, the zones of the first floor have a higher heating load than those of the ground floor. The cooling load is equal to 0.6 $kWh.m^{-2}$ and it seems to be quite low, as the building is not operating during the warmer months of the year, and it has a relatively high thermal mass. The zones of the first floor have a higher cooling load compared to the ones of the ground floor, again because they are more exposed. The electric light load of the whole building is equal to 2.8 $kWh.m^{-2}$, and it comes from the application of the "Always on during active occupancy hours" lighting control type during the simulations which can be found in Ladybug Tools Forum (2021) and represents the actual way the school building operates. Finally, the percentage of the thermal comfort of the whole volume during the occupancy hours of a year is 53.8 %, allowing a lot of space for improvements. Since the result though comes from the "adaptive comfort calculator" of the Ladybug 0.0.69 and Honeybee 0.0.66 Legacy Plug-ins which calculates the occupants' thermal comfort levels for solely naturally ventilated, free-running buildings and the building studied is not a free-running one, the analysis of the adaptive theory is not consistent, and it is conducted to only get an impression of a relevant exploration.

Going on to the current state's daylight simulations and in specific to the Radiance engine simulation results, the sDA was above 99 % for all thermal zones. Concerning the hourly average illuminance percentage in a year, almost all thermal zones gave results over their threshold value for over 90 % of the occupancy hours, with the exception of the east and west staircases which are not well naturally lit. The hourly uniformity percentages that are over defined thresholds in a year, are very low for most thermal zones, mainly because they have openings on their one side only. The ones with higher uniformities are those that represent the staircases of the building which have low average illuminances, as well as those that represent the corridor towards the north and some classrooms with a smaller depth.

Moving on to the Daysim engine simulation results used for dynamic-shading scenarios (for the two selected thermal zones), the hourly average illuminance percentages in a year that are over the threshold value of 300 lx are not affected by the application of interior shading. Concerning the hourly uniformity percentages in a year that are over the threshold value of 0.6, it is observed that for zone 6 it slightly rises once shading is applied, due to the decrease of the hourly average illuminance values, while for zone 17a it remains to the value of 0. Last, but not least, the point daylight glare probability (DGP) for the dynamic-shading scenarios of the two zones gave results below the 5 % threshold of the total time of occupation of the spaces. For the no-shading scenarios, zone 17a's point DGP exceeds the threshold by far, reaching the value of 18 %, while zone 6 maintains its point DGP below 5 %.

After the assessment of the existing situation, several passive strategies for the improvement of the above results were implemented and a parametric model was built with forty-eight alternatives in total. These interventions concerned two types of wall insulation, two types of floor and roof insulation, three different window retrofit options, two different types of interior shades and the addition light shelves. Moreover, the colour of the walls was altered from yellow to white stucco and the building was considered more airtight.

The annual daylight simulations ran for dynamic-shading scenarios through the Daysim simulation engine only for each one of the two selected thermal zones due to high time demands. They gave results that show that each iteration out of the twelve performed ones of each thermal zone, and in extension each of the forty-eight ones, has an sDA equal to 100 %. Going on to the hourly average illuminance percentages in a year that are over 300 lx for both types of space use, both zones' alternatives slightly dropped from the current state's mainly due to the new windows' transmittance values, but still, the percentages remained high. The hourly uniformity percentages in a year that are over the threshold of 0.6 for thermal zone 6 are higher than the current state's when a light shelf is used. On the contrary, every iteration of thermal zone 17a, ends up having a 0 % hourly uniformity which shows that neither of the daylight interventions were enough to raise this zone's hourly uniformity percentage in a year. The DGP percentages for both shading and no-shading scenarios of thermal zone 6 are below the 5 % threshold and lower than the current state's results. The results of each iteration of thermal zone 17a are all well below the 5 % threshold for the dynamic shading scenarios, while they range from 9.4 % to 14 % for the no-shading scenarios which means they exceed the threshold of 5 %, but they are now lower compared to the current state's 18 %.

Finally, the parametric energy model ran and produced forty-eight possible models. According to the results, the heating load of the whole conditioned volume dropped by at least 61.2 % compared to the current state's value, while the cooling load rose, but only very slightly. The heating load of thermal zones 6 and 17a dropped by at least 36.5 % and 35.6 % respectively compared to the current state's values, while the cooling loads of the zones slightly rose in most cases, but still not significantly. For the whole conditioned volume, the electric light load remained around the current state's 2.8 $kWh.m^{-2}$ with only a slight drop in some scenarios. For thermal zone 6 it ranges between 0.8 $kWh.m^{-2}$ and 0.9 $kWh.m^{-2}$ in contrast to the current state's 2.7 $kWh.m^{-2}$, and for thermal zone 17a, between 1.4 $kWh.m^{-2}$ and 1.5 $kWh.m^{-2}$ in contrast to the current state's 3.2 $kWh.m^{-2}$. Finally, the percentage of thermal comfort of the whole conditioned volume during its occupancy hours rose by at least 37.4%, but again, these results give only an impression of a relevant exploration.

Eventually, a csv file was created for all the forty-eight iterations of the parametric model. In it, all the different applied passive strategies and all the energy and daylight outcomes of the whole building and of each one of the two selected thermal zones were included. The file was then uploaded to the Design Explorer space exploration online tool, where the alternatives can be visualized in a user-friendly way and the different performances can be compared based on quantitative metrics.

## 4.2 Future Research

The study could be further developed by getting the daylight simulation results of all the thermal zones of the building and creating electric light schedules for all the iterations of all of them. This way the electric light load would be reduced even more.

Moreover, the thermal comfort of the building should be assessed through a different method, such as the Predicted Mean Vote (PMV) evaluation method and not one that is used for free-running buildings.

Furthermore, each thermal zone could also be individually approached and improved, concerning its energy and its daylight metrics, for an even better performance both of each zone individually and of the whole conditioned volume. This means that the selection of certain passive strategies such as the choice of windows, the choice of interior shades and the addition of light shelves, could be customized for each thermal zone.

Finally, more passive strategies could be examined and applied to the parametric model, concerning both the energy and the daylight part, such as exterior shades, planting of trees and other plants, etc.

# 5. INDEX

## 5.1 List of Figures

## 5.2 List of Tables

# 6. REFERENCE LIST


Alexandri, E. and Karapetsis, A., 2016. *Indoor Environmental Quality and its Impacts on Health – Case Study: School Buildings.* In: EinB2016: 5th International Conference "ENERGY in BUILDINGS 2016", 12 November 2016, Athens, Greece.

ANSI/ASHRAE Standard 62.1-2010, 2010. *Ventilation for Acceptable Indoor Air Quality*. Atlanta, GA, United States of America: American Society of Heating, Refrigerating and Air-Conditioning Engineers, Inc.

Big Ladder Software, 2021. *https://bigladdersoftware.com/epx/docs/8-6/input-output-reference/group-surface-construction-elements.html*. Accessed 11.03.2022.

CE Center, 2022. Top Five Tips for Successful Daylighting Design 2016. *https://continuingeducation.bnpmedia.com/courses/lutron/top-five-tips-for-successful-daylighting-design/?p=4*. Accessed 12.03.2022.

CEN European Daylight Standard (EN 17037), 2018. *https://velcdn.azureedge.net/~/media/marketing/ee/professional/28mai2019%20seminar/veluxen17037tallinn28052019.pdf*. Accessed 06.03.2022.

Daschalaki, E. and Sermpetzoglou, V., 2011. *Energy performance and indoor environmental quality in Hellenic schools*. Energy Buildings 43, pp. 718 - 727.

Daylighting Metrics Static vs. Dynamic Assessment, 2019. *https://www.webpages.uidaho.edu/arch570/DaylightMetrics.pdf*. Accessed 11.04.2021.

Design Explorer, 2019. *https://tt-acm.github.io/DesignExplorer/*. Accessed 28.02.2022.

Dramini.gr, 2022. *https://www.dramini.gr/423-350e-gia-leitoyrgikes-dapanes-scholeion-ston-n-dramas/.* Accessed 21.02.2022.

EN 12464-1, 2011. *Light and lighting - Lighting of work places - Part 1: Indoor work places.* Dublin, Ireland: National Standards Authority of Ireland.

EnergyPlus Weather Data, 2021. *https://energyplus.net/weather-location/europe_wmo_region_6/GRC//GRC_Thessaloniki.166220_IWEC*. Accessed 06.03.2022.

EnergyPlus 8.8.0, 2017. *userCustomEPLibrary.idf.* EnergyPlus 8.8.0. Accessed 15.03.2021.

Eortologio.net, 2013. *https://www.eortologio.net/argies/year/2009.* Accessed 06.03.2022.

GitHub, 2022. *https://github.com/ladybug-tools/honeybee-legacy/wiki/Materials-%E2%80%90-High-Performance-Window.* Accessed 11.03.2022.

Government Gazette (2019) *Research, exploitation and management of the geothermal potential of the country, establishment of the Hellenic Authority for Geological and Mineral Surveys, ownership separation of gas distribution networks, and other ordinances. Part A: Research, exploitation and management of the geothermal potential of the country.* (A'45). Greece: Greek Parliament.

Government Gazette (2013) *Energy Efficiency of Buildings: Harmonization with the Directive 2010/31 / EU of the European Parliament and of the Council, and other ordinances. Article 4: Determination of the minimum energy efficiency requirements.* (A’42). Greece: Greek Parliament.

Grasshopper Docs, 2020. *https://grasshopperdocs.com/index.html*. Accessed 06.03.2022.

Honeybee Energy Modeling, 2016. *https://docs.google.com/presentation/d/1tl1fUmlU41j-ZHQE8_VRuESaZ1F06kUqDuS1anJSaY8/edit#slide=id.g1185a3b12c_0_0*. Accessed 06.03.2022.

Hydra, 2020. *https://hydrashare.github.io/hydra/*. Accessed 12.04.2021.

IES Virtual Environment 6.4, 2012. *Apache-Tables User Guide*. *https://www.iesve.com/downloads/help/ve2012/Thermal/ApacheTables.pdf*. Accessed 13.03.2022.

Keco, E., 2017. *A Study on the Thermal Performance of School Buildings in Albania*. Vienna. Master Thesis: Vienna University of Technology.

Ladybug Tools Forum, 2021. *https://discourse.ladybug.tools/*. Accessed 06.03.2022.

Mackey, C., 2014. *Honeybee Energy Modeling.* YouTube, 2022. *https://www.youtube.com/watch?v=m8ncENwXpek&list=PLruLh1AdY-SgW4uDtNSMLeiUmA8YXEHT_*. Accessed 12.03.2022.

Marmaridou, E., 2013. *Boys' High School of Drama.* Thessaloniki. 2Θ4 14: Optional Course of the History of Architecture: Aristotle University of Thessaloniki.

MASEA Geprüfte Datenbank, 2022. https://www.masea-ensan.de/. Accessed 06.03.2022.

OpenStudio 3.0.1, 2020. *OpenStudioMasterTemplate.idf.* OpenStudio 3.0.1. Accessed 15.03.2021.

Paraschou, K., 2010. *Restoration of the "Boys' High School" of Drama - Assessment of its bearing capacity – Interventions*. Thessaloniki. Master Thesis: Aristotle University of Thessaloniki.

Regional Unit of Drama, 2022. https://web.archive.org/web/20180906132455/http://www.pedramas.eu/index.php. Accessed 28.02.2022

T.O.T.E.E. 20701-1/2017, 2017. *Detailed national specifications of parameters for the calculation of the energy efficiency of buildings and the issue of the energy performance certificate - According to the revision of K.EN.AK. (2017).* Athens, Greece: Technical Chamber of Greece.

Tsiouka, P., 2018. C*apture of energy consumption of school units: The example of the 105th Primary School of Athens.* Athens. Master Thesis: Harokopio University of Athens.

Vasiliadis, I., 2010. *The "Boys' High School" of Drama.* Drama. Schoolwork of the pupils of the Boys´ High School of Drama: Boys´ High School of Drama.

# 7. APPENDIX

## 7.1 Constructions of the school building

### 7.1.1 EnergyPlus opaque constructions

Table A-1 Basement wall to ground (sources: EnergyPlus, OpenStudio, Masea and ArchiPhysik databases, 2020)

| **Reinforced ConcreteWalltoGround 30** | **d [m]** | **λ [W.m$^{-1}$.K$^{-1}$]** | **c [J.kg$^{-1}$.K$^{-1}$]** | **ρ [kg.m$^{-3}$]** | **Thermal Absorp-tance** | **Solar Absorp-tance** | **Visible Absorp-tance** | **Roughness** |
|---|---|---|---|---|---|---|---|---|
| Reinforced Concrete | 0.30 | 2.50 | 1000 | 2400 | 0.90 | 0.70 | 0.70 | Medium-Rough |

Table A-2 Semi-basement wall to ground (sources: EnergyPlus, OpenStudio, Masea and ArchiPhysik databases, 2020)

| **StoneWalltoGround77** | **d [m]** | **λ [W.m$^{-1}$.K$^{-1}$]** | **c [J.kg$^{-1}$.K$^{-1}$]** | **ρ [kg.m$^{-3}$]** | **Thermal Absorp-tance** | **Solar Absorp-tance** | **Visible Absorp-tance** | **Roughness** |
|---|---|---|---|---|---|---|---|---|
| Limestone Masonry | 0.74 | 2.30 | 1000 | 2600 | 0.90 | 0.70 | 0.70 | Medium-Rough |
| Lime Plaster | 0.03 | 0.80 | 850 | 1700 | 0.90 | 0.70 | 0.70 | Medium-Rough |

Table A-3 Semi-basement exterior wall (sources: EnergyPlus, OpenStudio, Masea and ArchiPhysik databases, 2020)

| **StoneWallExterior80** | **d [m]** | **λ [W.m$^{-1}$.K$^{-1}$]** | **c [J.kg$^{-1}$.K$^{-1}$]** | **ρ [kg.m$^{-3}$]** | **Thermal Absorp-tance** | **Solar Absorp-tance** | **Visible Absorp-tance** | **Roughness** |
|---|---|---|---|---|---|---|---|---|
| Lime Plaster | 0.03 | 0.80 | 850 | 1700 | 0.90 | 0.70 | 0.70 | Medium-Rough |
| Limestone Masonry | 0.74 | 2.30 | 1000 | 2600 | 0.90 | 0.70 | 0.70 | Medium-Rough |
| Lime Plaster | 0.03 | 0.80 | 850 | 1700 | 0.90 | 0.70 | 0.70 | Medium-Rough |

Table A-4 Semi-basement exterior wall (sources: EnergyPlus, OpenStudio, Masea and ArchiPhysik databases, 2020)

| **StoneWallExterior70** | **d [m]** | **λ [W.m$^{-1}$.K$^{-1}$]** | **c [J.kg$^{-1}$.K$^{-1}$]** | **ρ [kg.m$^{-3}$]** | **Thermal Absorp-tance** | **Solar Absorp-tance** | **Visible Absorp-tance** | **Roughness** |
|---|---|---|---|---|---|---|---|---|
| Lime Plaster | 0.03 | 0.80 | 850 | 1700 | 0.90 | 0.70 | 0.70 | Medium-Rough |
| Limestone Masonry | 0.64 | 2.30 | 1000 | 2600 | 0.90 | 0.70 | 0.70 | Medium-Rough |
| Lime Plaster | 0.03 | 0.80 | 850 | 1700 | 0.90 | 0.70 | 0.70 | Medium-Rough |

Table A-5 Semi-basement interior wall (sources: EnergyPlus, OpenStudio, Masea and ArchiPhysik databases, 2020)

| **StoneWallInterior80** | **d [m]** | **λ [W.m$^{-1}$.K$^{-1}$]** | **c [J.kg$^{-1}$.K$^{-1}$]** | **ρ [kg.m$^{-3}$]** | **Thermal Absorp-tance** | **Solar Absorp-tance** | **Visible Absorp-tance** | **Roughness** |
|---|---|---|---|---|---|---|---|---|
| Lime Plaster | 0.03 | 0.80 | 850 | 1700 | 0.90 | 0.70 | 0.70 | Medium-Rough |
| Limestone Masonry | 0.74 | 2.30 | 1000 | 2600 | 0.90 | 0.70 | 0.70 | Medium-Rough |
| Lime Plaster | 0.03 | 0.80 | 850 | 1700 | 0.90 | 0.70 | 0.70 | Medium-Rough |

Table A-6 Semi-basement interior wall (sources: EnergyPlus, OpenStudio, Masea and ArchiPhysik databases, 2020)

| **StoneWallInterior60** | **d [m]** | **λ [W.m$^{-1}$.K$^{-1}$]** | **c [J.kg$^{-1}$.K$^{-1}$]** | **ρ [kg.m$^{-3}$]** | **Thermal Absorp-tance** | **Solar Absorp-tance** | **Visible Absorp-tance** | **Roughness** |
|---|---|---|---|---|---|---|---|---|
| Lime Plaster | 0.03 | 0.80 | 850 | 1700 | 0.90 | 0.70 | 0.70 | Medium-Rough |
| Limestone Masonry | 0.54 | 2.30 | 1000 | 2600 | 0.90 | 0.70 | 0.70 | Medium-Rough |
| Lime Plaster | 0.03 | 0.80 | 850 | 1700 | 0.90 | 0.70 | 0.70 | Medium-Rough |

Table A-7 Semi-basement interior wall (sources: EnergyPlus, OpenStudio, Masea and ArchiPhysik databases, 2020)

| **SolidBrick WallInterior 15** | **d** **[m]** | **λ** **[W.m$^{-1}$.K$^{-1}$]** | **c** **[J.kg$^{-1}$.K$^{-1}$]** | **ρ** **[kg.m$^{-3}$]** | **Thermal Absorp-tance** | **Solar Absorp-tance** | **Visible Absorp-tance** | **Roughness** |
|---|---|---|---|---|---|---|---|---|
| Lime Plaster | 0.03 | 0.80 | 850 | 1700 | 0.90 | 0.70 | 0.70 | Medium-Rough |
| Solid Brick Masonry | 0.09 | 0.60 | 1000 | 1500 | 0.90 | 0.70 | 0.70 | Medium-Rough |
| Lime Plaster | 0.03 | 0.80 | 850 | 1700 | 0.90 | 0.70 | 0.70 | Medium-Rough |

Table A-8 Ground floor exterior wall (sources: EnergyPlus, OpenStudio, Masea and ArchiPhysik databases, 2020)

| **PerforatedBrickWallExterior70** | **d** **[m]** | **λ** **[W.m$^{-1}$.K$^{-1}$]** | **c** **[J.kg$^{-1}$.K$^{-1}$]** | **ρ** **[kg.m$^{-3}$]** | **Thermal Absorp-tance** | **Solar Absorp-tance** | **Visible Absorp-tance** | **Roughness** |
|---|---|---|---|---|---|---|---|---|
| Lime Plaster | 0.03 | 0.80 | 850 | 1700 | 0.90 | 0.70 | 0.70 | Medium-Rough |
| Perforated Brick Masonry | 0.64 | 0.51 | 1000 | 1500 | 0.90 | 0.70 | 0.70 | Medium-Rough |
| Lime Plaster | 0.03 | 0.80 | 850 | 1700 | 0.90 | 0.70 | 0.70 | Medium-Rough |

Table A-9 Ground floor exterior wall (sources: EnergyPlus, OpenStudio, Masea and ArchiPhysik databases, 2020)

| **Reinforced ConcretePerforatedBrickWallExterior70** | **d** **[m]** | **λ** **[W.m$^{-1}$.K$^{-1}$]** | **c** **[J.kg$^{-1}$.K$^{-1}$]** | **ρ** **[kg.m$^{-3}$]** | **Thermal Absorp-tance** | **Solar Absorp-tance** | **Visible Absorp-tance** | **Roughness** |
|---|---|---|---|---|---|---|---|---|
| Lime Plaster | 0.03 | 0.80 | 850 | 1700 | 0.90 | 0.70 | 0.70 | Medium-Rough |
| Reinforced Concrete | 0.30 | 2.50 | 1000 | 2400 | 0.90 | 0.70 | 0.70 | Medium-Rough |
| Perforated Brick Masonry | 0.34 | 0.51 | 1000 | 1500 | 0.90 | 0.70 | 0.70 | Medium-Rough |
| Lime Plaster | 0.03 | 0.80 | 850 | 1700 | 0.90 | 0.70 | 0.70 | Medium-Rough |

Table A-10 Ground floor exterior wall (sources: EnergyPlus, OpenStudio, Masea and ArchiPhysik databases, 2020)

| PerforatedBrickWallExterior30 | d [m] | λ [W.m$^{-1}$.K$^{-1}$] | c [J.kg$^{-1}$.K$^{-1}$] | ρ [kg.m$^{-3}$] | Thermal Absorp-tance | Solar Absorp-tance | Visible Absorp-tance | Roughness |
|---|---|---|---|---|---|---|---|---|
| Lime Plaster | 0.03 | 0.80 | 850 | 1700 | 0.90 | 0.70 | 0.70 | Medium-Rough |
| Perforated Brick Masonry | 0.24 | 0.51 | 1000 | 1500 | 0.90 | 0.70 | 0.70 | Medium-Rough |
| Lime Plaster | 0.03 | 0.80 | 850 | 1700 | 0.90 | 0.70 | 0.70 | Medium-Rough |

Table A-11 Ground floor exterior wall (sources: EnergyPlus, OpenStudio, Masea and ArchiPhysik databases, 2020)

| Reinforced Concrete Wall Exterior30 | d [m] | λ [W.m$^{-1}$.K$^{-1}$] | c [J.kg$^{-1}$.K$^{-1}$] | ρ [kg.m$^{-3}$] | Thermal Absorp-tance | Solar Absorp-tance | Visible Absorp-tance | Roughness |
|---|---|---|---|---|---|---|---|---|
| Lime Plaster | 0.03 | 0.80 | 850 | 1700 | 0.90 | 0.70 | 0.70 | Medium-Rough |
| Reinforced Concrete | 0.24 | 2.50 | 1000 | 2400 | 0.90 | 0.70 | 0.70 | Medium-Rough |
| Lime Plaster | 0.03 | 0.80 | 850 | 1700 | 0.90 | 0.70 | 0.70 | Medium-Rough |

Table A-12 Ground floor interior wall (sources: EnergyPlus, OpenStudio, Masea and ArchiPhysik databases, 2020)

| StoneWallInterior70 | d [m] | λ [W.m$^{-1}$.K$^{-1}$] | c [J.kg$^{-1}$.K$^{-1}$] | ρ [kg.m$^{-3}$] | Thermal Absorp-tance | Solar Absorp-tance | Visible Absorp-tance | Roughness |
|---|---|---|---|---|---|---|---|---|
| Lime Plaster | 0.03 | 0.80 | 850 | 1700 | 0.90 | 0.70 | 0.70 | Medium-Rough |
| Limestone Masonry | 0.64 | 2.30 | 1000 | 2600 | 0.90 | 0.70 | 0.70 | Medium-Rough |
| Lime Plaster | 0.03 | 0.80 | 850 | 1700 | 0.90 | 0.70 | 0.70 | Medium-Rough |

Table A-13 Ground floor interior wall (sources: EnergyPlus, OpenStudio, Masea and ArchiPhysik databases, 2020)

| PerforatedBrickWallInterior70 | d [m] | λ [W.m$^{-1}$.K$^{-1}$] | c [J.kg$^{-1}$.K$^{-1}$] | ρ [kg.m$^{-3}$] | Thermal Absorp-tance | Solar Absorp-tance | Visible Absorp-tance | Roughness |
|---|---|---|---|---|---|---|---|---|
| Lime Plaster | 0.03 | 0.80 | 850 | 1700 | 0.90 | 0.70 | 0.70 | Medium-Rough |
| Perforated Brick Masonry | 0.64 | 0.51 | 1000 | 1500 | 0.90 | 0.70 | 0.70 | Medium-Rough |
| Lime Plaster | 0.03 | 0.80 | 850 | 1700 | 0.90 | 0.70 | 0.70 | Medium-Rough |

Table A-14 Ground floor interior wall (sources: EnergyPlus, OpenStudio, Masea and ArchiPhysik databases, 2020)

| PerforatedBrickWallInterior20 | d [m] | λ [W.m$^{-1}$.K$^{-1}$] | c [J.kg$^{-1}$.K$^{-1}$] | ρ [kg.m$^{-3}$] | Thermal Absorp-tance | Solar Absorp-tance | Visible Absorp-tance | Roughness |
|---|---|---|---|---|---|---|---|---|
| Perforated Brick Masonry | 0.20 | 0.51 | 1000 | 1500 | 0.90 | 0.70 | 0.70 | Medium-Rough |

Table A-15 Ground floor interior wall (sources: EnergyPlus, OpenStudio, Masea and ArchiPhysik databases, 2020)

| Reinforced ConcreteWallInterior30 | d [m] | λ [W.m$^{-1}$.K$^{-1}$] | c [J.kg$^{-1}$.K$^{-1}$] | ρ [kg.m$^{-3}$] | Thermal Absorp-tance | Solar Absorp-tance | Visible Absorp-tance | Roughness |
|---|---|---|---|---|---|---|---|---|
| Lime Plaster | 0.03 | 0.80 | 850 | 1700 | 0.90 | 0.70 | 0.70 | Medium-Rough |
| Reinforced Co | 0.24 | 2.50 | 1000 | 2400 | 0.90 | 0.70 | 0.70 | Medium-Rough |
| Lime Plaster | 0.03 | 0.80 | 850 | 1700 | 0.90 | 0.70 | 0.70 | Medium-Rough |

Table A-16 Ground floor interior wall (sources: EnergyPlus, OpenStudio, Masea and ArchiPhysik databases, 2020)

| **PerforatedBrickWallInterior20** | **d** [m] | **λ** [W.m$^{-1}$.K$^{-1}$] | **c** [J.kg$^{-1}$.K$^{-1}$] | **ρ** [kg.m$^{-3}$] | **Thermal Absorp-tance** | **Solar Absorp-tance** | **Visible Absorp-tance** | **Roughness** |
|---|---|---|---|---|---|---|---|---|
| Lime Plaster | 0.03 | 0.80 | 850 | 1700 | 0.90 | 0.70 | 0.70 | Medium-Rough |
| Perforated Brick Masonry | 0.14 | 0.51 | 1000 | 1500 | 0.90 | 0.70 | 0.70 | Medium-Rough |
| LimePlaster | 0.03 | 0.80 | 850 | 1700 | 0.90 | 0.70 | 0.70 | Medium-Rough |

Table A-17 Ground floor interior wall (sources: EnergyPlus, OpenStudio, Masea and ArchiPhysik databases, 2020)

| **PerforatedBrickWallInterior30** | **d** [m] | **λ** [W.m$^{-1}$.K$^{-1}$] | **c** [J.kg$^{-1}$.K$^{-1}$] | **ρ** [kg.m$^{-3}$] | **Thermal Absorp-tance** | **Solar Absorp-tance** | **Visible Absorp-tance** | **Roughness** |
|---|---|---|---|---|---|---|---|---|
| Lime Plaster | 0.03 | 0.80 | 850 | 1700 | 0.90 | 0.70 | 0.70 | Medium-Rough |
| Perforated Brick Masonry | 0.24 | 0.51 | 1000 | 1500 | 0.90 | 0.70 | 0.70 | Medium-Rough |
| Lime Plaster | 0.03 | 0.80 | 850 | 1700 | 0.90 | 0.70 | 0.70 | Medium-Rough |

Table A-18 Ground floor interior wall (sources: EnergyPlus, OpenStudio, Masea and ArchiPhysik databases, 2020)

| **StonePerforatedBrickWallInterior 100** | **d** [m] | **λ** [W.m$^{-1}$.K$^{-1}$] | **c** [J.kg$^{-1}$.K$^{-1}$] | **ρ** [kg.m$^{-3}$] | **Thermal Absorp-tance** | **Solar Absorp-tance** | **Visible Absorp-tance** | **Roughness** |
|---|---|---|---|---|---|---|---|---|
| Lime Plaster | 0.03 | 0.80 | 850 | 1700 | 0.90 | 0.70 | 0.70 | Medium-Rough |
| Limestone Masonry | 0.67 | 2.30 | 1000 | 2600 | 0.90 | 0.70 | 0.70 | Medium-Rough |
| Perforated Brick Masonry | 0.27 | 0.51 | 1000 | 1500 | 0.90 | 0.70 | 0.70 | Medium-Rough |
| Lime Plaster | 0.03 | 0.80 | 850 | 1700 | 0.90 | 0.70 | 0.70 | Medium-Rough |

Table A-19 Ground floor interior wall (sources: EnergyPlus, OpenStudio, Masea and ArchiPhysik databases, 2020)

| StoneReinforcedConcreteWallInterior100 | d [m] | λ [W.m$^{-1}$.K$^{-1}$] | c [J.kg$^{-1}$.K$^{-1}$] | ρ [kg.m$^{-3}$] | Thermal Absorp-tance | Solar Absorp-tance | Visible Absorp-tance | Roughness |
|---|---|---|---|---|---|---|---|---|
| Lime Plaster | 0.03 | 0.80 | 850 | 1700 | 0.90 | 0.70 | 0.70 | Medium-Rough |
| Limestone Masonry | 0.67 | 2.30 | 1000 | 2600 | 0.90 | 0.70 | 0.70 | Medium-Rough |
| Reinforced Concrete | 0.27 | 2.50 | 1000 | 2400 | 0.90 | 0.70 | 0.70 | Medium-Rough |
| Lime Plaster | 0.03 | 0.80 | 850 | 1700 | 0.90 | 0.70 | 0.70 | Medium-Rough |

Table A-20 Mezzanine exterior wall (sources: EnergyPlus, OpenStudio, Masea and ArchiPhysik databases, 2020)

| StoneWallPlasterboard71.25 | d [m] | λ [W.m$^{-1}$.K$^{-1}$] | c [J.kg$^{-1}$.K$^{-1}$] | ρ [kg.m$^{-3}$] | Thermal Absorp-tance | Solar Absorp-tance | Visible Absorp-tance | Roughness |
|---|---|---|---|---|---|---|---|---|
| Lime Plaster | 0.03 | 0.80 | 850 | 1700 | 0.90 | 0.70 | 0.70 | Medium-Rough |
| Limestone Masonry | 0.67 | 2.30 | 1000 | 2600 | 0.90 | 0.70 | 0.70 | Medium-Rough |
| Knauf Plasterboard | 0.0125 | 0.19 | 4 | 664 | 0.90 | 0.70 | 0.70 | Medium-Rough |

Table A-21 First floor exterior wall (sources: EnergyPlus, OpenStudio, Masea and ArchiPhysik databases, 2020)

| StoneWallExterior60 | d [m] | λ [W.m$^{-1}$.K$^{-1}$] | c [J.kg$^{-1}$.K$^{-1}$] | ρ [kg.m$^{-3}$] | Thermal Absorp-tance | Solar Absorp-tance | Visible Absorp-tance | Roughness |
|---|---|---|---|---|---|---|---|---|
| Lime Plaster | 0.03 | 0.80 | 850 | 1700 | 0.90 | 0.70 | 0.70 | Medium-Rough |
| Limestone Masonry | 0.54 | 2.30 | 1000 | 2600 | 0.90 | 0.70 | 0.70 | Medium-Rough |
| Lime Plaster | 0.03 | 0.80 | 850 | 1700 | 0.90 | 0.70 | 0.70 | Medium-Rough |

Table A-22 First floor exterior wall (sources: EnergyPlus, OpenStudio, Masea and ArchiPhysik databases, 2020)

| ReinforcedConcretePerforatedBrickWallExterior60 | d [m] | λ [W.m$^{-1}$.K$^{-1}$] | c [J.kg$^{-1}$.K$^{-1}$] | ρ [kg.m$^{-3}$] | Thermal Absorp-tance | Solar Absorp-tance | Visible Absorp-tance | Roughness |
|---|---|---|---|---|---|---|---|---|
| Lime Plaster | 0.03 | 0.80 | 850 | 1700 | 0.90 | 0.70 | 0.70 | Medium-Rough |
| Reinforced Concrete | 0.30 | 2.50 | 1000 | 2400 | 0.90 | 0.70 | 0.70 | Medium-Rough |
| Perforated Brick Masonry | 0.24 | 0.51 | 1000 | 1500 | 0.90 | 0.70 | 0.70 | Medium-Rough |
| Lime Plaster | 0.03 | 0.80 | 850 | 1700 | 0.90 | 0.70 | 0.70 | Medium-Rough |

Table A-23 First floor exterior wall (sources: EnergyPlus, OpenStudio, Masea and ArchiPhysik databases, 2020)

| PerforatedBrickWallExterior60 | d [m] | λ [W.m$^{-1}$.K$^{-1}$] | c [J.kg$^{-1}$.K$^{-1}$] | ρ [kg.m$^{-3}$] | Thermal Absorp-tance | Solar Absorp-tance | Visible Absorp-tance | Roughness |
|---|---|---|---|---|---|---|---|---|
| Lime Plaster | 0.03 | 0.80 | 850 | 1700 | 0.90 | 0.70 | 0.70 | Medium-Rough |
| Perforated Brick Masonry | 0.54 | 0.51 | 1000 | 1500 | 0.90 | 0.70 | 0.70 | Medium-Rough |
| Lime Plaster | 0.03 | 0.80 | 850 | 1700 | 0.90 | 0.70 | 0.70 | Medium-Rough |

Table A-24 First floor interior wall (sources: EnergyPlus, OpenStudio, Masea and ArchiPhysik databases, 2020)

| StonePerforatedBrickWallInterior90 | d [m] | λ [$W.m^{-1}.K^{-1}$] | c [$J.kg^{-1}.K^{-1}$] | ρ [$kg.m^{-3}$] | Thermal Absorp-tance | Solar Absorp-tance | Visible Absorp-tance | Roughness |
|---|---|---|---|---|---|---|---|---|
| Lime Plaster | 0.03 | 0.80 | 850 | 1700 | 0.90 | 0.70 | 0.70 | Medium-Rough |
| Limestone Masonry | 0.57 | 2.30 | 1000 | 2600 | 0.90 | 0.70 | 0.70 | Medium-Rough |
| Perforated Brick Masonry | 0.27 | 0.51 | 1000 | 1500 | 0.90 | 0.70 | 0.70 | Medium-Rough |
| Lime Plaster | 0.03 | 0.80 | 850 | 1700 | 0.90 | 0.70 | 0.70 | Medium-Rough |

Table A-25 First floor interior wall (sources: EnergyPlus, OpenStudio, Masea and ArchiPhysik databases, 2020)

| StoneReinforcedConcreteWallInterior90 | d [m] | λ [$W.m^{-1}.K^{-1}$] | c [$J.kg^{-1}.K^{-1}$] | ρ [$kg.m^{-3}$] | Thermal Absorp-tance | Solar Absorp-tance | Visible Absorp-tance | Roughness |
|---|---|---|---|---|---|---|---|---|
| Lime Plaster | 0.03 | 0.80 | 850 | 1700 | 0.90 | 0.70 | 0.70 | Medium-Rough |
| Limestone Masonry | 0.57 | 2.30 | 1000 | 2600 | 0.90 | 0.70 | 0.70 | Medium-Rough |
| Reinforced Concrete | 0.27 | 2.50 | 1000 | 2400 | 0.90 | 0.70 | 0.70 | Medium-Rough |
| Lime Plaster | 0.03 | 0.80 | 850 | 1700 | 0.90 | 0.70 | 0.70 | Medium-Rough |

Table A-26 Ground floor slab to ground (sources: EnergyPlus, OpenStudio, Masea and ArchiPhysik databases, 2020)

| **Reinforced ConcreteCementMosaicSlabtoGround15** | **d [m]** | **λ [W.m$^{-1}$.K$^{-1}$]** | **c [J.kg$^{-1}$.K$^{-1}$]** | **ρ [kg.m$^{-3}$]** | **Thermal Absorp-tance** | **Solar Absorp-tance** | **Visible Absorp-tance** | **Roughness** |
|---|---|---|---|---|---|---|---|---|
| Reinforced Concrete | 0.12 | 2.50 | 1000 | 2400 | 0.90 | 0.70 | 0.70 | Medium-Rough |
| Cement Mosaic | 0.03 | 1.20 | 1000 | 1900 | 0.90 | 0.70 | 0.70 | Medium-Rough |

Table A-27 Ground floor slab to ground (sources: EnergyPlus, OpenStudio, Masea and ArchiPhysik databases, 2020)

| **Reinforced ConcreteCementMosaicSlab25** | **d [m]** | **λ [W.m$^{-1}$.K$^{-1}$]** | **c [J.kg$^{-1}$.K$^{-1}$]** | **ρ [kg.m$^{-3}$]** | **Thermal Absorp-tance** | **Solar Absorp-tance** | **Visible Absorp-tance** | **Roughness** |
|---|---|---|---|---|---|---|---|---|
| Reinforced Concrete | 0.22 | 2.50 | 1000 | 2400 | 0.90 | 0.70 | 0.70 | Medium-Rough |
| Cement Mosaic | 0.03 | 1.20 | 1000 | 1900 | 0.90 | 0.70 | 0.70 | Medium-Rough |

Table A-28 Ground floor slab to unheated (sources: EnergyPlus, OpenStudio, Masea and ArchiPhysik databases, 2020)

| **Reinforced ConcreteCementMosaicSlabtoUnheated15** | **d [m]** | **λ [W.m$^{-1}$.K$^{-1}$]** | **c [J.kg$^{-1}$.K$^{-1}$]** | **ρ [kg.m$^{-3}$]** | **Thermal Absorp-tance** | **Solar Absorp-tance** | **Visible Absorp-tance** | **Roughness** |
|---|---|---|---|---|---|---|---|---|
| Reinforced Concrete | 0.12 | 2.50 | 1000 | 2400 | 0.90 | 0.70 | 0.70 | Medium-Rough |
| Cement Mosaic | 0.03 | 1.20 | 1000 | 1900 | 0.90 | 0.70 | 0.70 | Medium-Rough |

Table A-29 Ground floor adiabatic ceiling (sources: EnergyPlus, OpenStudio, Masea and ArchiPhysik databases, 2020)

| CementMosaicReinforcedConcretePlasterCeiling26.5 | d [m] | λ [W.m-1.K-1] | c [J.kg-1.K-1] | ρ [kg.m-3] | Thermal Absorp-tance | Solar Absorp-tance | Visible Absorp-tance | Roughness |
|---|---|---|---|---|---|---|---|---|
| Cement Mosaic | 0.03 | 1.20 | 1000 | 1900 | 0.90 | 0.70 | 0.70 | Medium-Rough |
| Reinforced Concrete | 0.22 | 2.50 | 1000 | 2400 | 0.90 | 0.70 | 0.70 | Medium-Rough |
| Lime Plaster | 0.015 | 0.80 | 850 | 1700 | 0.90 | 0.70 | 0.70 | Medium-Rough |

Table A-30 Mezzanine slab to unheated (sources: EnergyPlus, OpenStudio, Masea and ArchiPhysik databases, 2020)

| PlasterReinforcedConcreteCeramicTilesSlabtoUnheated43 | d [m] | λ [W.m-1.K-1] | c [J.kg-1.K-1] | ρ [kg.m-3] | Thermal Absorp-tance | Solar Absorp-tance | Visible Absorp-tance | Roughness |
|---|---|---|---|---|---|---|---|---|
| Lime Plaster | 0.015 | 0.80 | 850 | 1700 | 0.90 | 0.70 | 0.70 | Medium-Rough |
| Reinforced Concrete | 0.385 | 2.50 | 1000 | 2400 | 0.90 | 0.70 | 0.70 | Medium-Rough |
| Ceramic Tiles | 0.03 | 1.05 | 1000 | 2000 | 0.90 | 0.70 | 0.70 | Medium-Rough |

Table A-31 Mezzanine slab to unheated (sources: EnergyPlus, OpenStudio, Masea and ArchiPhysik databases, 2020)

| PlasterReinforcedConcreteCeramicTilesSlabtoUnheated33 | d [m] | λ [W.m-1.K-1] | c [J.kg-1.K-1] | ρ [kg.m-3] | Thermal Absorp-tance | Solar Absorp-tance | Visible Absorp-tance | Roughness |
|---|---|---|---|---|---|---|---|---|
| Lime Plaster | 0.015 | 0.80 | 850 | 1700 | 0.90 | 0.70 | 0.70 | Medium-Rough |
| Reinforced Concrete | 0.285 | 2.50 | 1000 | 2400 | 0.90 | 0.70 | 0.70 | Medium-Rough |
| Ceramic Tiles | 0.03 | 1.05 | 1000 | 2000 | 0.90 | 0.70 | 0.70 | Medium-Rough |

Table A-32 First floor ceiling to unheated (sources: EnergyPlus, OpenStudio, Masea and ArchiPhysik databases, 2020)

| **AirWoodLimePlasterCeilingtoUnheated41.5** | **d [m]** | **λ [W.m⁻¹.K⁻¹]** | **c [J.kg⁻¹.K⁻¹]** | **ρ [kg.m⁻³]** | **Thermal Absorp-tance** | **Solar Absorp-tance** | **Visible Absorp-tance** | **Roughness** |
|---|---|---|---|---|---|---|---|---|
| F05 Ceiling Air Space Resistance | - | 0.18 | - | - | - | - | - | - |
| Hardwood | 0.115 | 0.13 | 1500 | 650 | 0.90 | 0.70 | 0.70 | Rough |
| Lime Plaster | 0.015 | 0.80 | 850 | 1700 | 0.90 | 0.70 | 0.70 | Medium-Rough |

Table A-33 First floor ceiling to unheated (sources: EnergyPlus, OpenStudio, Masea and ArchiPhysik databases, 2020)

| **AirLimePlasterCeilingtoUnheated41.5** | **d [m]** | **λ [W.m⁻¹.K⁻¹]** | **c [J.kg⁻¹.K⁻¹]** | **ρ [kg.m⁻³]** | **Thermal Absorp-tance** | **Solar Absorp-tance** | **Visible Absorp-tance** | **Roughness** |
|---|---|---|---|---|---|---|---|---|
| F05 Ceiling Space Resistance | - | 0.18 | - | - | - | - | - | - |
| Lime Plaster | 0.015 | 0.80 | 850 | 1700 | 0.90 | 0.70 | 0.70 | Medium-Rough |

Table A-34 First floor ceiling to unheated (sources: EnergyPlus, OpenStudio, Masea and ArchiPhysik databases, 2020)

| **AirWoodReinforcedConcreteLimePlasterCeilingtoUnheated61.5** | **d [m]** | **λ [W.m⁻¹.K⁻¹]** | **c [J.kg⁻¹.K⁻¹]** | **ρ [kg.m⁻³]** | **Thermal Absorp-tance** | **Solar Absorp-tance** | **Visible Absorp-tance** | **Roughness** |
|---|---|---|---|---|---|---|---|---|
| F05 Ceiling Space Resistance | - | 0.18 | - | - | - | - | - | - |
| Hardwood | 0.115 | 0.13 | 1500 | 650 | 0.90 | 0.70 | 0.70 | Rough |
| Reinforced Concrete | 0.20 | 2.50 | 1000 | 2400 | 0.90 | 0.70 | 0.70 | Medium-Rough |
| Lime Plaster | 0.015 | 0.80 | 850 | 1700 | 0.90 | 0.70 | 0.70 | Medium-Rough |

Table A-35 First floor ceiling to unheated (sources: EnergyPlus, OpenStudio, Masea and ArchiPhysik databases, 2020)

| **AirReinforcedConcreteLimePlasterCeilingtoUnheated61.5** | **d** [m] | **λ** [W.m$^{-1}$.K$^{-1}$] | **c** [J.kg$^{-1}$.K$^{-1}$] | **ρ** [kg.m$^{-3}$] | **Thermal Absorp-tance** | **Solar Absorp-tance** | **Visible Absorp-tance** | **Roughness** |
|---|---|---|---|---|---|---|---|---|
| F05 Ceiling Space Resistance | - | 0.18 | - | - | - | - | - | - |
| Reinforced Concrete | 0.20 | 2.50 | 1000 | 2400 | 0.90 | 0.70 | 0.70 | MediumRough |
| Lime Plaster | 0.015 | 0.80 | 850 | 1700 | 0.90 | 0.70 | 0.70 | MediumRough |

Table A-36 First floor ceiling to unheated (sources: EnergyPlus, OpenStudio, Masea, ArchiPhysik and Fibran databases, 2020)

| **Roof** | **d** [m] | **λ** [W.m$^{-1}$.K$^{-1}$] | **c** [J.kg$^{-1}$.K$^{-1}$] | **ρ** [kg.m$^{-3}$] | **Thermal Absorp-tance** | **Solar Absorp-tance** | **Visible Absorp-tance** | **Roughness** |
|---|---|---|---|---|---|---|---|---|
| Ceramic Tiles | 0.03 | 1.05 | 1000 | 2000 | 0.90 | 0.70 | 0.70 | Medium-Rough |
| XPS40050 | 0.05 | 0.033 | 1450 | 38 | 0.90 | 0.70 | 0.70 | Medium-Rough |

Table A-37 Air wall (sources: EnergyPlus database, 2020)

| **Air Wall** | **d** [m] | **λ** [W.m$^{-1}$.K$^{-1}$] | **c** [J.kg$^{-1}$.K$^{-1}$] | **ρ** [kg.m$^{-3}$] | **Thermal Absorp-tance** | **Solar Absorp-tance** | **Visible Absorp-tance** | **Roughness** |
|---|---|---|---|---|---|---|---|---|
| Air | 0.01 | 0.6 | 1000 | 800 | 0.95 | 0.70 | 0.70 | Medium-Smooth |

### 7.1.2 EnergyPlus window constructions

Table A-38 Wooden window (source: T.O.T.E.E., 2017)

| **Wooden Window No Mass** | **U-value** [W.m$^{-2}$.K$^{-1}$] | **SHGC** | **Visible transmittance** |
|---|---|---|---|
| | 4.7 | 0.79 | 0.945 |

Table A-39 Iron glass door (source: T.O.T.E.E., 2017)

| Iron Glass Door No Mass | U-value [W.m$^{-2}$.K$^{-1}$] | SHGC | Visible transmittance |
|---|---|---|---|
| | 5.8 | 0.76 | 0.74 |

### 7.1.3 EnergyPlus shade materials

Table A-40 Draperies shading (source: ASHRAE, 2001)

| Semi open Weave Medium Color Draperies | Reflectance | Transmittance | Emissivity | Thickness | Conductivity |
|---|---|---|---|---|---|
| | 0.4 | 0.36 | 0.9 | 0.001 | - |

Table A-41 Plaster board shading (source: ASHRAE, 2001)

| Plaster Board | Reflectance | Transmittance | Emissivity | Thickness | Conductivity |
|---|---|---|---|---|---|
| | 0.4 | 0 | 0.9 | 0.0125 | 0.13 |

### 7.1.4 Radiance opaque materials

Table A-42 Yellow stucco properties for daylight simulation (source: github.com, 2021)

| Yellow stucco | Red reflectance | Green reflectance | Blue reflectance |
|---|---|---|---|
| | 0.839 | 0.800 | 0.753 |

### 7.1.5 Radiance glass materials

Table A-43 Wooden-frame windows' properties for daylight simulation (source: NFRC Directory, 2021)

| Single Pane | Red transmittance | Green transmittance | Blue transmittance |
|---|---|---|---|
| | 0.945 | 0.945 | 0.945 |
| **Double Pane** | **Red transmittance** | **Green transmittance** | **Blue transmittance** |
| | 0.845 | 0.845 | 0.845 |

### 7.1.6 Radiance translucent materials

Table A-44 Draperies' properties for daylight simulation (source: Ladybug Tools Forum, 2021)

| Semi open Weave Medium Color Draperies | Red diffusive reflectance | Green diffusive reflectance | Blue diffusive reflectance | Specular reflection | Diffusive transmis -sion | Specular transmis-sion | Roughness |
|---|---|---|---|---|---|---|---|
| | 0.998 | 0.998 | 0.998 | 0.01 | 0.2 | 0.385 | 0.079 |

## 7.2 Occupancy schedules

Table A-45 Zones 1,2 occupancy schedule (source: "Boys' high school" class schedule, 2018-19)

| Zones 1,2 | Monday | Tuesday | Wednesday | Thursday | Friday | Saturday | Sunday |
|---|---|---|---|---|---|---|---|
| 08:00-08:59 | 0.5 | 0.5 | 0.5 | 0.5 | 0.5 | 0 | 0 |
| 09:00-09:59 | 0.5 | 0.5 | 0.5 | 0.5 | 0.5 | 0 | 0 |
| 10:00-10:59 | 0.5 | 0.5 | 0.5 | 0.5 | 0.5 | 0 | 0 |
| 11:00-11:59 | 0.5 | 0.5 | 0.5 | 0.25 | 0.5 | 0 | 0 |
| 12:00-12:59 | 0.25 | 0.5 | 0.5 | 0.5 | 0.5 | 0 | 0 |
| 13:00-13:59 | 0.25 | 0.25 | 0.5 | 0.5 | 0.25 | 0 | 0 |
| 14:00-14:59 | 0.5 | 0 | 0.5 | 0 | 0 | 0 | 0 |

Table A-46 Zones 3,4,23,24 occupancy schedule (source: "Boys' high school" class schedule, 2018-19)

| Zones 3,4,23,24 | Monday | Tuesday | Wednesday | Thursday | Friday | Saturday | Sunday |
|---|---|---|---|---|---|---|---|
| 08:00-08:59 | 0 | 0 | 0 | 0 | 0 | 0 | 0 |
| 09:00-09:59 | 0 | 0 | 0 | 0 | 0 | 0 | 0 |
| 10:00-10:59 | 0 | 0 | 0 | 0 | 0 | 0 | 0 |
| 11:00-11:59 | 0 | 0 | 0 | 0 | 0 | 0 | 0 |
| 12:00-12:59 | 0 | 0 | 0 | 0 | 0 | 0 | 0 |
| 13:00-13:59 | 0 | 0 | 0 | 0 | 0 | 0 | 0 |
| 14:00-14:59 | 0 | 0 | 0 | 0 | 0 | 0 | 0 |

Table A-47 Zones 5,6 occupancy schedule (source: "Boys' high school" class schedule, 2018-19)

| Zones 5,6 | Monday | Tuesday | Wednesday | Thursday | Friday | Saturday | Sunday |
|---|---|---|---|---|---|---|---|
| 08:00-08:59 | 0.75 | 0.75 | 0.75 | 0.75 | 0.75 | 0 | 0 |
| 09:00-09:59 | 0.75 | 0.75 | 0.75 | 0.75 | 0.75 | 0 | 0 |
| 10:00-10:59 | 0.75 | 0.75 | 0.75 | 0.75 | 0.75 | 0 | 0 |
| 11:00-11:59 | 0.75 | 0.75 | 0.75 | 0.75 | 0.75 | 0 | 0 |
| 12:00-12:59 | 0.75 | 0.75 | 0.75 | 0.75 | 0 | 0 | 0 |
| 13:00-13:59 | 0 | 0.75 | 0.75 | 0.75 | 0.75 | 0 | 0 |
| 14:00-14:59 | 0.75 | 0 | 0.75 | 0 | 0 | 0 | 0 |

Table A-48 Zones 7,8,17,18,27,28 occupancy schedule (source: “Boys’ high school” class schedule, 2018-19)

| Zones 7,8,17,18, 27,28 | Monday | Tuesday | Wednesday | Thursday | Friday | Saturday | Sunday |
|---|---|---|---|---|---|---|---|
| 08:00-08:59 | 0.5 | 0.5 | 0.5 | 0.5 | 0.5 | 0 | 0 |
| 09:00-09:59 | 0.5 | 0.5 | 0.5 | 0.5 | 0.5 | 0 | 0 |
| 10:00-10:59 | 0.5 | 0.5 | 0.5 | 0.5 | 0.5 | 0 | 0 |
| 11:00-11:59 | 0.5 | 0.5 | 0.5 | 0.5 | 0.5 | 0 | 0 |
| 12:00-12:59 | 0.5 | 0.5 | 0.5 | 0.5 | 0.5 | 0 | 0 |
| 13:00-13:59 | 0.5 | 0.5 | 0.5 | 0.5 | 0.5 | 0 | 0 |
| 14:00-14:59 | 0.5 | 0.5 | 0.5 | 0.5 | 0.5 | 0 | 0 |

Table A-49 Zones 9a,10a,9b,10b,14a,14b occupancy schedule
(source: “Boys’ high school” class schedule, 2018-19)

| Zones 9a,10a,9b, 10b,14a,14b | Monday | Tuesday | Wednesday | Thursday | Friday | Saturday | Sunday |
|---|---|---|---|---|---|---|---|
| 08:00-08:59 | 0.1 | 0.1 | 0.1 | 0.1 | 0.1 | 0 | 0 |
| 09:00-09:59 | 0.1 | 0.1 | 0.1 | 0.1 | 0.1 | 0 | 0 |
| 10:00-10:59 | 0.1 | 0.1 | 0.1 | 0.1 | 0.1 | 0 | 0 |
| 11:00-11:59 | 0.1 | 0.1 | 0.1 | 0.1 | 0.1 | 0 | 0 |
| 12:00-12:59 | 0.1 | 0.1 | 0.1 | 0.1 | 0.1 | 0 | 0 |
| 13:00-13:59 | 0.1 | 0.1 | 0.1 | 0.1 | 0.1 | 0 | 0 |
| 14:00-14:59 | 0 | 0 | 0 | 0 | 0 | 0 | 0 |

Table A-50 Zones 11,12,13a,13b,13c,13d,13e,31,32,33a,33b,33c,33d,33e occupancy schedule
(source: “Boys’ high school” class schedule, 2018-19)

| Zones 11,12,13a, 13b,13c,13d, 13e,31,32, 33a,33b,33c, 33d, 33e | Monday | Tuesday | Wednesday | Thursday | Friday | Saturday | Sunday |
|---|---|---|---|---|---|---|---|
| 08:00-08:59 | 0.2 | 0.2 | 0.2 | 0.2 | 0.2 | 0 | 0 |
| 09:00-09:59 | 0.2 | 0.2 | 0.2 | 0.2 | 0.2 | 0 | 0 |
| 10:00-10:59 | 0.2 | 0.2 | 0.2 | 0.2 | 0.2 | 0 | 0 |
| 11:00-11:59 | 0.2 | 0.2 | 0.2 | 0.2 | 0.2 | 0 | 0 |
| 12:00-12:59 | 0.2 | 0.2 | 0.2 | 0.2 | 0.2 | 0 | 0 |
| 13:00-13:59 | 0.2 | 0.2 | 0.2 | 0.2 | 0.2 | 0 | 0 |
| 14:00-14:59 | 0 | 0 | 0 | 0 | 0 | 0 | 0 |

Table A-51 Zones 15,16 occupancy schedule (source: “Boys’ high school” class schedule, 2018-19)

| Zones 15,16 | Monday | Tuesday | Wednesday | Thursday | Friday | Saturday | Sunday |
|---|---|---|---|---|---|---|---|
| 08:00-08:59 | 0.75 | 0.75 | 0.75 | 0.75 | 0.75 | 0 | 0 |
| 09:00-09:59 | 0.75 | 0.75 | 0.75 | 0.75 | 0.75 | 0 | 0 |
| 10:00-10:59 | 0.75 | 0.75 | 0.75 | 0.75 | 0.75 | 0 | 0 |
| 11:00-11:59 | 0.75 | 0.38 | 0.38 | 0.75 | 0.38 | 0 | 0 |
| 12:00-12:59 | 0.75 | 0.75 | 0.75 | 0.75 | 0.38 | 0 | 0 |
| 13:00-13:59 | 0.75 | 0.75 | 0.75 | 0.75 | 0.75 | 0 | 0 |
| 14:00-14:59 | 0.75 | 0 | 0.75 | 0 | 0 | 0 | 0 |

Table A-52 Zone 19 occupancy schedule (source: “Boys’ high school” class schedule, 2018-19)

| Zone 19 | Monday | Tuesday | Wednesday | Thursday | Friday | Saturday | Sunday |
|---|---|---|---|---|---|---|---|
| 08:00-08:59 | 0.05 | 0.05 | 0.05 | 0.05 | 0.05 | 0 | 0 |
| 09:00-09:59 | 0.05 | 0.05 | 0.05 | 0.05 | 0.05 | 0 | 0 |
| 10:00-10:59 | 0.05 | 0.05 | 0.05 | 0.05 | 0.05 | 0 | 0 |
| 11:00-11:59 | 0.05 | 0.05 | 0.05 | 0.05 | 0.05 | 0 | 0 |
| 12:00-12:59 | 0.05 | 0.05 | 0.05 | 0.05 | 0.05 | 0 | 0 |
| 13:00-13:59 | 0.05 | 0.05 | 0.05 | 0.05 | 0.05 | 0 | 0 |
| 14:00-14:59 | 0.05 | 0.05 | 0.05 | 0.05 | 0.05 | 0 | 0 |

Table A-53 Zones 21,22 occupancy schedule (source: “Boys’ high school” class schedule, 2018-19)

| Zones 21,22 | Monday | Tuesday | Wednesday | Thursday | Friday | Saturday | Sunday |
|---|---|---|---|---|---|---|---|
| 08:00-08:59 | 0.5 | 0.5 | 0.5 | 0.5 | 0.5 | 0 | 0 |
| 09:00-09:59 | 0.5 | 0.5 | 0.5 | 0.5 | 0.5 | 0 | 0 |
| 10:00-10:59 | 0.5 | 0.25 | 0.5 | 0.5 | 0.5 | 0 | 0 |
| 11:00-11:59 | 0.5 | 0.5 | 0.5 | 0.5 | 0.5 | 0 | 0 |
| 12:00-12:59 | 0.5 | 0.5 | 0.25 | 0.5 | 0.5 | 0 | 0 |
| 13:00-13:59 | 0.5 | 0.5 | 0.5 | 0.5 | 0.25 | 0 | 0 |
| 14:00-14:59 | 0.5 | 0.5 | 0.5 | 0.25 | 0.5 | 0 | 0 |

Table A-54 Zones 25,26 occupancy schedule (source: “Boys’ high school” class schedule, 2018-19)

| Zones 25,26 | Monday | Tuesday | Wednesday | Thursday | Friday | Saturday | Sunday |
|---|---|---|---|---|---|---|---|
| 08:00-08:59 | 0.75 | 0.75 | 0.75 | 0.75 | 0.75 | 0 | 0 |
| 09:00-09:59 | 0.75 | 0.75 | 0.75 | 0.75 | 0.75 | 0 | 0 |
| 10:00-10:59 | 0.75 | 0.75 | 0.75 | 0.75 | 0.75 | 0 | 0 |
| 11:00-11:59 | 0.75 | 0.75 | 0.75 | 0.75 | 0.75 | 0 | 0 |
| 12:00-12:59 | 0.75 | 0.75 | 0.75 | 0.75 | 0.75 | 0 | 0 |
| 13:00-13:59 | 0.75 | 0.75 | 0.75 | 0.75 | 0.75 | 0 | 0 |
| 14:00-14:59 | 0 | 0.75 | 0.75 | 0.75 | 0.75 | 0 | 0 |

Table A-55 Zones 35a1,35a2,35b occupancy schedule (source: “Boys’ high school” class schedule, 2018-19)

| Zones 35a1,35a2,35b | Monday | Tuesday | Wednesday | Thursday | Friday | Saturday | Sunday |
|---|---|---|---|---|---|---|---|
| 08:00-08:59 | 0.60 | 0.60 | 0.60 | 0.60 | 0.60 | 0 | 0 |
| 09:00-09:59 | 0.60 | 0.60 | 0.60 | 0.60 | 0.60 | 0 | 0 |
| 10:00-10:59 | 0.45 | 0.45 | 0.60 | 0.60 | 0.60 | 0 | 0 |
| 11:00-11:59 | 0.45 | 0.60 | 0.60 | 0.60 | 0.60 | 0 | 0 |
| 12:00-12:59 | 0.45 | 0.60 | 0.60 | 0.60 | 0.60 | 0 | 0 |
| 13:00-13:59 | 0.45 | 0.60 | 0.60 | 0.60 | 0.60 | 0 | 0 |
| 14:00-14:59 | 0.60 | 0.45 | 0.60 | 0.60 | 0.60 | 0 | 0 |

## 7.3 Hot and cold days temperature demands

Table A-56 Cold days - minimum allowed temperature (source: T.O.T.E.E., 2017)

| All thermal zones | Monday | Tuesday | Wednesday | Thursday | Friday | Saturday | Sunday |
|---|---|---|---|---|---|---|---|
| 00:00-00:59 | 16 | 16 | 16 | 16 | 16 | 16 | 16 |
| 01:00-01:59 | 16 | 16 | 16 | 16 | 16 | 16 | 16 |
| 02:00-02:59 | 16 | 16 | 16 | 16 | 16 | 16 | 16 |
| 03:00-03:59 | 16 | 16 | 16 | 16 | 16 | 16 | 16 |
| 04:00-04:59 | 16 | 16 | 16 | 16 | 16 | 16 | 16 |
| 05:00-05:59 | 16 | 16 | 16 | 16 | 16 | 16 | 16 |
| 06:00-06:59 | 16 | 16 | 16 | 16 | 16 | 16 | 16 |
| 07:00-07:59 | 20 | 20 | 20 | 20 | 20 | 16 | 16 |
| 08:00-08:59 | 20 | 20 | 20 | 20 | 20 | 16 | 16 |
| 09:00-09:59 | 20 | 20 | 20 | 20 | 20 | 16 | 16 |
| 10:00-10:59 | 20 | 20 | 20 | 20 | 20 | 16 | 16 |
| 11:00-11:59 | 20 | 20 | 20 | 20 | 20 | 16 | 16 |
| 12:00-12:59 | 20 | 20 | 20 | 20 | 20 | 16 | 16 |
| 13:00-13:59 | 20 | 20 | 20 | 20 | 20 | 16 | 16 |
| 14:00-14:59 | 20 | 20 | 20 | 20 | 20 | 16 | 16 |
| 15:00-15:59 | 16 | 16 | 16 | 16 | 16 | 16 | 16 |
| 16:00-16:59 | 16 | 16 | 16 | 16 | 16 | 16 | 16 |
| 17:00-17:59 | 16 | 16 | 16 | 16 | 16 | 16 | 16 |
| 18:00-18:59 | 16 | 16 | 16 | 16 | 16 | 16 | 16 |
| 19:00-19:59 | 16 | 16 | 16 | 16 | 16 | 16 | 16 |
| 20:00-20:59 | 16 | 16 | 16 | 16 | 16 | 16 | 16 |
| 21:00-21:59 | 16 | 16 | 16 | 16 | 16 | 16 | 16 |
| 22:00-22:59 | 16 | 16 | 16 | 16 | 16 | 16 | 16 |
| 23:00-23:59 | 16 | 16 | 16 | 16 | 16 | 16 | 16 |

Table A-57 Hot days - maximum allowed temperature (source: T.O.T.E.E., 2017)

| All thermal zones | Monday | Tuesday | Wednesday | Thursday | Friday | Saturday | Sunday |
|---|---|---|---|---|---|---|---|
| 00:00-00:59 | 35 | 35 | 35 | 35 | 35 | 35 | 35 |
| 01:00-01:59 | 35 | 35 | 35 | 35 | 35 | 35 | 35 |
| 02:00-02:59 | 35 | 35 | 35 | 35 | 35 | 35 | 35 |
| 03:00-03:59 | 35 | 35 | 35 | 35 | 35 | 35 | 35 |
| 04:00-04:59 | 35 | 35 | 35 | 35 | 35 | 35 | 35 |
| 05:00-05:59 | 35 | 35 | 35 | 35 | 35 | 35 | 35 |
| 06:00-06:59 | 35 | 35 | 35 | 35 | 35 | 35 | 35 |
| 07:00-07:59 | 26 | 26 | 26 | 26 | 26 | 35 | 35 |
| 08:00-08:59 | 26 | 26 | 26 | 26 | 26 | 35 | 35 |
| 09:00-09:59 | 26 | 26 | 26 | 26 | 26 | 35 | 35 |
| 10:00-10:59 | 26 | 26 | 26 | 26 | 26 | 35 | 35 |
| 11:00-11:59 | 26 | 26 | 26 | 26 | 26 | 35 | 35 |
| 12:00-12:59 | 26 | 26 | 26 | 26 | 26 | 35 | 35 |
| 13:00-13:59 | 26 | 26 | 26 | 26 | 26 | 35 | 35 |
| 14:00-14:59 | 26 | 26 | 26 | 26 | 26 | 35 | 35 |
| 15:00-15:59 | 35 | 35 | 35 | 35 | 35 | 35 | 35 |
| 16:00-16:59 | 35 | 35 | 35 | 35 | 35 | 35 | 35 |
| 17:00-17:59 | 35 | 35 | 35 | 35 | 35 | 35 | 35 |
| 18:00-18:59 | 35 | 35 | 35 | 35 | 35 | 35 | 35 |
| 19:00-19:59 | 35 | 35 | 35 | 35 | 35 | 35 | 35 |
| 20:00-20:59 | 35 | 35 | 35 | 35 | 35 | 35 | 35 |
| 21:00-21:59 | 35 | 35 | 35 | 35 | 35 | 35 | 35 |
| 22:00-22:59 | 35 | 35 | 35 | 35 | 35 | 35 | 35 |
| 23:00-23:59 | 35 | 35 | 35 | 35 | 35 | 35 | 35 |

## 7.4 Iterative energy simulation results of the parametric, improved model

Table A-58 Iterative energy simulation results of the parametric, improved model for the whole conditioned volume

| | Wall Insulation Thickness [m] | Floor/Ceiling Insulation Thickness [m] | Window U-value [W.m-2.K-1] | Interior Shade Transmit-tance | Light Shelf (0=yes) (1=no) | Heating Demand [kWh.m-2] | Cooling Demand [kWh.m-2] | Electric Light Demand [kWh.m-2] | Percent of Time Comfortable [%] |
|---|---|---|---|---|---|---|---|---|---|
| Scenario 1 | 0.08 | 0.05 | 1.59 | 0.6 | 0 | 21.2 | 0.9 | 2.7 | 77.1 |
| Scenario 2 | 0.16 | 0.05 | 1.59 | 0.6 | 0 | 19.1 | 1 | 2.7 | 77.2 |
| Scenario 3 | 0.08 | 0.1 | 1.59 | 0.6 | 0 | 20.2 | 1 | 2.7 | 76.5 |
| Scenario 4 | 0.16 | 0.1 | 1.59 | 0.6 | 0 | 18.1 | 1.1 | 2.7 | 76.4 |
| Scenario 5 | 0.08 | 0.05 | 2.67 | 0.6 | 0 | 21.3 | 1.4 | 2.7 | 74.7 |
| Scenario 6 | 0.16 | 0.05 | 2.67 | 0.6 | 0 | 19.2 | 1.5 | 2.7 | 74.6 |
| Scenario 7 | 0.08 | 0.1 | 2.67 | 0.6 | 0 | 20.4 | 1.6 | 2.7 | 74.3 |
| Scenario 8 | 0.16 | 0.1 | 2.67 | 0.6 | 0 | 18.3 | 1.7 | 2.7 | 73.9 |
| Scenario 9 | 0.08 | 0.05 | 1.3 | 0.6 | 0 | 22.8 | 0.6 | 2.8 | 78.9 |
| Scenario 10 | 0.16 | 0.05 | 1.3 | 0.6 | 0 | 20.7 | 0.6 | 2.8 | 79.5 |
| Scenario 11 | 0.08 | 0.1 | 1.3 | 0.6 | 0 | 21.8 | 0.6 | 2.8 | 78.9 |
| Scenario 12 | 0.16 | 0.1 | 1.3 | 0.6 | 0 | 19.7 | 0.7 | 2.8 | 79.3 |
| Scenario 13 | 0.08 | 0.05 | 1.59 | 0.45 | 0 | 21.2 | 0.9 | 2.7 | 77.1 |
| Scenario 14 | 0.16 | 0.05 | 1.59 | 0.45 | 0 | 19.2 | 1 | 2.7 | 77.3 |
| Scenario 15 | 0.08 | 0.1 | 1.59 | 0.45 | 0 | 20.3 | 1 | 2.7 | 76.5 |
| Scenario 16 | 0.16 | 0.1 | 1.59 | 0.45 | 0 | 18.2 | 1.1 | 2.7 | 76.4 |
| Scenario 17 | 0.08 | 0.05 | 2.67 | 0.45 | 0 | 21.4 | 1.4 | 2.7 | 75 |
| Scenario 18 | 0.16 | 0.05 | 2.67 | 0.45 | 0 | 19.3 | 1.5 | 2.7 | 74.7 |
| Scenario 19 | 0.08 | 0.1 | 2.67 | 0.45 | 0 | 20.4 | 1.6 | 2.7 | 74.4 |
| Scenario 20 | 0.16 | 0.1 | 2.67 | 0.45 | 0 | 18.4 | 1.7 | 2.7 | 74.1 |
| Scenario 21 | 0.08 | 0.05 | 1.3 | 0.45 | 0 | 22.8 | 0.6 | 2.8 | 78.9 |
| Scenario 22 | 0.16 | 0.05 | 1.3 | 0.45 | 0 | 20.8 | 0.6 | 2.8 | 79.5 |
| Scenario 23 | 0.08 | 0.1 | 1.3 | 0.45 | 0 | 21.8 | 0.6 | 2.8 | 78.9 |
| Scenario 24 | 0.16 | 0.1 | 1.3 | 0.45 | 0 | 19.7 | 0.7 | 2.8 | 79.3 |
| Scenario 25 | 0.08 | 0.05 | 1.59 | 0.6 | 1 | 21.2 | 0.9 | 2.7 | 77.1 |
| Scenario 26 | 0.16 | 0.05 | 1.59 | 0.6 | 1 | 19.1 | 1 | 2.7 | 77.2 |
| Scenario 27 | 0.08 | 0.1 | 1.59 | 0.6 | 1 | 20.2 | 1 | 2.7 | 76.5 |
| Scenario 28 | 0.16 | 0.1 | 1.59 | 0.6 | 1 | 18.1 | 1.1 | 2.7 | 76.4 |
| Scenario 29 | 0.08 | 0.05 | 2.67 | 0.6 | 1 | 21.3 | 1.4 | 2.7 | 74.7 |
| Scenario 30 | 0.16 | 0.05 | 2.67 | 0.6 | 1 | 19.2 | 1.5 | 2.7 | 74.6 |
| Scenario 31 | 0.08 | 0.1 | 2.67 | 0.6 | 1 | 20.4 | 1.6 | 2.7 | 74.3 |
| Scenario 32 | 0.16 | 0.1 | 2.67 | 0.6 | 1 | 18.3 | 1.7 | 2.7 | 73.9 |
| Scenario 33 | 0.08 | 0.05 | 1.3 | 0.6 | 1 | 22.8 | 0.6 | 2.8 | 78.9 |
| Scenario 34 | 0.16 | 0.05 | 1.3 | 0.6 | 1 | 20.7 | 0.6 | 2.8 | 79.5 |
| Scenario 35 | 0.08 | 0.1 | 1.3 | 0.6 | 1 | 21.8 | 0.6 | 2.8 | 78.9 |
| Scenario 36 | 0.16 | 0.1 | 1.3 | 0.6 | 1 | 19.7 | 0.7 | 2.8 | 79.3 |
| Scenario 37 | 0.08 | 0.05 | 1.59 | 0.45 | 1 | 21.2 | 0.9 | 2.7 | 77.1 |
| Scenario 38 | 0.16 | 0.05 | 1.59 | 0.45 | 1 | 19.2 | 1 | 2.7 | 77.3 |
| Scenario 39 | 0.08 | 0.1 | 1.59 | 0.45 | 1 | 20.3 | 1 | 2.7 | 76.5 |
| Scenario 40 | 0.16 | 0.1 | 1.59 | 0.45 | 1 | 18.2 | 1.1 | 2.7 | 74.4 |
| Scenario 41 | 0.08 | 0.05 | 2.67 | 0.45 | 1 | 21.4 | 1.4 | 2.7 | 74.9 |
| Scenario 42 | 0.16 | 0.05 | 2.67 | 0.45 | 1 | 19.3 | 1.5 | 2.7 | 74.8 |
| Scenario 43 | 0.08 | 0.1 | 2.67 | 0.45 | 1 | 20.4 | 1.6 | 2.7 | 74.5 |
| Scenario 44 | 0.16 | 0.1 | 2.67 | 0.45 | 1 | 18.4 | 1.7 | 2.7 | 74.1 |
| Scenario 45 | 0.08 | 0.05 | 1.3 | 0.45 | 1 | 22.8 | 0.6 | 2.8 | 78.9 |
| Scenario 46 | 0.16 | 0.05 | 1.3 | 0.45 | 1 | 20.8 | 0.6 | 2.8 | 79.5 |
| Scenario 47 | 0.08 | 0.1 | 1.3 | 0.45 | 1 | 21.8 | 0.6 | 2.8 | 78.9 |
| Scenario 48 | 0.16 | 0.1 | 1.3 | 0.45 | 1 | 19.7 | 0.7 | 2.8 | 79.3 |
| Current | - | - | 4.7 | 0.36 | 1 | 58.8 | 0.6 | 2.8 | 53.8 |

Table A-59 Iterative energy simulation results of the parametric, improved model for thermal zone 6

| | Wall Insulation Thickness [m] | Floor/Ceiling Insula ion Thickness [m] | Window U-value [W.m-2.K-1] | Interior Shade Transmit-tance | Light Shelf (0=yes) (1=no) | Heating Demand [kWh.m-2] | Cooling Demand [kWh.m-2] | Electric Light Demand [kWh.m-2] |
|---|---|---|---|---|---|---|---|---|
| Iteration 1 | 0.08 | 0.05 | 1.59 | 0.6 | 0 | 21.7 | 0.6 | 0.8 |
| Iteration 2 | 0.16 | 0.05 | 1.59 | 0.6 | 0 | 21.6 | 0.7 | 0.8 |
| Iteration 3 | 0.08 | 0.1 | 1.59 | 0.6 | 0 | 21.6 | 0.7 | 0.8 |
| Iteration 4 | 0.16 | 0.1 | 1.59 | 0.6 | 0 | 21 | 0.7 | 0.8 |
| Iteration 5 | 0.08 | 0.05 | 2.67 | 0.6 | 0 | 22.4 | 1 | 0.8 |
| Iteration 6 | 0.16 | 0.05 | 2.67 | 0.6 | 0 | 22 | 1 | 0.8 |
| Iteration 7 | 0.08 | 0.1 | 2.67 | 0.6 | 0 | 22.4 | 1.2 | 0.8 |
| Iteration 8 | 0.16 | 0.1 | 2.67 | 0.6 | 0 | 21.6 | 1.2 | 0.8 |
| Iteration 9 | 0.08 | 0.05 | 1.3 | 0.6 | 0 | 22.62 | 0.2 | 0.9 |
| Iteration 10 | 0.16 | 0.05 | 1.3 | 0.6 | 0 | 22 | 0.2 | 0.9 |
| Iteration 11 | 0.08 | 0.1 | 1.3 | 0.6 | 0 | 22.6 | 0.3 | 0.9 |
| Iteration 12 | 0.16 | 0.1 | 1.3 | 0.6 | 0 | 21.9 | 0.3 | 0.8 |
| Iteration 13 | 0.08 | 0.05 | 1.59 | 0.45 | 0 | 21.7 | 0.6 | 0.8 |
| Iteration 14 | 0.16 | 0.05 | 1.59 | 0.45 | 0 | 21 | 0.6 | 0.8 |
| Iteration 15 | 0.08 | 0.1 | 1.59 | 0.45 | 0 | 21.6 | 0.7 | 0.8 |
| Iteration 16 | 0.16 | 0.1 | 1.59 | 0.45 | 0 | 21 | 0.7 | 0.8 |
| Iteration 17 | 0.08 | 0.05 | 2.67 | 0.45 | 0 | 22 | 1 | 0.8 |
| Iteration 18 | 0.16 | 0.05 | 2.67 | 0.45 | 0 | 21.7 | 1 | 0.8 |
| Iteration 19 | 0.08 | 0.1 | 2.67 | 0.45 | 0 | 22.4 | 1.2 | 0.8 |
| Iteration 20 | 0.16 | 0.1 | 2.67 | 0.45 | 0 | 21.6 | 1.2 | 0.8 |
| Iteration 21 | 0.08 | 0.05 | 1.3 | 0.45 | 0 | 22.6 | 0.2 | 0.9 |
| Iteration 22 | 0.16 | 0.05 | 1.3 | 0.45 | 0 | 22 | 0.2 | 0.9 |
| Iteration 23 | 0.08 | 0.1 | 1.3 | 0.45 | 0 | 22.6 | 0.3 | 0.9 |
| Iteration 24 | 0.16 | 0.1 | 1.3 | 0.45 | 0 | 21.9 | 0.3 | 0.9 |
| Iteration 25 | 0.08 | 0.05 | 1.59 | 0.6 | 1 | 21.7 | 0.6 | 0.8 |
| Iteration 26 | 0.16 | 0.05 | 1.59 | 0.6 | 1 | 21 | 0.6 | 0.8 |
| Iteration 27 | 0.08 | 0.1 | 1.59 | 0.6 | 1 | 21.6 | 0.7 | 0.8 |
| Iteration 28 | 0.16 | 0.1 | 1.59 | 0.6 | 1 | 21 | 0.7 | 0.8 |
| Iteration 29 | 0.08 | 0.05 | 2.67 | 0.6 | 1 | 22.4 | 1 | 0.8 |
| Iteration 30 | 0.16 | 0.05 | 2.67 | 0.6 | 1 | 21.7 | 1 | 0.8 |
| Iteration 31 | 0.08 | 0.1 | 2.67 | 0.6 | 1 | 22.4 | 1.2 | 0.8 |
| Iteration 32 | 0.16 | 0.1 | 2.67 | 0.6 | 1 | 21.6 | 1.2 | 0.8 |
| Iteration 33 | 0.08 | 0.05 | 1.3 | 0.6 | 1 | 22.6 | 1.2 | 0.9 |
| Iteration 34 | 0.16 | 0.05 | 1.3 | 0.6 | 1 | 22 | 1.2 | 0.9 |
| Iteration 35 | 0.08 | 0.1 | 1.3 | 0.6 | 1 | 22.6 | 0.3 | 0.9 |
| Iteration 36 | 0.16 | 0.1 | 1.3 | 0.6 | 1 | 21.9 | 0.3 | 0.9 |
| Iteration 37 | 0.08 | 0.05 | 1.59 | 0.45 | 1 | 21.7 | 0.6 | 0.8 |
| Iteration 38 | 0.16 | 0.05 | 1.59 | 0.45 | 1 | 21 | 0.6 | 0.8 |
| Iteration 39 | 0.08 | 0.1 | 1.59 | 0.45 | 1 | 21.6 | 0.7 | 0.8 |
| Iteration 40 | 0.16 | 0.1 | 1.59 | 0.45 | 1 | 21 | 0.7 | 0.8 |
| Iteration 41 | 0.08 | 0.05 | 2.67 | 0.45 | 1 | 22.4 | 1 | 0.8 |
| Iteration 42 | 0.16 | 0.05 | 2.67 | 0.45 | 1 | 21.7 | 1 | 0.8 |
| Iteration 43 | 0.08 | 0.1 | 2.67 | 0.45 | 1 | 22.4 | 1.2 | 0.8 |
| Iteration 44 | 0.16 | 0.1 | 2.67 | 0.45 | 1 | 21.6 | 1.2 | 0.8 |
| Iteration 45 | 0.08 | 0.05 | 1.3 | 0.45 | 1 | 22.6 | 1.2 | 0.9 |
| Iteration 46 | 0.16 | 0.05 | 1.3 | 0.45 | 1 | 22 | 1.2 | 0.9 |
| Iteration 47 | 0.08 | 0.1 | 1.3 | 0.45 | 1 | 22.6 | 0.3 | 0.9 |
| Iteration 48 | 0.16 | 0.1 | 1.3 | 0.45 | 1 | 21.9 | 0.3 | 0.9 |
| Current | - | - | 4.7 | 0.36 | 1 | 35.6 | 0.2 | 2.7 |

Table A-60 Iterative energy simulation results of the parametric, improved model for thermal zone 17a

| | Wall Insulation Thickness [m] | Floor/Ceiling Insula ion Thickness [m] | Window U-value [W.m-2.K-1] | Interior Shade Transmit-tance | Light Shelf (0=yes) (1=no) | Heating Demand [kWh.m-2] | Cooling Demand [kWh.m-2] | Electric Light Demand [kWh.m-2] |
|---|---|---|---|---|---|---|---|---|
| Iteration 1 | 0.08 | 0.05 | 1.59 | 0.6 | 0 | 10.2 | 0.4 | 1.5 |
| Iteration 2 | 0.16 | 0.05 | 1.59 | 0.6 | 0 | 10 | 0.4 | 1.5 |
| Iteration 3 | 0.08 | 0.1 | 1.59 | 0.6 | 0 | 10 | 0.7 | 1.5 |
| Iteration 4 | 0.16 | 0.1 | 1.59 | 0.6 | 0 | 9.8 | 0.7 | 1.5 |
| Iteration 5 | 0.08 | 0.05 | 2.67 | 0.6 | 0 | 9.9 | 1.3 | 1.5 |
| Iteration 6 | 0.16 | 0.05 | 2.67 | 0.6 | 0 | 9.8 | 1.3 | 1.5 |
| Iteration 7 | 0.08 | 0.1 | 2.67 | 0.6 | 0 | 9.7 | 1.8 | 1.5 |
| Iteration 8 | 0.16 | 0.1 | 2.67 | 0.6 | 0 | 9.6 | 1.8 | 1.5 |
| Iteration 9 | 0.08 | 0.05 | 1.3 | 0.6 | 0 | 11.5 | 0.2 | 1.5 |
| Iteration 10 | 0.16 | 0.05 | 1.3 | 0.6 | 0 | 11.3 | 0.2 | 1.5 |
| Iteration 11 | 0.08 | 0.1 | 1.3 | 0.6 | 0 | 11.3 | 0.2 | 1.5 |
| Iteration 12 | 0.16 | 0.1 | 1.3 | 0.6 | 0 | 11.1 | 0.2 | 1.5 |
| Iteration 13 | 0.08 | 0.05 | 1.59 | 0.45 | 0 | 10.2 | 0.4 | 1.5 |
| Iteration 14 | 0.16 | 0.05 | 1.59 | 0.45 | 0 | 10.1 | 0.4 | 1.5 |
| Iteration 15 | 0.08 | 0.1 | 1.59 | 0.45 | 0 | 10 | 0.7 | 1.5 |
| Iteration 16 | 0.16 | 0.1 | 1.59 | 0.45 | 0 | 9.8 | 0.7 | 1.5 |
| Iteration 17 | 0.08 | 0.05 | 2.67 | 0.45 | 0 | 9.9 | 1.3 | 1.5 |
| Iteration 18 | 0.16 | 0.05 | 2.67 | 0.45 | 0 | 9.8 | 1.3 | 1.5 |
| Iteration 19 | 0.08 | 0.1 | 2.67 | 0.45 | 0 | 9.7 | 1.8 | 1.5 |
| Iteration 20 | 0.16 | 0.1 | 2.67 | 0.45 | 0 | 9.6 | 1.8 | 1.5 |
| Iteration 21 | 0.08 | 0.05 | 1.3 | 0.45 | 0 | 11.6 | 0.2 | 1.5 |
| Iteration 22 | 0.16 | 0.05 | 1.3 | 0.45 | 0 | 11.3 | 0.2 | 1.5 |
| Iteration 23 | 0.08 | 0.1 | 1.3 | 0.45 | 0 | 11.3 | 0.2 | 1.5 |
| Iteration 24 | 0.16 | 0.1 | 1.3 | 0.45 | 0 | 11.1 | 0.2 | 1.5 |
| Iteration 25 | 0.08 | 0.05 | 1.59 | 0.6 | 1 | 10.2 | 0.4 | 1.5 |
| Iteration 26 | 0.16 | 0.05 | 1.59 | 0.6 | 1 | 10 | 0.4 | 1.5 |
| Iteration 27 | 0.08 | 0.1 | 1.59 | 0.6 | 1 | 10 | 0.7 | 1.5 |
| Iteration 28 | 0.16 | 0.1 | 1.59 | 0.6 | 1 | 9.8 | 0.7 | 1.5 |
| Iteration 29 | 0.08 | 0.05 | 2.67 | 0.6 | 1 | 9.9 | 1.3 | 1.5 |
| Iteration 30 | 0.16 | 0.05 | 2.67 | 0.6 | 1 | 9.8 | 1.3 | 1.5 |
| Iteration 31 | 0.08 | 0.1 | 2.67 | 0.6 | 1 | 9.7 | 1.8 | 1.5 |
| Iteration 32 | 0.16 | 0.1 | 2.67 | 0.6 | 1 | 9.6 | 1.8 | 1.5 |
| Iteration 33 | 0.08 | 0.05 | 1.3 | 0.6 | 1 | 11.5 | 0.2 | 1.5 |
| Iteration 34 | 0.16 | 0.05 | 1.3 | 0.6 | 1 | 11.3 | 0.2 | 1.5 |
| Iteration 35 | 0.08 | 0.1 | 1.3 | 0.6 | 1 | 11.3 | 0.2 | 1.5 |
| Iteration 36 | 0.16 | 0.1 | 1.3 | 0.6 | 1 | 11.1 | 0.2 | 1.5 |
| Iteration 37 | 0.08 | 0.05 | 1.59 | 0.45 | 1 | 10.2 | 0.4 | 1.5 |
| Iteration 38 | 0.16 | 0.05 | 1.59 | 0.45 | 1 | 10.1 | 0.4 | 1.5 |
| Iteration 39 | 0.08 | 0.1 | 1.59 | 0.45 | 1 | 10 | 0.7 | 1.5 |
| Iteration 40 | 0.16 | 0.1 | 1.59 | 0.45 | 1 | 9.8 | 0.7 | 1.5 |
| Iteration 41 | 0.08 | 0.05 | 2.67 | 0.45 | 1 | 9.9 | 1.3 | 1.4 |
| Iteration 42 | 0.16 | 0.05 | 2.67 | 0.45 | 1 | 9.8 | 1.3 | 1.4 |
| Iteration 43 | 0.08 | 0.1 | 2.67 | 0.45 | 1 | 9.7 | 1.8 | 1.4 |
| Iteration 44 | 0.16 | 0.1 | 2.67 | 0.45 | 1 | 9.6 | 1.8 | 1.4 |
| Iteration 45 | 0.08 | 0.05 | 1.3 | 0.45 | 1 | 11.6 | 0.2 | 1.5 |
| Iteration 46 | 0.16 | 0.05 | 1.3 | 0.45 | 1 | 11.3 | 0.2 | 1.5 |
| Iteration 47 | 0.08 | 0.1 | 1.3 | 0.45 | 1 | 11.3 | 0.2 | 1.5 |
| Iteration 48 | 0.16 | 0.1 | 1.3 | 0.45 | 1 | 11.1 | 0.2 | 1.5 |
| Current | - | - | 4.7 | 0.36 | 1 | 18 | 0 | 3.2 |

## 7.5 School building boundary conditions

| Boundary Condition | Colour |
|---|---|
| Wall to Exterior | |
| Wall to Ground | |
| Roof to Exterior | |
| Slab to Exterior | |
| Slab to Ground | |
| Door/Window to Exterior | |

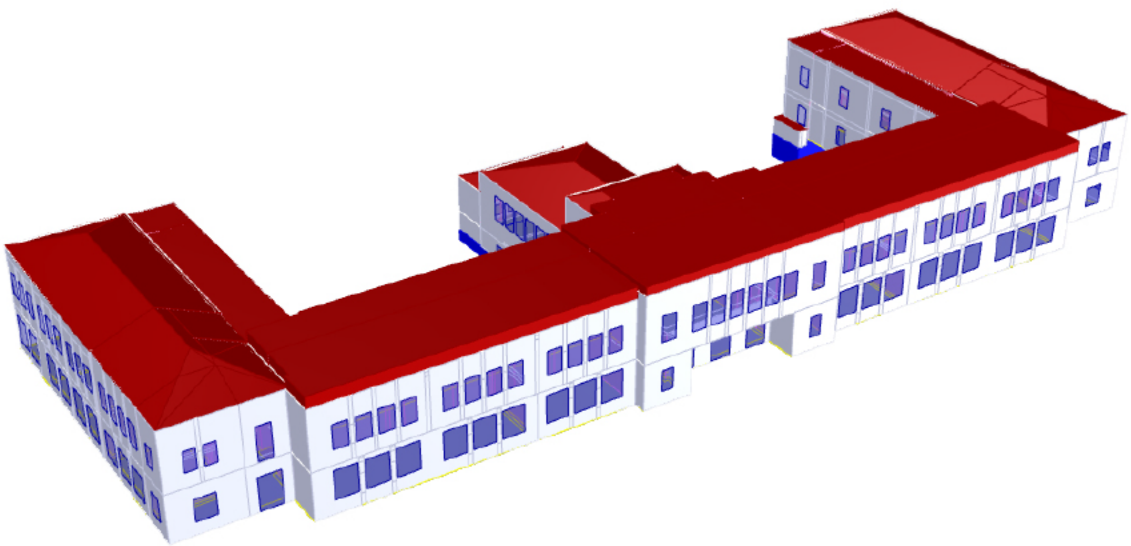

*Figure A-1 Boundary conditions of the school building realized in Grasshopper and visualized through the Rhino interface*

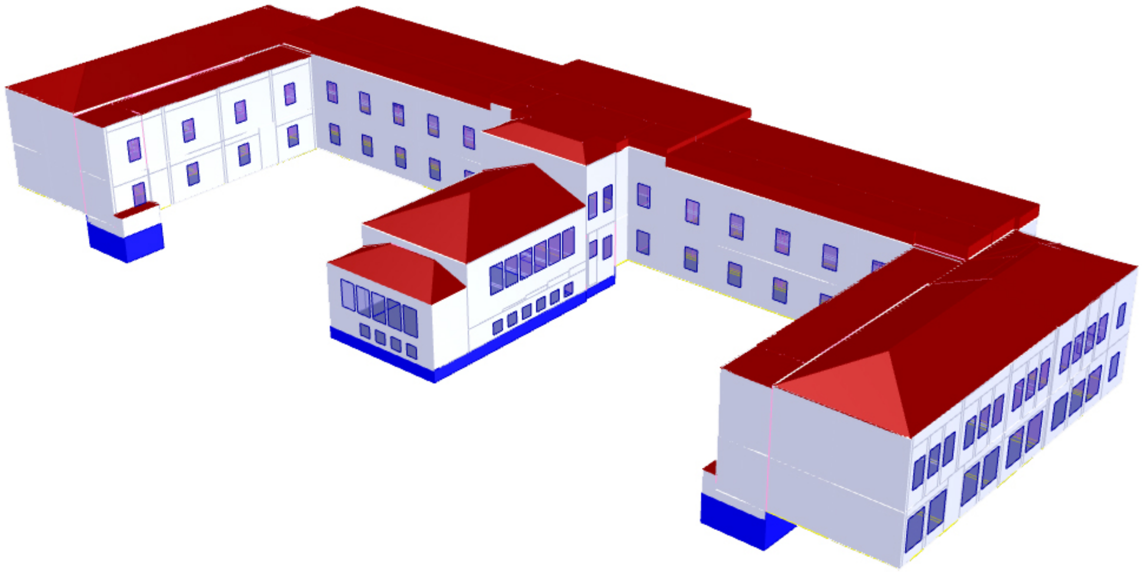

*Figure A-2 Boundary conditions of the school building realized in Grasshopper and visualized through the Rhino interface*

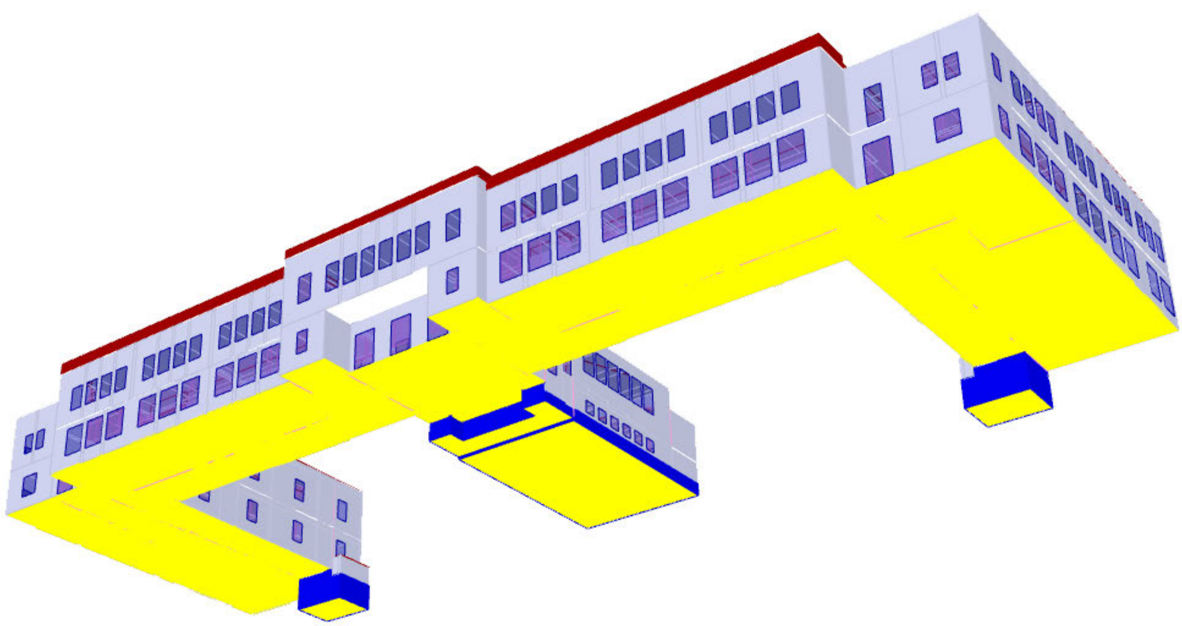

*Figure A-3 Boundary conditions of the school building realized in Grasshopper and visualized through the Rhino interface*